

---

**CHAPTER****TWO**

---

**SIBBORK: MODEL DEVELOPMENT**

*“Any model represents an abstraction of reality. The problem is not whether, but what to leave out.” - Clark, Jones & Holling (1979)*

*“Always code as if the guy who ends up using/maintaining your code is a violent psychopath who knows where you live.” - John Woods (1991)*

The original project direction focused on the re-parameterization of an existing gap dynamics model ZELIG for the simulation of boreal ecosystems. ZELIG was initially developed for temperate forests (*Smith and Urban*, 1988; *Urban*, 1990), and although the 3-D light subroutine has been applied to simulate a high-latitude light environment (*Weishampel and Urban*, 1996), the model had not been previously applied toward the simulation of Eurasian boreal ecosystems, and there were numerous incompatibilities between the existing ZELIG model and boreal forest processes. For example, ZELIG employed the Thornthwaite-Mather equation for the calculation of potential evapotranspiration (PET) based on monthly temperature and precipitation, and latitude corrections for day length. However, the correction factors have not been validated for latitudes above 50° N (*Botkin*, 1993), which rendered this approach inappropriate for the estimation of the water budget within Siberian boreal ecosystems located between 50° N and 71° N. The 3-D light ray tracing subroutine was created for flat terrain and, in its original form (*Weishampel*, 1994), was not compatible with complex terrain features. However, approximately half of the Siberian boreal forest is located in mountainous terrain (*Atlas of the USSR*, 1983), so modifications to the 3-D light ray tracing subroutine were needed in order to more appropriately compute the light environment for these areas. Each process in ZELIG was evaluated for compatibility with application toward the simulation of high-latitude environments and ecosystems and, wherever necessary, new formulations were developed. In order to extend the capabilities of the original ZELIG model to simulate the temperature, radiation, and edaphic gradients encountered in the mountains, model structure and several processes were substantially modified. The resulting gap dynamics model was deemed different enough from ZELIG

to warrant a rebranding and was coined SIBBORK - the SIBerian BOReal forest simulator, which was calibrated to the Krasnoyarsk region in central Siberia.

SIBBORK is a spatially-explicit individual-based gap model for predicting ecosystem change in boreal forests. It was designed as an open source model, utilizing publicly-available software and datasets. The new model is a descendant of ZELIG, an existing individual-based gap dynamics model (*Urban* 1990, 2000; *Urban et al.* 1991, 1993) and retains many of ZELIG's functionalities. First, ZELIG was functionally translated from Fortran to Python for the purpose of interfacing with ArcGIS, since a spatially-explicit model produces spatially explicit output, and GIS (ArcGIS, open source: QGIS, Grass) could be used to display model output in georeferenced space. Thereafter, the model was substantially altered through modifications to the 3-D light subroutine, species-specific parameterizations and governing equations, simulation of canopy architecture and terrain representations, and specification of the simulation area and plot size. Alteration was geared toward improving model functionality based on advances in ecology and technology, and specifically tailored to the boreal forest ecosystem. Additionally, an array of analysis scripts were created for ease of processing output from replicate model runs and for visualization of model outputs. A simplified diagram of process flow in SIBBORK is shown in [Figure 2.1](#).

SIBBORK's predecessor, ZELIG, was originally developed at the University of Virginia based on the FORET model (*Shugart and West*, 1977; *Shugart*, 1984; *Leemans et al.*, 1989), which is not spatially-explicit, for the simulation of North American temperate forests (*Smith and Urban*, 1988; *Urban*, 1990). It has since been adapted to temperate forests in China (*Jiang et al.*, 1999), the Pacific Northwest (*Urban et al.*, 1993; *Busing and Solomon*, 2004), Alaska (*Weishampel et al.*, 1992), the northern hardwood and mixed forests in Canada (*Larocque et al.*, 2006; *Larocque et al.*, 2011), the tropical dry forests in Puerto Rico (*Holm et al.*, 2012; *Bond-Lamberty et al.*, 2015), as well as the tropical forests in the Amazon region (*Holm et al.*, 2014). A detailed process flow diagram for ZELIG is shown in [Figure 2.2](#). The blue rectangles and arrows symbolize the processing, the orange rectangles list the inputs and the green rectangles summarize the outputs for each subroutine.

The current working version of SIBBORK is v3.0, however, each stage in development has it's own importance. SIBBORK v1.0 represents ZELIG (Fortran) functionality, implemented in Python. This version includes 1-D and 2-D light subroutines, in which the light penetration through the canopy is computed solely from directly overhead (1-D), as in classical gap dynamic models, or from overhead and from the south directions (2-D), respectively. The Fortran and Python versions of the model were run concurrently and model output was qualitatively and quantitatively evaluated to validate the functionality of the “translation”. There was no difference in model output of tree height, diameter at breast height (DBH), and biomass distributions for monospecies stands simulated via ZELIG v1.0 (Fortran) and SIBBORK v1.0 (Python) starting from bare ground, from identical initial conditions, and with a fixed seed in the random number generators.

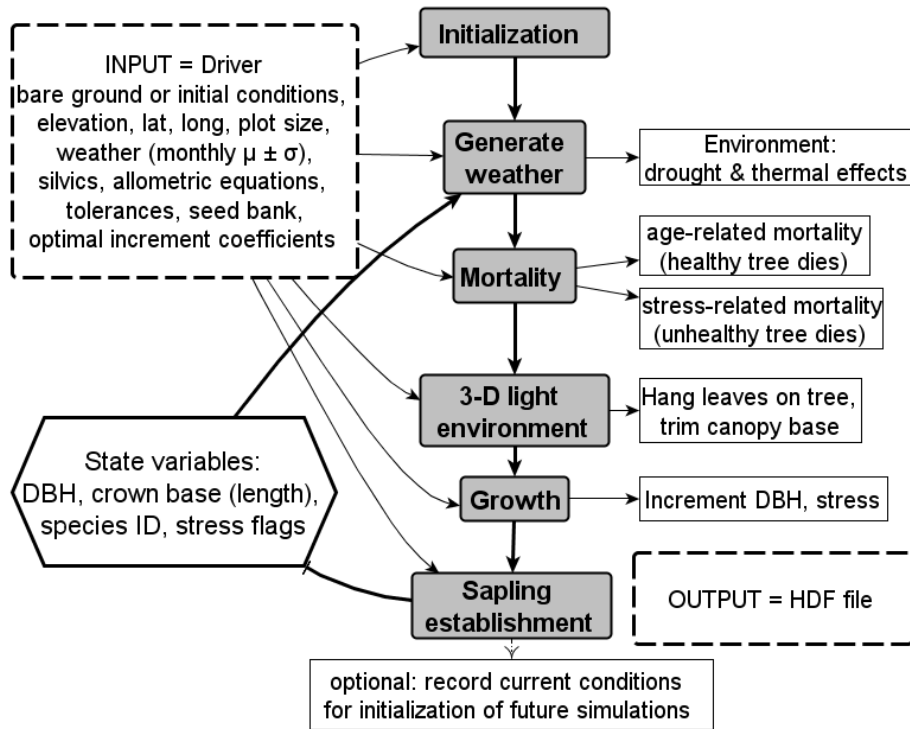


**Fig. 2.1:** Conceptual diagram of process flow in SIBBORK. Pre-processing includes analysis of climatological, radiation, and edaphic factors for the location of interest and generation of topography using Geographic Information System software. The model is initialized with conditions specified in the driver file. Weather is generated at daily and monthly timesteps. Annually, saplings are established, trees are grown, and some trees die due to natural or stress-related mortality. State variables are updated annually. HDF output file contains a record of state variables at user-specified increments. Height, basal area, biovolume, biomass, and leaf area are computed at the individual level as a function of DBH during post-processing, and optionally aggregated to the stand-level, with the additional option to specify masks based on terrain features.

In SIBBORK v2.0, the weather, sapling establishment, and tree growth subroutines were modified, and the parameterization representing the interaction between trees and the surrounding environment was enhanced. The representation of terrain in the simulation was developed using ArcGIS. The 3-D light subroutine developed by Weishampel (1994) was functionally implemented in Python and significantly modified to enhance the representation of the complex light regime at northern latitudes. Although the 3-D light subroutine worked with complex terrain at this stage, it was very computationally expensive (runtime on a 9-ha 1,000-year simulation was on the order of 12 hours). Model output and state variables were recorded to a hierarchical data format (HDF) file.

Sibbork v3.0 further improved the 3-D light subroutine to facilitate ray-tracing in complex terrain and accelerate it via the Numba library, which compiles the python code. Leaf area calculation was improved using a combination of approaches from the literature and field-based observations. Multiple scripts and a GUI were created to facilitate analysis and visualization of model output, including a timeseries output of simulated forest structure color-coded by

species. The functions that have been modified from ZELIG to SIBBORK are outlined in red in Figure 2.2, and added functionality is shown via red rectangles and arrows. Features that are unique to SIBBORK are listed in Figure 2.4.

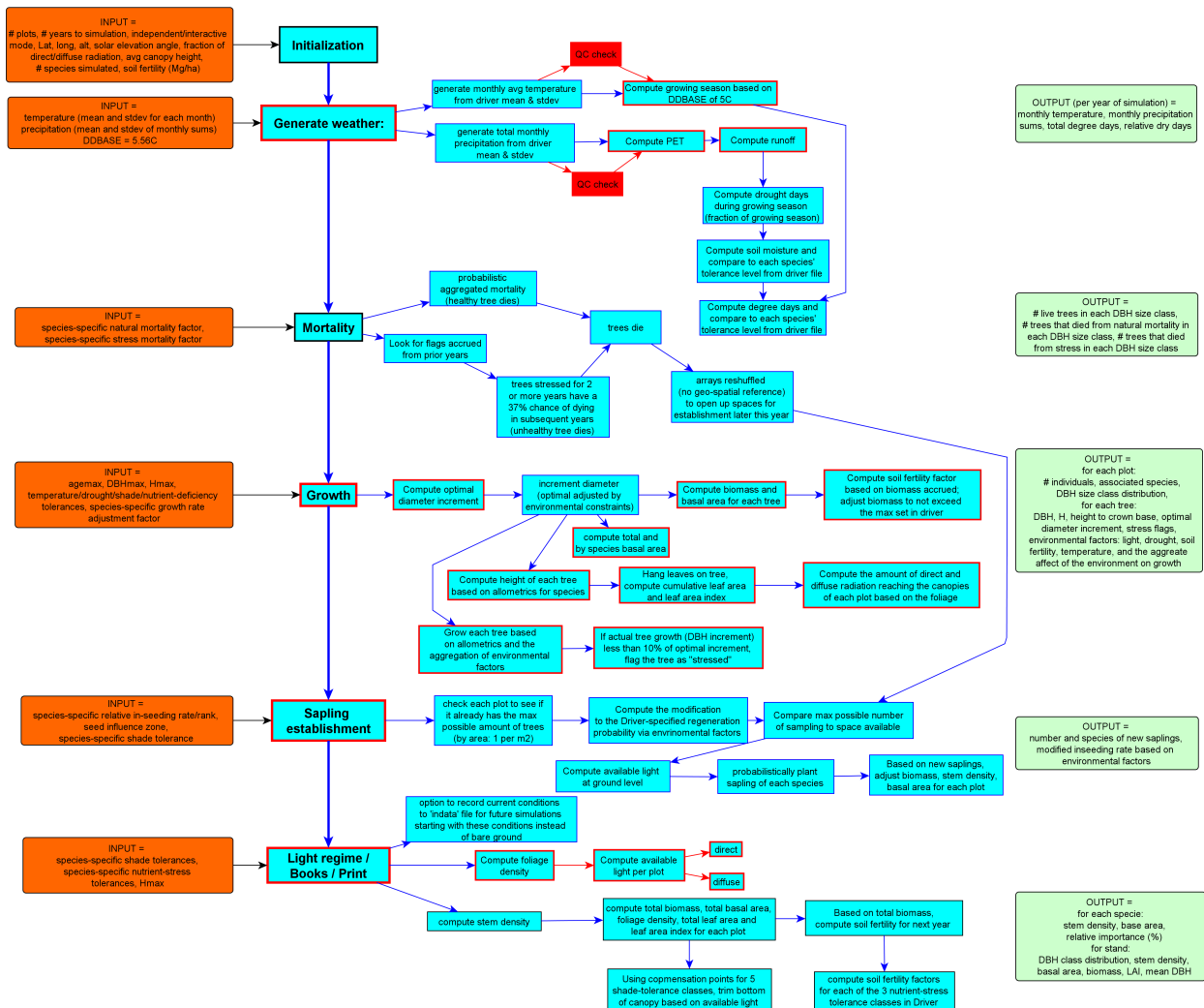


**Fig. 2.2:** SIBBORK is based on the ZELIG gap model, with significant modifications to the sapling establishment, tree growth, and 3-D light subroutines, as well as environmental interaction parameterizations. New features symbolized via red rectangles/arrows; features modified from ZELIG outlined in red.

## 2.1 Environment

SIBBORK simulates tree processes in a 3-dimensional environment, which includes topographic, radiation, climatic, and edaphic gradients. Topography and radiation are specified at the plot-level. Topography is specified as elevation above sea level in meters. Within each plot, the elevation is constant and the terrain is uniform. Radiation is computed in ArcGIS and specified as a sum of  $W\text{m}^{-2}$  for each month of the year. The radiation calculation takes into account

Function	ZELIG	SIBBORK
Monthly temperature	random from a gaussian around a mean	same, with added QC check
Monthly precipitation	random from a gaussian around a mean	same, but flush negative rain to 0, added QC check
Growing degree base	5.56° C	broadleaf: 5° C
Potential Evapotranspiration	Thorntwaite-Mather equation	modified Penman equation
Runoff	uses PET, field capacity and wilting point	same, but uses AET instead of PET
Optimal diameter increment	based on JABOWA	based on Bragg (2001, 2003)
Soil fertility	based on optimal biomass increment	based on actual potential biomass increment
Heat tolerance	parabolic	user-specified: parabolic or non-linear
Stress flags	if does not achieve 10% of optimal diameter increment	species-specific thresholds based on forestry yield tables
Maximum stem density	1 stem / m <sup>2</sup>	user-specified
Height	same form polynomial with species-specific coefficients	species-specific equations (incl. piecewise)
Leaf Area	same equation for all species, f(DBH)	species-specific, based on Breda (2003) and forestry yield tables
Plot size	100 m <sup>2</sup>	user-specified
Simulation domain	Single plot, transect of plots, or grid of interactive plots	user-specified number of plots in an interactive grid, single plot, transect of plots, or grid of independent plots grid of independent plots
Terrain	Flat	Flat, artificial 3-D, or real 3-D
Light mode	1-D, 2-D, 3-D	1-D, 2-D, or 3-D, with complex terrain
Driver file	fixed-format text	self-documenting python code
Model output file	(pretty-print) text, csv	HDF

**Fig. 2.3:** Functionality comparison between ZELIG and SIBBORK

latitude, elevation, slope steepness, aspect, direct:diffuse ratio, and atmospheric transmissivity. Soil characteristics include field capacity, wilting point and site index. Field capacity and wilting point are estimated from the total available water. These parameters are specified in the driver and are the same for all plots in the simulation. Conversely, site index is estimated based on forestry yield tables and refers to the limit on gross primary productivity. Site index is a plot-level parameter. Temperature and precipitation represent the simplified weather conditions. Temperature is specified at the plot-level, and is adjusted using the environmental lapse rate based on elevation above or below a reference weather station. Monthly precipitation is the same for all plots, due to lack of field data and uncertainty in downscaling precipitation from climate and meso-scale models. A simplified precipitation gradient can be specified based on slope aspect (windward/leeward), however, all plots with a given slope aspect will receive the same precipitation. Light-ray tracing is computed within a 50-m thick layer of the atmosphere above the ground surface. The 50-m thickness was selected to exceed the maximum observed tree heights in the Siberian boreal forest and to limit the computational space (*Shvidenko et al.*, 2006; *Ershov and Isaev*, 2006; *Neigh et al.*, 2013). Vegetation is simulated within this 3-dimensional environment.

Feature	Description	Origin
<i>Simulation of 3-D space</i>		
Spatially-explicit simulation of 3-D terrain	The model intakes a 2-D matrix that can specify real terrain from a Digital Elevation model or user-generated artificial terrain (flat, sloped, etc.)	A new feature that allows terrain heterogeneity. Plots in a grid (homogeneously flat terrain) were simulated with ZELIG by Weishampel and Urban (1996).
Wrap-around to simulate continuous forest	The southernmost boundary of the simulation area is wrapped around to be continuous with the northernmost boundary, and the eastern boundary is wrapped around to be continuous with the western boundary to ensure continuity with regards to light ray tracing.	This feature remains from the previous versions of ZELIG, however, in SIBBORK this feature can be toggled on/off to simulate forest fragmentation.
3-D light ray tracing that works with the 3-D terrain	Light ray tracing does not allow light to travel through the terrain. To facilitate wrap-around, ray trace is permitted to continue elevated terrain along the edge of the simulation area.	A new algorithm that allows the 3-D light subroutine originally developed by Weishampel (1993) to work with 3-D terrain.
Independent vs. interactive plot modes	Independent mode: trees on a plot receive only from directly overhead and do not shade trees on other plots. Interactive mode: trees on a plot receive light from 7 paired sun azimuth-elevation angles and shade trees on nearby plots.	An improved version of a feature from ZELIG, which now gives the user the ability to specify the shape and extent of the simulation area, and the plot size.
Differential air (and soil) temperature in complex terrain	Air temperature is computed at the plot level using weather station data, radiation inputs, and seasonal lapse rates.	A new empirically-based algorithm.
Soil moisture and drainage	Soil moisture is computed as a fraction of total available water content based on soil type. Runoff represents gravitational water, and is contributed as runoff to the water budget of the plot directly downslope.	A new algorithm based on soil type and terrain characteristics. Soil and water content data are available from global datasets.
<i>Species-specific parameterization</i>		
Total (above- & below-ground) biomass	Most models do not consider or compute below-ground biomass. SIBBORK is parameterized to compute the species-specific total sum of above- and below-ground biomass based on yield tables with this data.	A new empirically-based algorithm that improves simulated biomass estimates at the individual and stand levels.
Foliage biomass	Species-specific piece-wise calculation based on DBH and total biomass.	A new empirically-based algorithm.
Total leaf area	Species-specific computations of leaf area as a function of foliage biomass, leaf area index (LAI), and specific leaf area (SLA).	A new algorithm that synthesizes regional yield table data and published datasets.

<i>Inputs</i>		
JSON (JavaScript Object Notation) file format	Standardized file format with user-friendly formatting and incorporation of documentation strings for every input variable.	A new feature, as previous versions of ZELIG and its derivatives utilize Text file format, in which inputs must be specified at a fixed location within the document with no option of in-line documentation.
Input file pickled and stored with simulation output	The input file is stored with the output HDF file and cannot be altered, therefore preserving the user-specified simulation parameters for future reference.	This is a new feature that permanently associates the input data with the model output generated with those inputs, eliminating the possibility of manually associating the input file with an output file generated from other inputs.
Ease of creating matrix inputs for topography, soil nutrition, and maximum ground-level light gradients.	Although the maximum available light at ground level (also used for top of canopy) is computed using the Solar Radiation Calculator (ref) in ArcGIS, the topography and site index input ASCII files can be generated manually or with a script.	This is a new feature that facilitates generation of artificial terrain (e.g. flat, different slopes and aspects) for model testing, and allows the utilization of actual terrain from a Digital Elevation Model in the simulation.
<i>Outputs</i>		
HDF file format	Multi-dimensional matrix output format that makes it possible to store all of the model output in one file, greatly simplifying the parsing of model output.	A new feature that eliminates the need to parse pretty-print text output documents common to many models, including ZELIG and FAREAST.
2-D and 3-D matrix outputs to visualize the simulated environment and vegetation across the landscape	Information about the simulated environment is stored at the plot level. All tree parameters are stored at the individual level within each plot. This facilitates analysis at the individual, plot, and stand levels.	A new feature that facilitates visualization and animation of model outputs in 4-D space-time in Geographic Information Systems or as matrix-based gifs.
<i>Documentation</i>		
User's Manual, tutorials, and extensive comments within the code and driver file	Documentation of every input parameter, function and subroutine in the model code. Step-by-step tutorials on model implementation, re-parameterization to new species and locations, modification of the HDF output record, and model testing. In-line code commentary.	A new feature that is often overlooked in model development or lost as model development branches.

**Fig. 2.4:** Description and origins of new and improved SIBBORK v3.0 features.

### 2.1.1 Spatial domain

#### Plot Size

The spatial unit of the simulation is a plot approximately the size of the canopy of a dominant tree. Trees of different species will develop crowns of different sizes, however, the average canopy size can be deduced from the ecosystem in focus. Tropical trees, e.g. Bunyan, may develop canopies 20-m across or more, whereas Dahurian larch, which dominates vast regions of north-central Siberia, is characterized by a long, thin, almost-cylindrical canopy of just a few meters in diameter. The goal is to appropriately simulate the leaf area index (LAI), which, in the simulation, is a ratio of total leaf area to plot size. If the plot is significantly smaller than the horizontal canopy cross-section, the simulated LAI will be exaggerated. The plot size is set by the user in the digital elevation input file. In the current analysis and application of SIBBORK, 100  $m^2$  plots were used. However, analysis assessing the dependence of model output on plot size was conducted and the results are reported in Chapter 5, which confirmed the appropriateness of the 100  $m^2$  plot size for the central Siberian boreal forest.

#### Simulation Area

The spatial domain includes all of the plots in the simulation, and is determined by whether the simulation is run in 1-D, 2-D or 3-D mode. In the 1-D mode, the user-specified number of plots are simulated independently, without spatial interactions, and with a simplified light representation ([Figure 2.5a](#)). There are two options for simulating independent plots: (1) all plots are collocated at the same point location and experience the same environmental conditions, and (2) plots are distributed in a grid across environmental gradient(s), but trees on a plot do not interact with trees on adjacent and nearby plots. In the latter, each plot can have different environmental conditions from its neighbors, which expands on ZELIG capabilities.

In the 2-D mode, the plots are aligned along a north-south transect ([Figure 2.5b](#)). Each plot is adjacent to two neighboring plots - to the north and to the south, respectively, with a wrap-around from the northern-most plot to the southern-most plot. The trees on each plot interact with trees on plots to the north through shading. The shadow is wrapped around from the north edge to enter the simulation domain from the south edge.

In the 3-D mode ([Figure 2.5c](#)), the plots are aligned in a grid. Each plot has eight immediate neighbors, and trees on one plot interact with trees on adjacent and nearby plots through shading along seven compass directions (no shade directly to the south in the extratropical northern hemisphere).

The plot size and the spatial extent of the simulation domain are specified in a 2-D matrix format of plot-level elevations in an ASCII file (DEM), which can be generated in ArcGIS or by the user. Plot-level radiation inputs are computed in

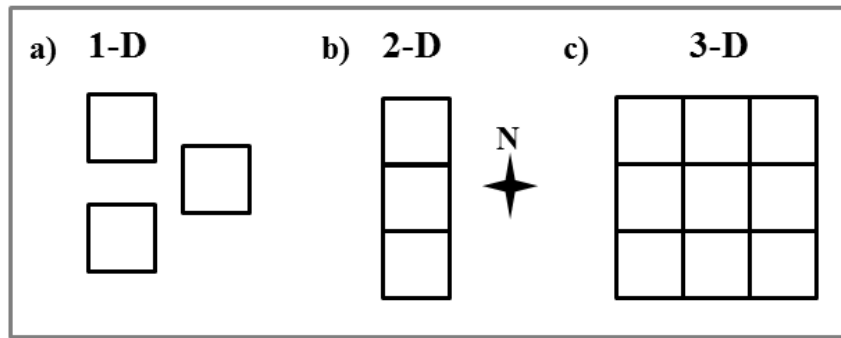


**Fig. 2.5:** User-specified simulation modes in SIBBORK: (a) Independent plots, no interactions between trees on these plots. (b) Transect of plots oriented south to north. Trees on a plot cast shade onto plots to the north. (c) Grid mode. Trees on a plot cast shade onto plots to the southeast, east, northeast, north, northwest, west and southwest. Each square represents one plot.

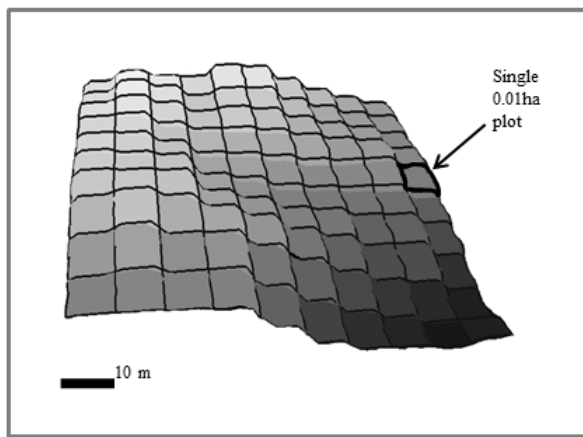


**Fig. 2.6:** A sample simulation area for 3-D grid mode: 0.01ha plots along a topographic gradient - a gentle, southeast-facing slope. Lower elevations are symbolized by darker grey. Each plot in the 3-D simulation mode has hydrologic, temperature, and radiation variables based on its location along the simulated terrain.

ArcGIS based on the topography specified in this file. Plot size for calibration and testing of the model remained at  $100\text{ m}^2$  (0.01ha). A sample 1-ha simulation domain is shown in Figure 2.6.

Urban and his colleagues conducted a sensitivity analysis on ZELIG to assess the dependence of model output on the spatial extent simulated (*Urban et al.*, 1991). They found that aggregation at the plot-level compared to larger spatial domains (hectare) results in greater interannual and inter-replicate variability in stand structure. The scale of output aggregation in SIBBORK is user-specified, however, it is important to understand that the simulated changes in stand structure and composition over time will vary depending on whether the analysis is conducted at the fine (plot-level) or coarse (landscape-level) scale.

### Initial Conditions

The simulation can be initialized from bare ground or a specific initial condition. Bare ground represents the conditions following a stand-replacing disturbance, such as clear-cutting or an intense wildfire or clear-cutting. Initialization from a set of initial conditions places a specified number of trees of a given species and size on each plot. Initial conditions may be obtained from field measurements, random assignment, or previous model runs, and specify the average tree size and stem density for species of interest. For example, it is possible to initialize the model as a young birch stand with diameters at breast height (DBH) in the range  $5 \pm 1\text{cm}$ , which over the course of the simulation may be replaced by other species.

### 2.1.2 Weather

Weather conditions affect the duration of the growing season, the annual growing degrees sum, and the soil moisture available for plant growth. Weather is modeled stochastically in the simulation at a daily timestep based the monthly averages of observed temperature and precipitations records from the World Meteorological Organization (WMO) weather station(s) within 100km radius of the location of interest. WMO weather records in Russia extend back 50-120 years, cover all ecotones of interest, and are in the public domain (NCDC, 2005a, b).

In order to prevent the occasional simulation of unrealistically high or low temperatures generated from the gaussian distribution centered around the average monthly temperature, a quality control (QC) check has been added. If a temperature is simulated outside of the observed absolute minimum to absolute maximum range, this number is discarded, and another number is generated. The distributions of observed and simulated monthly temperatures are shown in [Figure 2.7](#) for an average growing season at  $57^{\circ}\text{N}$   $95^{\circ}\text{E}$ , elevation 180m above mean sea level (amsl). Using the DEM and the standard environmental lapse rate of  $6.5^{\circ}\text{Ckm}^{-1}$ , temperature is computed for each plot that is at a different elevation than the reference weather station. Air temperature is used to compute the growing degree days above the base temperature of  $5^{\circ}\text{C}$ . Observed and simulated growing degree day sums for 55 consecutive years (length of record) are shown in [Figure 2.8](#). Monthly precipitation is also simulated from a gaussian distribution using average monthly sums of water-equivalent precipitation. Monthly precipitation totals are increased by 10% to account for potential windloss (*Bonan*, 1988a). The shape of the simulated distribution of monthly precipitation on flat terrain closely resembles the precipitation records acquired at the same elevation ([Figure 2.9](#)).

Climate change is simulated in two ways: static and dynamic. Static climate change simply adjusts the simulated monthly temperature and precipitation by a specified coefficient before relaying these values to the vegetation processes. The coefficient of change is constant throughout the simulation. In this manner, vegetation processes can be simulated in an environment that experiences a stable climate of, for example,  $2^{\circ}\text{C}$  warmer and 10% dryer than the historic record (based on 20<sup>th</sup> century observations). Dynamic climate change is represented by adjustment coeffi-

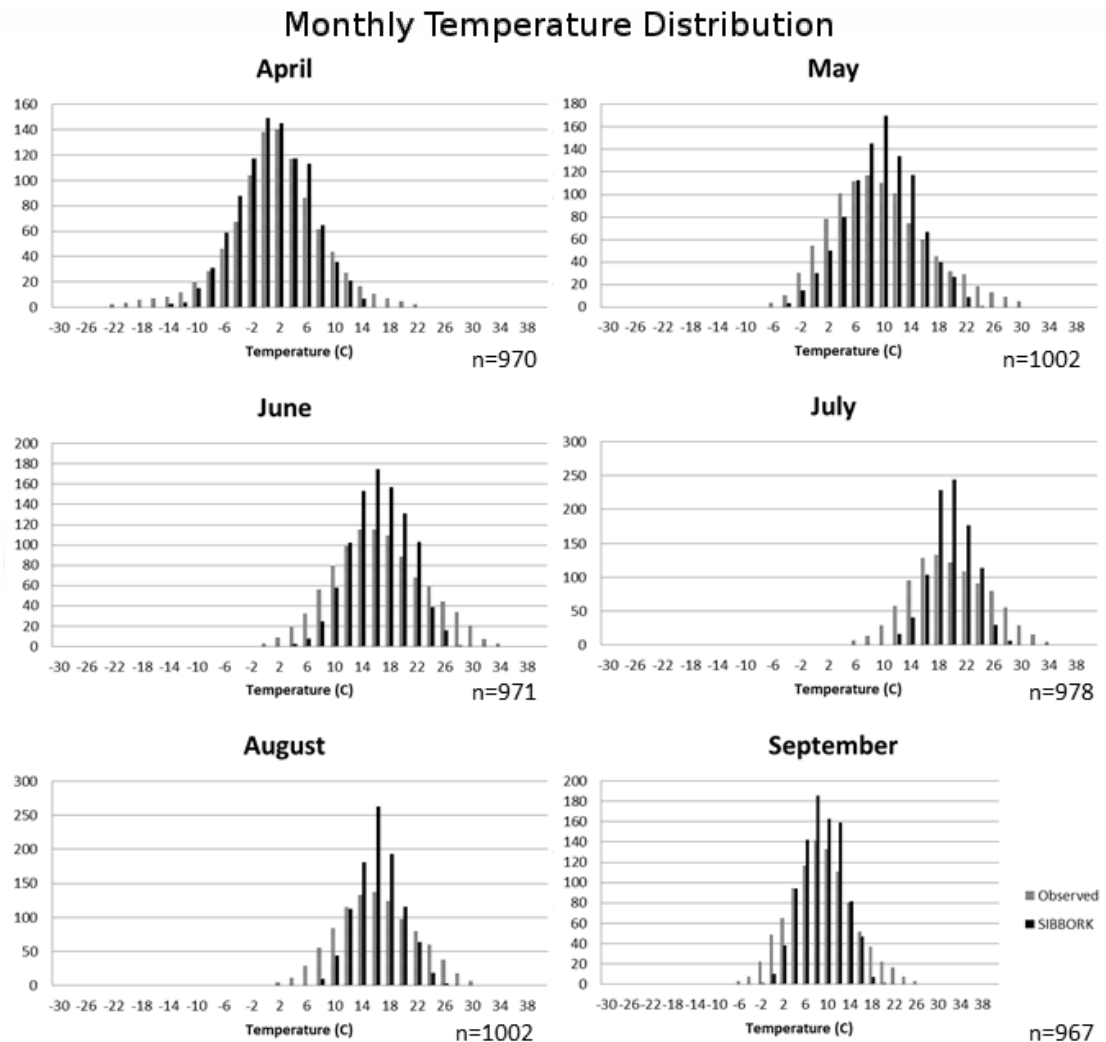


**Fig. 2.7:** Distributions of observed and simulated daily temperature for the months within the growing season. Although the distribution of observed temperatures is slightly wider, the average simulated annual total heat sum, expressed in growing degree days, is within 2% of the average observed value.

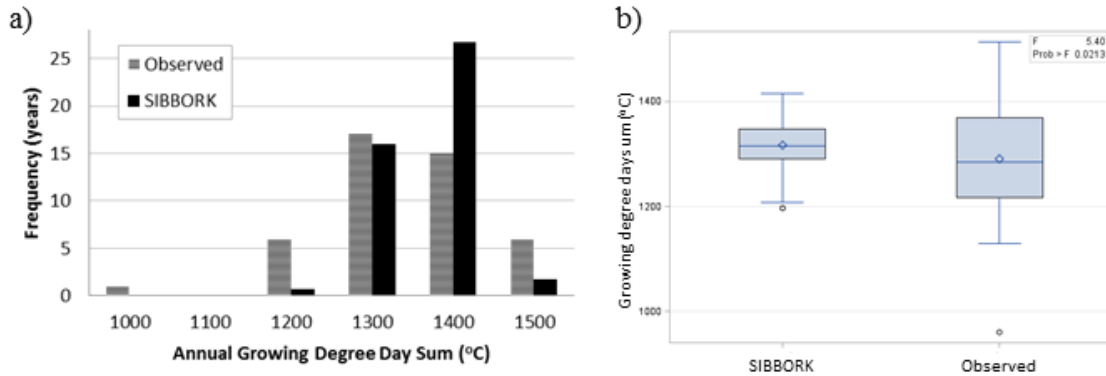


**Fig. 2.8:** Distributions of observed and simulated growing degree days. (a) Slightly greater variability is exhibited in the data record than in the simulation, however, if a larger sample size is considered, colder and warmer years are also simulated, which expands the variability for the annual growing degree days sum in the simulation. (b) SIBBORK annual growing degree day sums are not statistically significantly different from observed values at the nearest WMO station at the 0.05 level (ANOVA:  $F=5.4$ ,  $p<0.0213$ ,  $n_{\text{obs}}=45$ ).

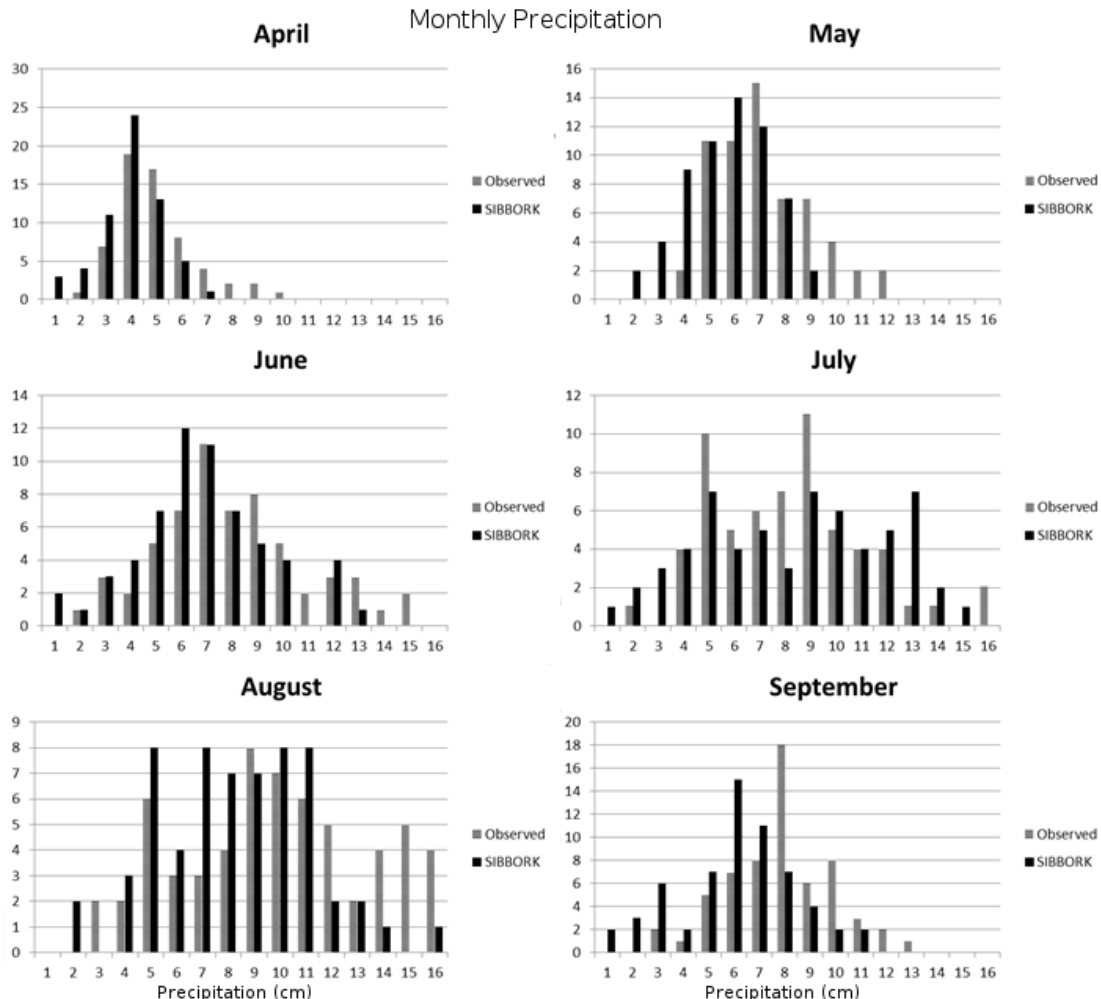


**Fig. 2.9:** Distributions of observed and simulated daily precipitation exhibit significant overlap throughout the growing season.

clients applied at annual or monthly increments. For example, average monthly temperatures may be linearly increased at a rate of  $1^{\circ}\text{C}$  per decade and/or precipitation may be decreased at a non-linear rate of 10% per decade (Figure 2.10). Climate change is initialized at a user-specified year in the simulation and continues for a specified duration. This approach is flexible enough to allow forest generation in a stable climate, then apply climate change for a desired period of time, then stabilize the climate at a desired threshold.

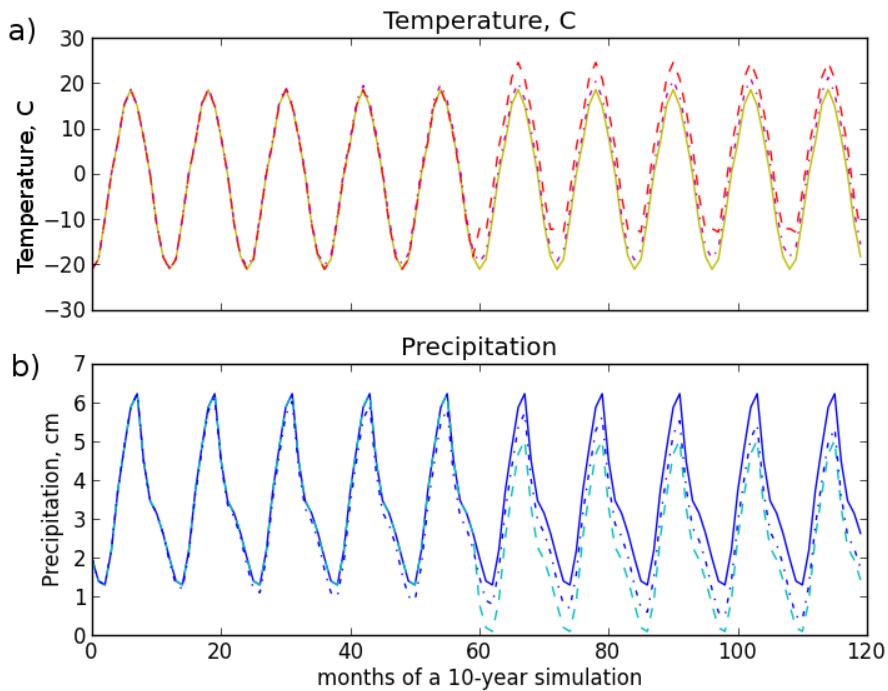


**Fig. 2.10:** The top graph depicts average monthly temperature (a), whereas the bottom graph depicts average monthly precipitation (b), over the course of a 10 year simulation. The solid lines depict the historical data record. The dashed line in (a) represents a step-wise  $7^{\circ}\text{C}$  increase in temperature in year 5. The dash-dot line represents a more gradual approach, in which each month's temperature is increased by a small fraction of a degree, so that a total of  $1.5^{\circ}\text{C}$  warming is observed over the 10 year simulation. In (b), precipitation can also be gradually decreased (dash-dot line) by a few mm per year to a total decrease of 1cm over the course of a 10-year simulation. Alternatively, precipitation can be changed once (decrease in year 5) and then maintained at the new level.

To simulate observed climate change, observed monthly and seasonal trends in temperature and precipitation changes were obtained from the Russian Hydrometeorology Office (*Gruza et al.*, 2015). Near-future climate change may be approximated via extrapolation of the observed trends.

### 2.1.3 Insolation

Solar radiation is required for photosynthesis, however, vegetation can be shaded by surrounding vegetation and by the terrain. A unique feature of SIBBORK is the incorporation of shading by topographic features, which generates

<b>ecotone</b>	<b>station</b>	<b>location (lat, long)</b>	<b>direct:diffuse ratio</b>
northern taiga	Turukhansk	65.8° N, 88.0° E	40 : 60
middle taiga	Vanavara	60.2° N, 102.2° E	45 : 55
southern taiga	Irkutsk	52.3° N, 104.4° E	50 : 50

**Fig. 2.11:** World Radiation Data Centre stations used for computing the direct:diffuse ratio for downwelling solar radiation, and for quality control check of computed radiation values in ArcGIS using Solar Area Calculator.

a differential distribution of radiation available for photosynthesis based on the location on the landscape. This is particularly important for the simulation of the southern Siberian boreal forest located in the complex terrain of Altay-Sayan and Zabaikal' e mountain ranges, as well as for the high latitude environment of northern taiga, where the unique annual pattern of radiation exhibits a large component of diffuse radiation for most of the year due to the flat angles of the sun. Available light is partitioned into direct and diffuse components using ratios derived based on radiation datasets from the central Siberian stations (World Radiation Data Centre: wrdc-mgo.nrel.gov).

Incident radiation (direct + diffuse) received at bare ground (or top of the canopy) is computed in  $W H m^{-2}$  at a monthly time step using the Area Solar Radiation tool in ArcGIS based on algorithms developed by Fu and Rich (1999a, 1999b, 2002) and the 30m X 30m resolution ASTER Digital Elevation Model (*METI and NASA*, 2011) resampled at a 10m X 10m resolution. In brief, the Area Solar Radiation tool computes incident direct radiation based on a viewshed from a set number of compass directions (user-defined: 8-32). Diffuse radiation is computed using the standard overcast diffuse model, in which incoming radiation depends on the sun's zenith angle. Default atmospheric transmissivity of 0.5 is used for central Siberia, as this fraction represents generally clear skies, and corresponds to the prevailing anticyclonic conditions throughout most of the year in this region. Transmissivity and the direct:diffuse ratio can be decreased to represent the radiation regime of particularly cloudy regions. Using the Area Solar Radiation algorithm, slopes of different grades and aspects receive differential amounts of total radiation throughout the year, which affects the monthly air temperature and the potential evapotranspiration of those locations. The differences in radiation received in complex terrain can be quite significant, as shown for the top of the canopy of a mixed forest in complex terrain (Figure 2.12a) and at the ground level below the canopy assuming a leaf area index of 1.3 (Figure 2.12b). This figure demonstrates the importance of including 3-dimensional terrain in the computation of available light for prediction of species distribution (potential vegetation) across the landscape.

A limitation of the approximation of incident radiation using the Solar Area Radiation calculator in ArcGIS is in the specification of the direct:diffuse light fraction. The same fraction is applied to all locations on the terrain, regardless of slope or aspect. This can be particularly incorrect when considering high latitude light regimes in the northern hemisphere, with larger direct radiation received on the south-facing slopes, and the light regime dominated by diffuse light on north-facing slopes. Based on radiation data from the World Radiation Data Centre (see station list in Figure 2.11), direct:diffuse light fraction computed for locations in southern, middle, and northern taiga are approximately

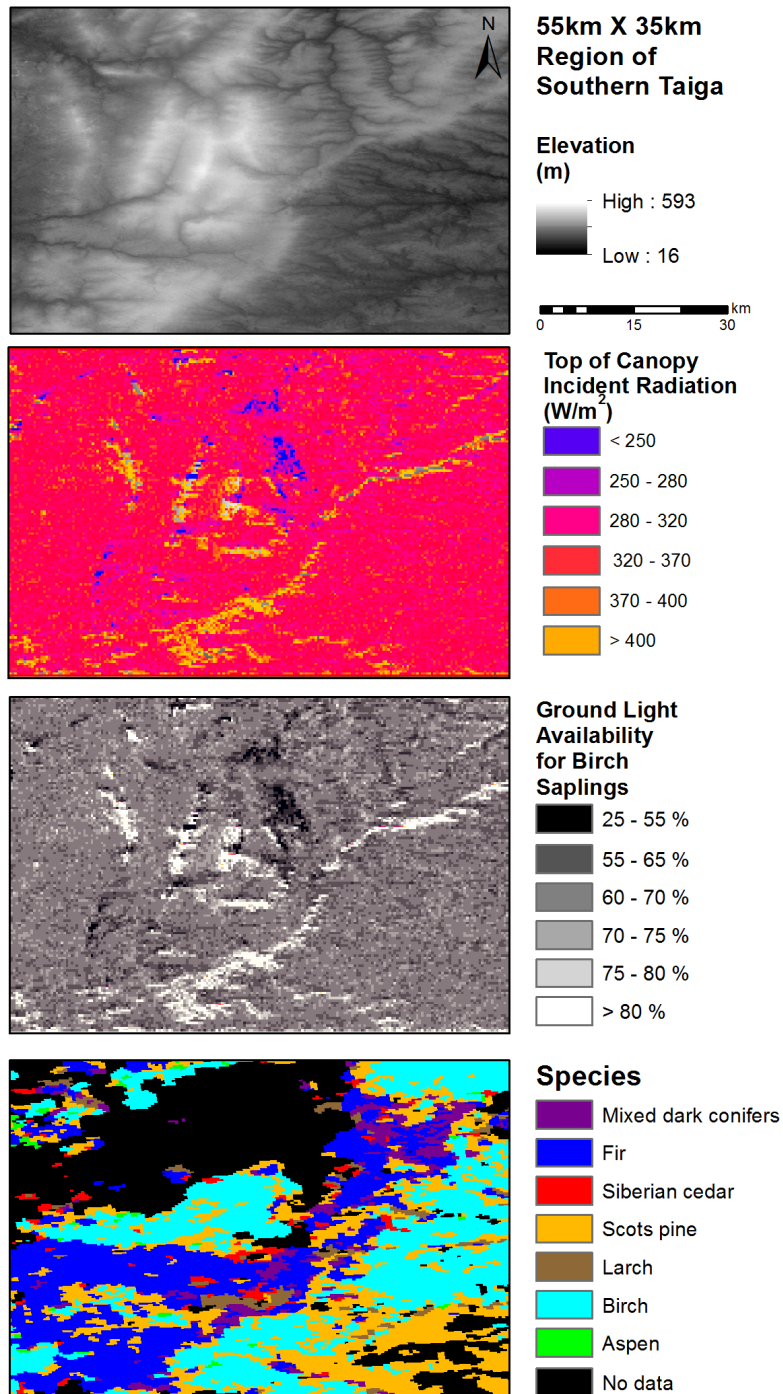


**Fig. 2.12:** Radiation input differs across the terrain based on elevation, slope, and aspect. (a) An area of complex terrain in southern taiga, east of the Yenisei River (from ASTER DEM, METI and NASA, 2011). (b) The average direct radiation experienced on different slopes within complex terrain in central Siberia on June 22nd, computed using ArcGIS Area Solar Calculator tool. (c) Model-predicted available light factor for birch at the ground level based on a closed canopy with a leaf area index of 1.3, computed as a fraction of light incident on top of the canopy, as in (b), or on bare ground. (d) A species composition map (Bartalev, 2010; Bartalev et al., 2011; Huttich et al., 2014) shows the observed distribution of birches along upper slopes, including a southeast-facing slope in the lower right quadrant, and an area of higher elevation in the center. Birches are found in this panel predominantly where the available ground-level light in (c) is greater than 50% of what birches require for regeneration.

50:50, 45:55, 40:60, respectively. These ratios are estimated averages for the duration of the growing season at each location, based on data from 1993, which is the most recent year for which data for all three locations is available.

## 2.1.4 Available Light

Shading by terrain is accounted for in the GIS-generated plot-level radiation values based on the resampled digital elevation model. Shading by vegetation, on the other hand, depends on foliage density and is computed within a 50-m thick layer of the atmosphere above the ground level using the Beer-Lambert Law:

$$AL_h = AL_o \times e^{-k \times DLA} \quad (2.1)$$

where  $AL_h$  is the available light at a given height  $h$  above the ground,  $AL_o$  is the top-of-canopy normalized radiation factor that includes shading due to terrain and aspect,  $k$  is a constant that describes light extinction through the canopy, and  $DLA$  represents the cumulative foliage density above height  $h$ .  $DLA$  is synonymous with leaf area index (LAI). Species-specific values of  $k$  vary in the range of 0.37 to 0.47 between species (Breda, 2003), and even greater variability is observed based on stand density and tree age (Johansson, 1989). An average value of 0.4 is employed in the simulation. Plotting this equation for LAI values of 1-10 results in Figure 2.13. In broadleaf and light conifer forests, LAI values of 1-5 are common (Brooks *et al.*, 1997a,b; Kull and Tulva, 2000; Shibistova *et al.*, 2002a,b; Shulze *et al.*, 2002; Lindroth *et al.*, 2008; Kobayashi *et al.*, 2010), whereas coniferous forests can accumulate LAI of up to 10 (Chen *et al.*, 2005), and LAIs as high as 18 have been reported for some boreal regions (DeAngelis *et al.*, 1981);, but these high values may be an artifact of using 2-sided leaf area to calculate the LAI (Asner, *et al.*, 2003). In general, significantly more shading within and below the canopy is observed within dark conifer forests of Siberia than in broadleaf or mixed stands.

The direct light simulation traces a sun ray from each of the 7 compass directions along a diagonal based on the average sun elevation angle in that direction (no direct light from the north in extratropical northern hemisphere). The direct radiation along each trace is scaled by the contribution of light from each compass direct over the course of the growing season. In contrast, diffuse light is computed along 8 diagonal paths through the canopy and from directly overhead. Light extinction is computed along these ray traces.

The shadow of a typical canopy dominant tree from central Siberia (24m, Simard *et al.*, 2011) can extend up to 100m, depending on foliage density and sun elevation angle. A sensitivity analysis for the maximum distance of a tree's shading effect for direct and diffuse light in the boreal ecosystem revealed that the maximum effect (tree shadow) of a 20m tree on unvegetated flat terrain at  $56^\circ N$  is approximately 100m for direct radiation, however, this depends on the sun angle. This maximum distance was obtained using the lowest sun elevation angle ( $5^\circ$ ) averaged for the

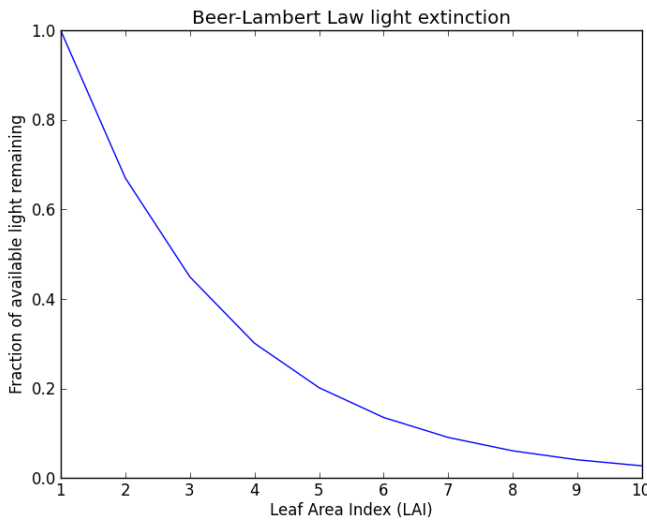


**Fig. 2.13:** At the top of the canopy, the fraction of available light is 1. Light extinction through the canopy follows an exponential function related to leaf area index (LAI). Broadleaf species generally do not establish in forests with LAI greater than 5, because not enough light filters through the canopy for them to maintain a positive carbon balance.

northeastern section during the growing season. The effect of trees on one plot with regards to diminishing the amount of diffuse light on adjacent and nearby plots extends up to 75m, which corresponds to approximately 7 plots in the simulation. Beyond that distance, the effects are considered negligible. Within a forest, light along a ray trace is likely to diminish due to the leaf area index (LAI) before reaching the distance of maximum shadow length. When the maximum possible tree height was taken into consideration (larch, 41m, *Shvidenko et al.*, 2006), the maximum distance for the shading effect could extend to 450m and 160m for direct and diffuse light, respectively, when computing the shading effect mathematically via the tangent of the sun elevation angle. The values are different, because the angles used to compute shading are different for direct and diffuse light components. The analysis in GIS, however, reveals that the effective shadow from the low sun elevation angle from the NE and NW is insignificant, i.e. less than 1% of direct radiation extinguished along this shadow path, and that the effective shadow length when the sun is in the east or west, at an average sun elevation angle of 19°, extends 130m for direct and diffuse light. Beyond that distance, 0.5% of the above-canopy radiation is occluded by the tree. This analysis helps to determine the smallest spatial domain that would not cause numerical instability upon wrap-around in the simulation. In the spatially-explicit version of ZELIG, the warp-around was shifted by one grid row, so that a tree does not shade itself (Figure 8.3 in *Shugart et al.*, 1988; Figure 2 in *Weishampel et al.*, 1996). In contrast, in SIBBORK, the shadow is kept in the same grid row upon wrap-around, but the size of the simulation domain is selected to exceed the longest possible shade to avoid having a tree shade itself.

## Light ray tracing for direct light computation

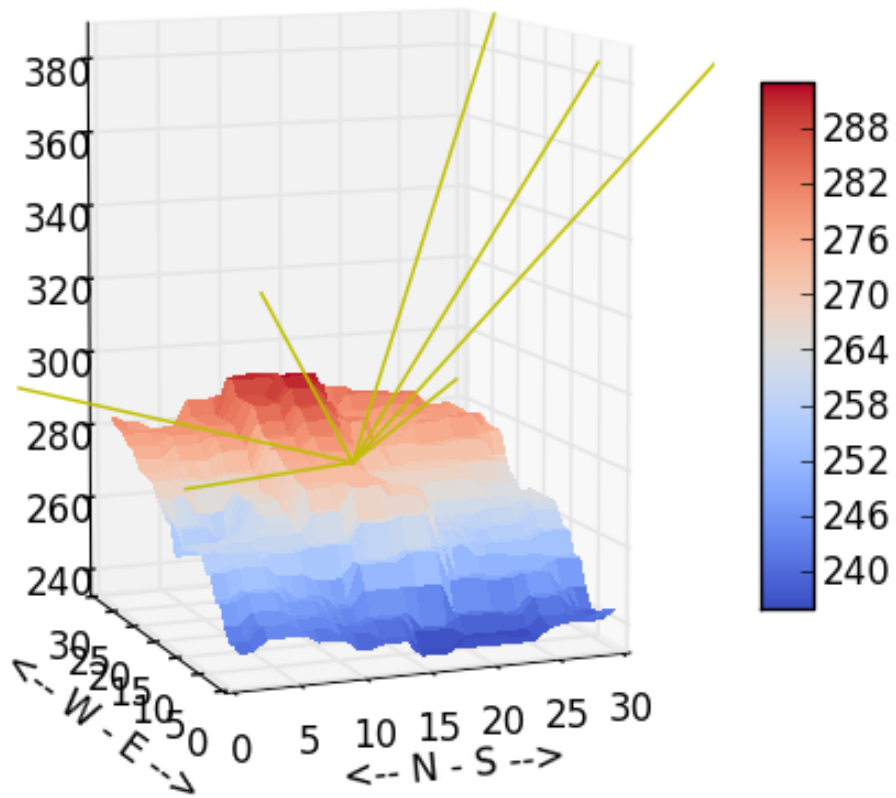


**Fig. 2.14:** Sun ray tracing for direct light computation from 7 of the 8 primary compass directions at 4 different angles, based on sun location during the growing season. The sun elevation angle is much greater to the SE, S and SW, than to the other directions. The lowest sun elevation angles are experienced from the NW and NE directions. There is no direct light from the N in Siberia. The colorbar symbolizes elevation (m) above sea level.

The annual computation of the light environment is spatially explicit, and has a spatial resolution of 10m x 10m x 1m (plot size x 1m vertical step). This is also the most computationally-expensive subroutine of this single-thread simulation, and has been accelerated using the Numba library (<http://www.numba.pydata.org>). The computational demand for the 3-D light subroutine increases exponentially with increasing spatial domain. Furthermore, the light ray tracing in complex terrain requires special parameterization. Originally, the light environment was computed within a volume above the complex terrain that was capped at 50m above the highest point on the terrain. In order to not increase the volume through which the light rays are traced above a complex terrain, the light is now computed only within a 50m thick column of the atmosphere above each plot, which may have a different elevation than adjacent or nearby plots. The trees can still shade each other on nearby plots, however, the light ray is capped at 50m above each elevation level. This simplification significantly decreases the computational demands of the light subroutine above simulated hilly or mountainous terrain.

## 2.1.5 Evapotranspiration

In ZELIG, potential evapotranspiration (PET) was computed via the Thornthwaite-Mather equation (*Thornthwaite and Mather, 1957*) using average monthly temperatures and correction coefficients for each month and latitude. This equation does not consider the available water (land surface limitations on evaporation), and is therefore intended for the calculation of PET only. It is known to underestimate PET by 20-30% (*Fisher et al., 2011*). Furthermore, the Thornthwaite-Mather equation has not been validated for PET calculations at high latitudes above 50° N (*Botkin, 1993*), and correction factors are not available for those regions. Fischer *et al.* (2011) recommends a radiation-based or a combination approach for estimating PET in boreal regions. For SIBBORK, a modified Penman equation (*Campbell, 1977*) was selected:

$$PET = \frac{a \times (Temperature + b) \times (Radiation)}{\lambda \times 1000} \quad (2.2)$$

where  $a$  and  $b$  are coefficients, with common values of  $0.025^{\circ}C^{-1}$  and  $3^{\circ} C$ , respectively, and  $\lambda$  is the latent heat of vaporization ( $2430 \text{ Jg}^{-1}$ ). Air *Temperature* and *Radiation* in this calculation are plot-wide parameters that change with each month of the year, and are in units of degrees Celsius and  $Jm^{-2}$  (converted from  $W\text{Hm}^{-2}$ ), respectively. The 1000 factor in the denominator converts PET to cm/month.

Due to the variation in air temperature and radiation input across complex terrain, evaporative demands (PET) are heterogeneous across the landscape. Figure 2.15a compares the annual PET computed via the modified Penman equation utilized in SIBBORK for southern taiga, middle taiga, and treeline locations (average of 10 years) to an overview map of PET for Russia (*Kolosova, 1982*).

The water budget for a single-layer soil was computed in ZELIG via

$$\text{runoff} = \text{SoilMoisture} + \text{Precipitation} - \text{PET} \quad (2.3)$$

where the *Soil Moisture* parameter refers to the previous month's soil moisture in a single-layer soil, which can be at field capacity, between field capacity and wilting point, or at wilting point. At the start of the simulation, the soil moisture is equal to field capacity. Any soil moisture at the end of this computation in excess of field capacity is considered runoff (overland flow and gravitational water). In certain regions of central Siberia, PET exceeds precipitation during the growing season. Equation (2.3) overestimates soil dryness, especially in regions underlain by permafrost. To estimate the soil moisture more realistically in SIBBORK, the water balance is computed as follows:

$$\text{runoff} = \text{SoilMoisture} + \text{Precipitation} - \text{AET} \quad (2.4)$$

where, *AET* is estimated as a fraction of PET (from equation (2.2)). This fraction, called evapotranspiration coefficient, is estimated at 60-70% in central Siberia (*Olchev and Novenko*, 2011) and 30-50% in the driest region of central Siberia near Yakutsk (*Ohta et al.*, 2008; *Matsumoto et al.*, 2008; *Maximov et al.*, 2008). The actual evapotranspiration depends on the structure and composition of the forest canopy (*Nakai et al.*, 2008), which changes over the course of succession or with altered environmental conditions, but the inclusion of a computation of AET with input from canopy parameters and the estimation of foliage growth based on AET would introduce a circular dependency and increase computational demand. Additionally, there is high interseasonal and interannual variability in the evapotranspiration coefficient (*Matsumoto et al.*, 2008). With the focus on the growing season and the central Siberian region along the Yenisei River meridian, the evapotranspiration coefficient of 0.7 appeared to adequately estimate the  $\frac{\text{AET}}{\text{PET}}$  ratio. Figure 2.15b demonstrates the fit between the AET computed by SIBBORK (10-year average) and Global Evapotranspiration dataset (*Zhang et al.*, 2010; [www.ntsg.umt.edu/project/et](http://www.ntsg.umt.edu/project/et), spatial resolution 4x8km at  $58^{\circ}\text{N}$  latitude). Furthermore, the observed moisture coefficient (ratio of precipitation to PET), which varies in the range of 1-2 along the Yenisei River meridian and dips below 1 in southern Siberia, is appropriately simulated by SIBBORK (Figure 2.15c). It is interesting to note that some of the greatest uncertainty in the estimation of PET and AET using modeling and remote sensing approaches is for boreal regions of Siberia and North America (*Zhang et al.*, 2010).

## 2.1.6 Growing Degrees

There is an optimal temperature range for tree processes, above and below which the rates of photosynthesis, respiration, and related processes are reduced (*Waring and Schlesinger*, 1985). Although the effectiveness of the photosyn-

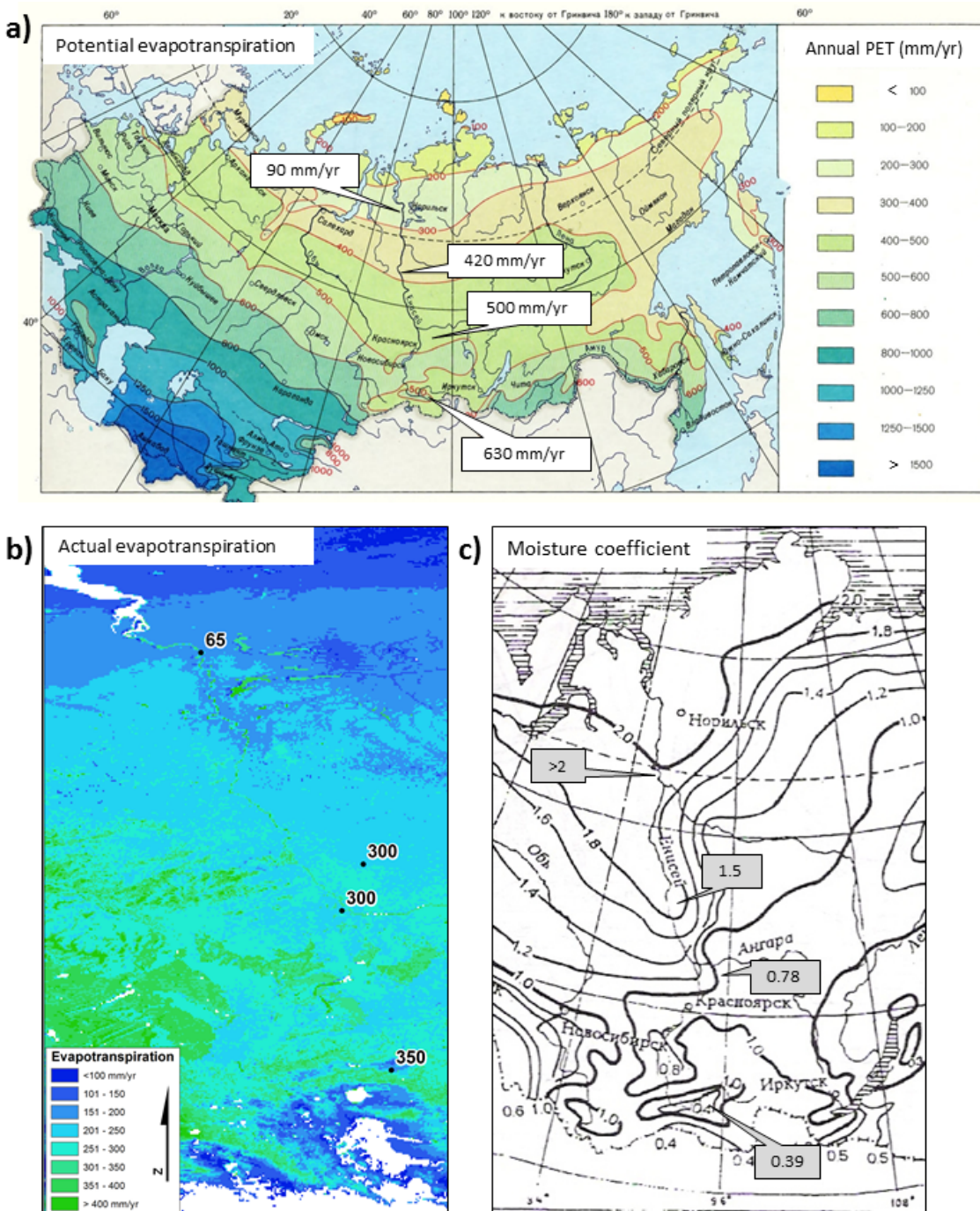


**Fig. 2.15:** Water budget variables for central Siberia. (a) Potential evapotranspiration is conveyed via the Kolosova (1982) map, with northern treeline, middle taiga, southern taiga, and southern treeline PET quantities (mm/yr) computed for the WMO weather stations of Dudinka, Severo-Enisejske, Enisejsk, and Kyzyl, respectively, and shown via insets oriented north-to-south on map. Note that the PET computed for Kyzyl is on the order of 600mm/yr. Kyzyl is located in an arid basin, surrounded by steppe vegetation. Forested hillsides in the vicinity experience a lower PET (230-500mm/yr), depending on aspect and elevation. (b) Actual evapotranspiration from the Global Evapotranspiration dataset (Zhang *et al.*, 2010) is shown in the background. The AET computed in SIBBORK for the same 4 locations as in (a) are shown via numerical labels (mm/yr). (c) The annual moisture coefficient from a map by Isachenko (1985, background) is compared to the same quantity computed in SIBBORK (grey insets). This ratio is unitless.

thetic process has a temperature dependency (Atkin *et al.*, 2007), temperatures extreme (high) enough to damage the photosynthetic apparatus do not occur in the Siberian boreal forest (Larcher, 1995). However, there is a lower limit on the temperatures necessary for photosynthesis. For conifers, this limit is closer to  $0^{\circ}\text{C}$ , whereas broadleaf trees initiate photosynthesis at temperatures above about  $5^{\circ}\text{C}$  (Shugart *et al.*, 1992; Chapman *et al.*, 2006). For the purpose of simplification in the model, it is assumed that all trees become photosynthetically active when the air temperature is above  $5^{\circ}\text{C}$ . For ease of convention, the annual accumulated heat load in the simulation is expressed in growing degree days above the base temperature of  $5^{\circ}\text{C}$  (Shugart *et al.*, 1992; Chapman *et al.*, 2006; Shuman, 2010). Whenever a daily air temperature exceeds this base temperature, growing degrees are accumulated. A day with an average daytime air temperature of  $14^{\circ}\text{C}$  would accumulate 9 growing degrees ( $GDD_5$ ) above the base temperature. In the model, daily temperatures are simulated and growing degrees are summed up. Some arboreal species, such as birch, function best in warmer climates and have a low tolerance for frost or cold weather ( $GDD_5$  minimum =  $410^{\circ}\text{C}$ ). Others, such as larch, can grow in very cold locations, and have a low growing degrees requirement ( $GDD_5$  minimum =  $300^{\circ}\text{C}$ ). Growing degrees are accumulated over the course of the year, and can be used to track the amount of heat available for vegetation processes, especially as climate changes.

In previous versions of ZELIG, each of the arboreal species had a minimum requirement of  $GDD_5$ , and a maximum heat tolerance (maximum  $GDD_5$ ), from which a parabolic curve for optimal growing degree days was derived (Pastor and Post, 1986). However, Bugmann and Solomon (2000) suggest that a nonlinear response may be the more appropriate parameterization of vegetation response to the accumulated annual  $GDD_5$ . Based on empirical evidence, SIBBORK was reparameterized such that trees will not experience stress from accumulated heat over the growing season, if soil moisture is not limiting (McDowell *et al.*, 2011; Bauweraerts *et al.*, 2014; Wertin *et al.*, 2012). However, too little warmth will be limiting to species with a certain growing degree requirement, and the minimum warmth requirement is specified for each species in SIBBORK, as it was in ZELIG.

The parabolic and the nonlinear vegetation response parameterizations to the  $GDD_5$  are shown in Figure 2.16. Historical annual average  $GDD_5$ , represented by a dashed line in Figure 2.16, summarizes the temperature conditions over the second half of the 20<sup>th</sup> century at a WMO weather station in central Siberia. The dashed line labeled “+  $2^{\circ}\text{C}$ ” denotes what the average  $GDD_5$  sum may be with a 2-degree increase in the annual average temperature. Note that with the parabolic parameterization of heat tolerance, larch (*Larix sibirica*) experiences significantly reduced growth - less than 20% of optimal. In the nonlinear parameterization, none of the three species are affected by heat alone, and growth is not decreased due to an increase in growing degrees, provided soil moisture is not limiting.

Growing degrees can be used to describe a characteristic of the environmental conditions, and the total annual heat load can be the most limiting factor to tree growth at certain locations in some years. Larch has the lowest minimum

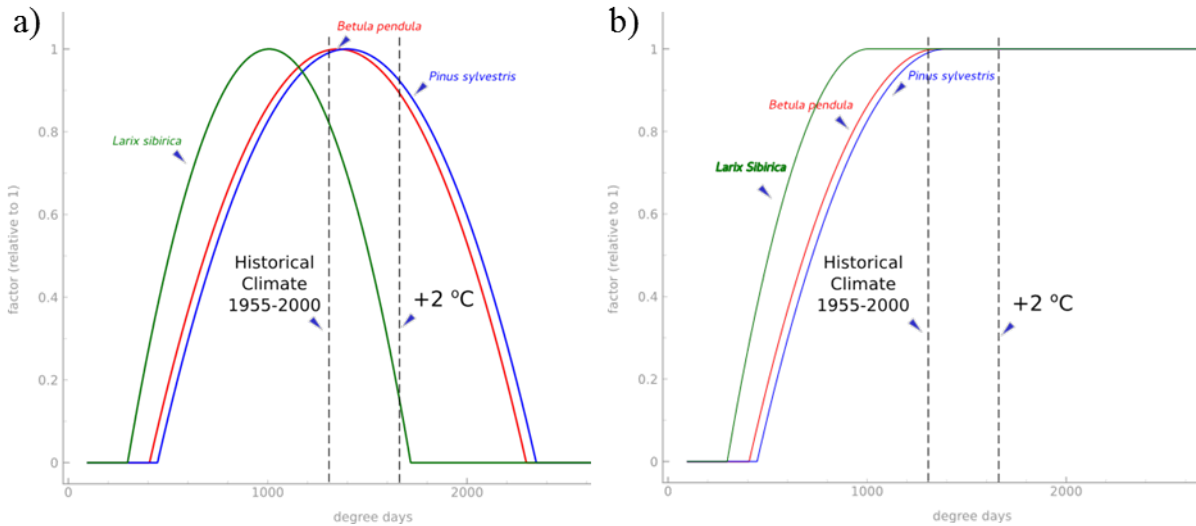


**Fig. 2.16:** Species response to annual accumulated heat load ( $GDD_5$ ) as was parameterized in ZELIG (a) and using the new, non-linear parameterization in SIBBORK (b).

$GDD_5$  requirement of boreal tree species ( $300^{\circ}C$ ). This limit corresponds to the forest-tundra boundary conditions (Tchekakova and Parfenova, 2006).

### 2.1.7 Soil Moisture

The water budget for the simulation is computed for a single-layer soil as follows:

$$SoilMoisture = SoilMoisture_{prev} + Precipitation - AET - runoff \quad (2.5)$$

where *Soil Moisture* represents the soil moisture available to plants, *SoilMoisture<sub>prev</sub>* refers to the total available water remaining in the soil from the previous month, and AET is computed as a fraction of PET.

The model is initialized with soil moisture at field capacity, which is a characteristic of soil type. When soil moisture exceeds field capacity, the excess water is considered as runoff and is removed from the simulation. When soil moisture decreases below zero, the trees reach the wilting point and photosynthesis is inhibited. Field capacity and wilting point are computed as a function of soil type and total available water from a soils database (Stolbovoi and McCullum, 2002). For the purposes of simplification and convention, a single wilting point is specified for all species in the simulation. When no soil type information is available, a wilting point of 15 bar is used. Figure 2.17 shows the process flow for the soil moisture computation in SIBBORK.

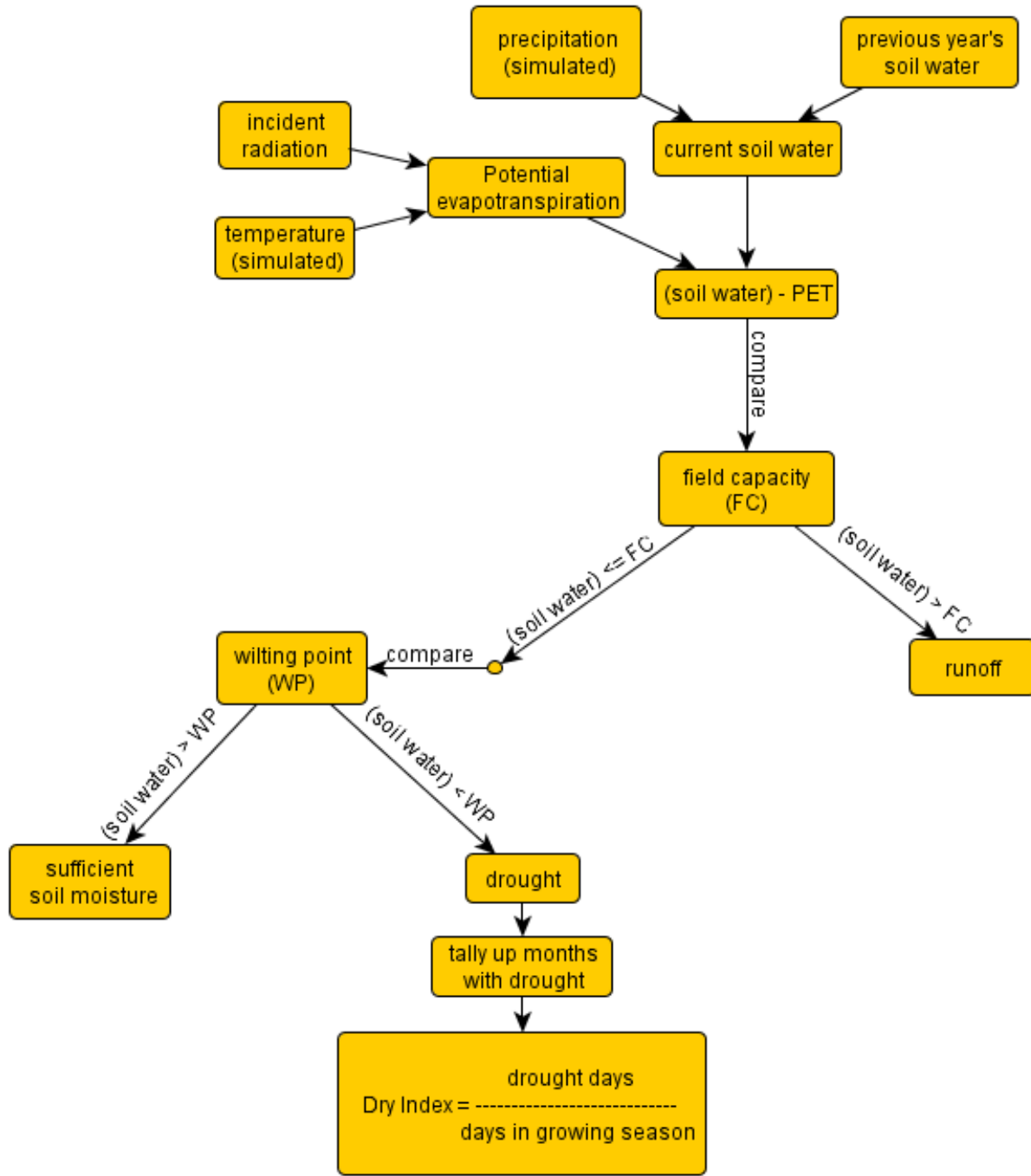


**Fig. 2.17:** The soil moisture in SIBBORK is assessed as a dryness index, which is computed as a fraction of the growing season with soil water content below wilting point.

## 2.1.8 Soil Fertility

Soil fertility exerts a limit on the maximum amount of biomass that can be accumulated on a hectare of land per year at a specified location. It is a cap on the annual productivity at a simulated site. This may be similar to a limit on gross primary productivity (GPP). In SIBBORK, there is no limit to total standing biomass, just to the rate at which it can be accumulated on an annual basis. When the vegetation on a simulated plot approaches this maximum rate of biomass accretion, trees experience suppressed growth scaled by species-specific tolerances to low soil nutrition.

Russian forestry utilizes a site index parameter to describe how different species may perform at a given site (I=good, V=poor). A species that requires a high amount of soil nutrition, e.g. fir, may grow poorly on the same soil on which a species with low nutrition requirements, e.g. pine, may grow well and reach a larger diameter at a younger age. In this case, site index V may be used to describe this location for fir, whereas for pine, the site index may be closer to I or II. In this manner, site index is a species-specific characteristic, but this is very difficult to parameterize for mixed species stands.

SITE INDEX					
Species	I	II	III	IV	V
<i>Abies sibirica</i> ‡	32 – 36.8 cm	27 – 31.8 cm	22.2 – 26.9 cm	17.2 – 22 cm	12.3 – 17.1 cm
<i>Larix sibirica</i> ‡	27.4 – 36.7 cm	20.2 – 27.2 cm	15 – 20.1 cm	11.1 – 14.9 cm	8.2 – 11 cm
<i>Betula spp.</i> *	15.5 – 18 cm	12.8 – 15.4 cm	12 – 14.7 cm	7.7 – 10.1 cm	7.8 – 11.1 cm
<i>Picea obovata</i> ‡	26.4 – 31 cm	23.4 – 26.3 cm	21.3 – 23.3 cm	19.6 – 21.2 cm	17.5 – 23.1 cm
<i>Pinus sibirica</i>	57.3 – 81.6 cm	39.6 – 56.8 cm	27.6 – 39.2 cm	19.2 – 27.3 cm	13.4 – 19 cm
<i>Pinus sylvestris</i> ‡	31.7 – 39.3 cm	24.6 – 31.5 cm	18.5 – 24.4 cm	13.1 – 18.3 cm	13.4 – 18.2 cm
<i>Populus spp.</i> *	19 – 22.5 cm	15.4 – 18.9 cm	11.7 – 15.3 cm	11.6 – 8.1 cm	8 – 4.5 cm

**Fig. 2.18:** Site index is estimated for monospecies stands based on average tree height at stand ages of 50 and 100 years. Here, the diameter-height relationship was used to convert the heights to diameters at breast height (DBH), so as to compute the site index - biovolume (function of DBH) relationship for the soil fertility parameterization.

For the purposes of simplification and generalizability, soil fertility in SIBBORK is derived from the forestry yield table parameter of Net Growth specified in tons per hectare (biomass) or cubic meters per hectare (biovolume) accumulated per year for monospecies stands of different site indices. Central Siberia is dominated by site index III and IV soils, whereas southern regions of central and western Siberia are dominated by site index II soils for the species that grow there (*Korpachev et al.*, 2010). However, site index III soils with larch may have greater annual productivity than site index III soils with fir. For simulations of monospecies stands, the soil fertility GPP limitation is taken directly from the forestry yield tables (*Shvidenko et al.*, 2006). For simulation of mixed species stands, the site index of the most productive species is used to determine the cap on GPP. For example, in middle taiga, cap levels of 6, 4 and 2

tons  $ha^{-1} yr^{-1}$ , which correspond to biovolume caps of 6, 5, and 4  $m^3 ha^{-1} yr^{-1}$ , are used for soils with site indices II, III, and IV, respectively.

## 2.2 Vegetation Processes

### 2.2.1 Sapling Establishment

Regeneration is a stochastic process affected by the seed rate specified in the driver file for each species in the simulation. Saplings establish up to a maximum per-plot stem density specified in the driver file. ZELIG utilizes a 1 stem/ $m^2$  maximum stem density, whereas SIBBORK allows the user to specify the stem density, which can exceed 1 stem/ $m^2$  in order to better represent dense pine forests observed in Siberia. The minimum stem density in SIBBORK is 1 stem/plot, which facilitates the simulation of open canopy forests encountered in northern taiga. When a sapling is established, it is not assigned an explicit x,y position within a plot. Instead, the uncertainty of its location on the simulated landscape is localized to within a specified plot. Saplings are planted with a DBH of  $2.5 \pm 0.25 cm$ . This size may be representative of a 40-year old larch in severely limiting environmental conditions, or a 5-year old birch under favorable conditions for the species. This discrepancy creates difficulty in comparing simulated stands with a specific age structure to observed stands, however, usually, the comparison is good to within a decade (i.e. 40-year old trees in the simulation compare well to 50-year old trees in the field). Saplings are established at the end of the simulation year, after mortality and growth have been accounted for. Sapling establishment is affected by the environmental factors of ground-level light, growing degrees, and soil moisture.

Some species, notably aspen, birch and spruce, reproduce by stump sprouting. This type of regeneration is currently not included in SIBBORK, although frameworks for this exist in FAREAST (*Yan and Shugart*, 2005) and later versions of ZELIG (*Larocque et al.*, 2006). Inclusion of stump sprouting in the model would likely increase the contribution of aspen and birch to stand composition, especially after disturbances, such as wildfire.

### 2.2.2 Tree Growth

Annual tree growth is a function of the species type, tree size, and the effects of environmental conditions. An optimal diameter growth increment (OGI) is computed for each tree based on its current size and species type. Estimation of OGI has been modified following methodology described by Bragg (2001, 2003) to account for growth of older, larger trees. Previous parameterization of OGI halted growth at an estimated maximum diameter. However, species-specific maximum diameters are difficult to estimate. The new parameterization utilizes maximum observed growth to

determine the actual relative diameter increment (ARI). The potential relative diameter increment (PRI) is computed by fitting a curve with the following form to a subset of the largest observed ARIs for a species:

$$PRI = a \times DBH^b \times c^{DBH} \quad (2.6)$$

The PRI represents optimal diameter increment for a species relative to its current size (DBH). Empirically-derived coefficients  $a$ ,  $b$ , and  $c$  are species-specific. OGI is computed via:

$$OGI = PRI \times DBH \quad (2.7)$$

annually for each tree in the simulation. This maximum gain in diameter represents the growth a tree would experience at a given size if it had access to unlimited resources. The OGI is scaled down by environmental constraints representative of the conditions in each year of the simulation and the species-specific tolerances to such resource limitations. The new parameterization for the optimal diameter increment does not constrict tree growth at an arbitrarily assigned maximum diameter, but does significantly reduce vigor for older trees.

Figure 2.19 demonstrates how the optimal growth diameter increment (OGI) is computed in SIBBORK for different species in the simulation. Based on forestry yield table regional averages of DBH at decadal time increments, pine has a larger PRI than birch (a), which means that each year a pine tree has the potential to grow more, relative to its current diameter, than a birch. The peak OGI (b) for birch is larger than pine, but pine continues to grow vigorously, while birch growth drastically decreases as it approaches a DBH of 40cm. According to this approach, a pine tree with a 40cm DBH could be expected to add a larger tree ring each year than a 40cm birch in non-limiting environmental conditions.

Forestry yield tables (*Shvidekno et al.*, 2006) represent regional averages. Using the Usolsky forestry inventory (*Ershov and Isaev*, 2006), a potential relative increment was computed for pine (c). Note that the PRI is larger for pine in Usolsky than in the yield tables. It is possible that the smaller spatial scale of the Usolsky forest inventory reflects pine growth in microclimates particularly suited for this species. The difference between ZELIG and SIBBORK parameterizations of OGI using Scots pine (*Pinus sylvestris*) as an example is shown in (d). The blue triangles represent the forestry yield table data. Values for older trees are often extrapolated from young tree measurements rather than measured directly. The black line is the ZELIG fit with a user-assigned maximum diameter of 56 cm. This curve fits the yield table data quite well. However, Scots pines diameters in the >1m range have been reported (*Shugart et al.*, 1992a). The blue line is fitted to the yield table data using the curve defined by equation (2.7). The fit is appropriate, and older trees are able to continue growing past 56cm in diameter. Setting the maximum diameter to 100 cm and using the ZELIG parameterization for OGI results in the black dashed line. The Usolsky forest inventory contains averages

for smaller areas, although the values in the inventory still represent averages and do not capture maximum growth of individual trees. The green squares represent a subset of the Usolsky inventory for areas where pine exhibited the most annual growth. The green line is the curve fitted to the Usolsky subset using Bragg methodology and equation (2.7). Although the ZELIG and the Bragg estimates based on Usolsky inventory data capture the rapid early increases in growth and the maximum diameter increment experienced by a pine tree without any environmental limitations, the growth experienced by older trees is represented quite differently by the two parameterizations. Expanding the parameterization for growth of older trees is particularly important for simulation of Siberian boreal forests, where more than half of the assessed stands were considered in the mature or over-mature stages in the 1990s (*Krankina et al.*, 1996).

Understanding that yield tables and Usolsky inventory data represent averages, and individual faster-growing trees may be found in the region, the OGI curve was modified to include a 15% increase over the Usolsky-based maximum OGI estimates, which is represented by the red line in Figure 2.19d. The OGI for each species in the simulation is presented in Figure 2.19e, with aspen (*Populus spp.*) showing the largest maximum diameter increment, but all conifers maintaining the potential even as they grow beyond 40cm DBH. Aspen and birch photosynthesis rates have been shown to be more than twice the rate of gas exchange in pine and spruce (*Smith and Hinckley*, 1995; *Brooks et al.*, 1997), which supports the relatively fast growth rates of these tree species shown in Figure 2.19e.

### 2.2.3 Tree Mortality

Mortality is a stochastic process modeled using a uniform random number generator along with species-specific silvicultural information specified in the driver file. Tree mortality can be from two sources: natural or stress-based. Natural mortality, also known as age-based mortality, is based on the principle that only 1% of individuals within a species survive to the maximum age, and therefore maximum size (max DBH, max height). Stress-related mortality is dependent on environmental conditions and species-specific tolerances to resource limitations. Natural and stress-induced mortality subroutines were retained from ZELIG, however, a new mortality trigger has been added coupled with disturbance triggers. This type of mortality allows the user to specify the species and the sizes of trees that will be removed from the simulation following a disturbance event.

#### Age-related Mortality

Age-related mortality is based on the principle that only 1% of individuals within a species will survive to the maximum age for that species, and follows the general trend described in the equation (2.8) and Figure 2.20 (*Shugart*, 1984). The important thing to note here, is that the 1% may be an appropriate estimate for forests without disturbances, however, inclusion of disturbances, such as wildfire or insect outbreaks, will significantly reduce the number

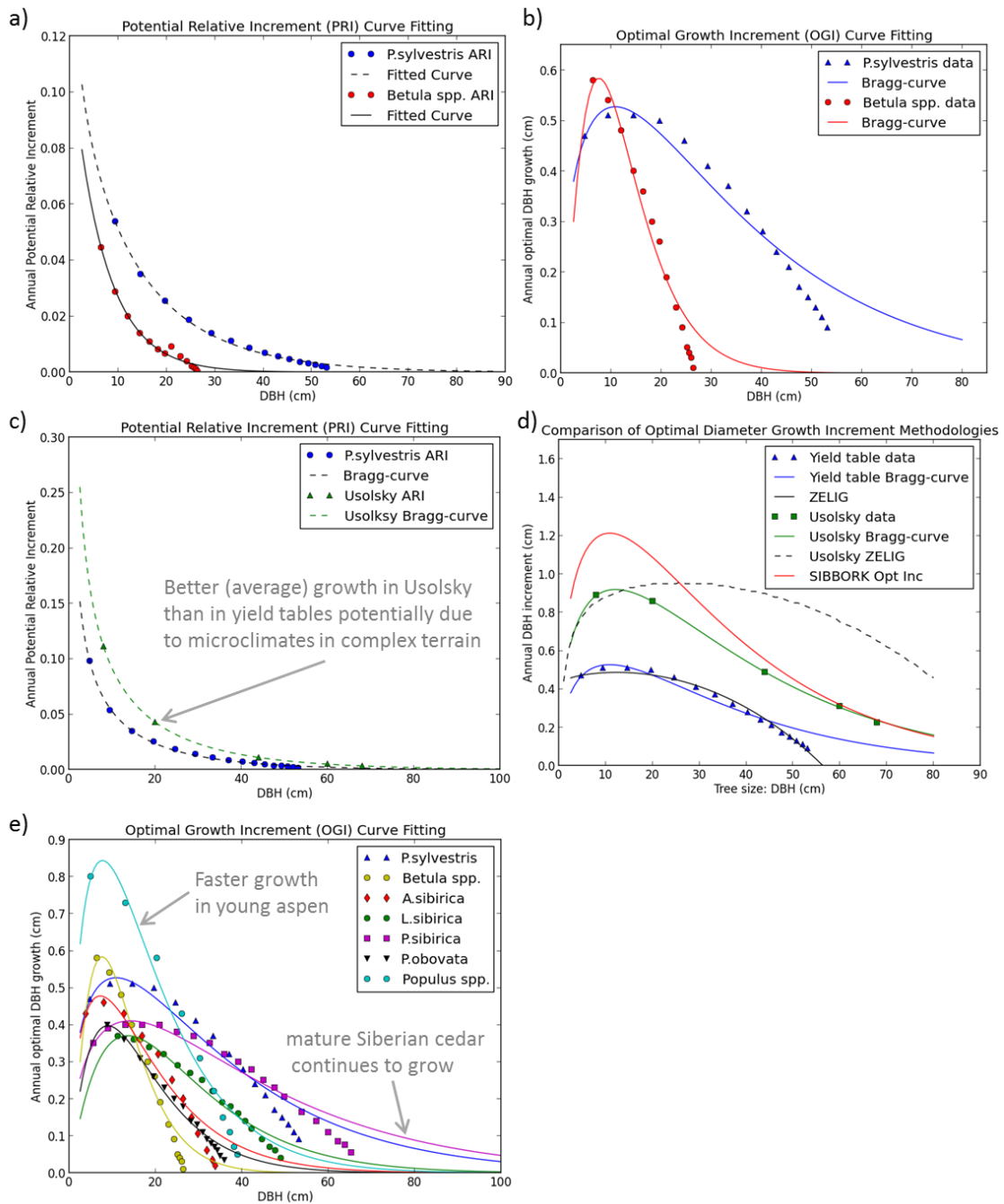


**Fig. 2.19:** Determining the optimal diameter increment based on species type and tree size. (a) Annual potential relative increment for pine and birch and (b) optimal diameter increment for pine and birch, based on forestry yield tables. (c) Forestry inventories representing a smaller spatial extent may capture greater annual tree growth than the regional averages in yield tables. (d) Comparison of ZELIG and SIBBORK methodologies for determining the annual optimal diameter increment based on species and tree size. (e) Optimal diameter increment for seven boreal species in SIBBORK.

of individual trees that survive to the species-specific maximum age (*Mielke et al.*, 1978).

$$\text{Probability} = 1 - e^{\frac{-4.605}{\text{AGE} \times \text{MAX}}}$$
 (2.8)

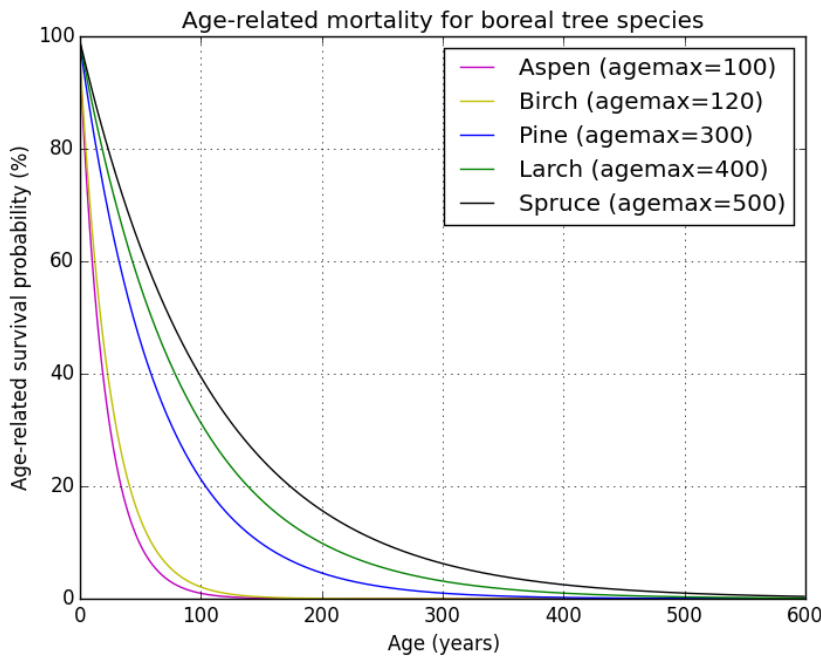


**Fig. 2.20:** The age-related mortality differs for the boreal trees, based on the estimated maximum age for the species. At each age, a tree has the specified probability of surviving to the next year, such that, for example, a 100-year old pine has a 20% chance of surviving to the next simulation year.

### Stress-based Mortality

Stress-based mortality is a result of species-specific tolerances to resource limitations. When resources, such as light, soil moisture and soil nutrition, are limited, the tree will not grow at the optimal rate for its size and species type. The annual optimal diameter increment (ODI) is decreased based on the limitations from environmental conditions. In ZELIG, when the actual diameter increment (growth) acquired by an individual in a given year is <10% of the optimal diameter for a tree of its size and species type, a stress flag is activated for that individual. In SIBBORK, species-specific thresholds for percent of ODI needed to induce stress are employed to decrease stress mortality of hardy species that are able to survive multiple consecutive slow growth years (*Keane et al.*, 2001). These thresholds were estimated from forestry yield tables for each species (*Shvidenko et al.*, 2006). Similar to ZELIG, after two consecutive years with a stress flag, the individual in SIBBORK has a 37% chance of dying in each of the subsequent years until the tree dies or until the stress flag is removed. The stress flag is removed when the tree achieves at least 10% of its

<b>species</b>	<b>stress-flag threshold (%ODI)</b>
<i>Abies sibirica</i>	6%
<i>Larix sibirica</i>	5%
<i>Betula pendula</i>	10%
<i>Picea obovata</i>	8%
<i>Pinus sibirica</i>	8%
<i>Pinus sylvestris</i>	10%
<i>Populus tremula</i>	10%

**Fig. 2.21:** The species-specific stress-flag thresholds were estimated based on the optimal diameter increment calculations (see Tree Growth section for detail) and the forestry yield table values for decadal diameter increments for mature (>75% of agemax) monospecies stands.

optimal diameter increment within a simulation year. Throughout a tree's lifetime, it may be stressed and released several times, based on environmental conditions and its species-specific tolerances to resource limitations.

SIBBORK is tailored toward the simulation of boreal ecosystems, although the framework is flexible enough to easily re-parameterize it to the simulation of any type of forest ecosystem for which appropriate forestry data are available. Boreal forests are dominated by hardy trees, which can survive in very limiting conditions for decades. Based on forestry yield tables (Shvidenko *et al.*, 2006), mature fir, spruce, Siberian cedar and especially larch can survive for decades while incrementing the DBH by less than 0.1mm per year (on average). To reflect this resilience, the threshold for stress flag assignment, which was 10% for all species in ZELIG, was restructured as a species-specific parameter, which allows Siberian larches to increase the DBH by as little as 5% of their annual ODI without being flagged for stress-based mortality. Species-specific stress-flag thresholds are listed in Figure 2.21.

## 2.3 Allometry

Species-specific allometric equations in SIBBORK represent fitted relationships for height, biovolume, above-ground biomass, above- and below-ground biomass, foliage biomass, and leaf area as functions of DBH. These relationships were derived from the regional yield tables for the southern and middle taiga regions of central Siberia listed in Figure 2.22 (Shvidenko *et al.*, 2006). Figure 2.23 conveys species-specific allometric equations employed in SIBBORK. The DBH and base of the canopy are two structure-related state variables tracked by SIBBORK from year to year (Figure 2.1). Other tree dimensions are computed as a function of DBH in post-processing. Some relationships are conveyed as piece-wise functions to preserve realism in tree structure. The equation form for the same variable, i.e. height, may differ from species to species, which presents a significant difference from species-specific parameterizations in ZELIG. This approach provides greater flexibility in using the equation(s) of best fit to describe the allometric relationships for each species.

Species	Regional forestry yield tables used for deriving allometry
<i>Abies sibirica</i>	Fir stands of mountain ecoregions of the Central Siberian Plateau
<i>Larix sibirica</i>	Larch stands of maximal productivity in Middle Siberia (ecoregions of middle and south taiga); Larch forests of Yenisei Krjazh and south of Krasnoyarskii krai (ecoregions of mountain taiga forests and subtaiga); Larch forests of Angara River basin (ecoregions of middle and south taiga)
<i>Betula spp</i>	Birch stands in south and middle taiga ecoregions of Siberia
<i>Pinus sibirica</i>	Fully-stocked mixed cedar forests of the Central Siberian Plateau; Mixed cedar stands of Central Siberian Plateau
<i>Pinus sylvestris</i>	Fully-stocked pine stands in middle taiga, south taiga, sub-taiga and forest steppe ecoregions of Central and East Siberia
<i>Picea obovata</i>	Fully-stocked spruce forests of Middle Siberia (ecoregions of southern and middle taiga)
<i>Populus spp.</i>	Fully-stocked aspen stands of Central and East Siberia (ecoregions of middle and southern taiga); Aspen stands in south taiga ecoregions of Central Siberia

**Fig. 2.22:** Regional forestry yield tables used for deriving allometric relationships for different species in SIBBORK.

### 2.3.1 Height

The height equations in SIBBORK represent curves of best fit derived from yield table data for each species. The form of the equation differs between species. To make sure this is the best approach, height equations from ZELIG, a Monte Carlo gap model FAREAST (*Yan and Shugart, 2005*) and yield tables were compared for all seven species in SIBBORK. The comparison revealed that the previous ZELIG parameterization, which computes tree height via a second-order polynomial with species-specific coefficients based on estimated maximum diameter and height that a tree of a given species can attain, did not always match the form of the height-diameter relationship presented in the yield table data. When a second-order polynomial equation is used to compute height as a function of DBH, height begins to decrease for large trees. This is not the case in nature. SIBBORK predominantly utilizes piece-wise functions to estimate tree height as a function of DBH to reflect fast vertical growth in young stems, and slower growth rate for mature trees. [Figure 2.24](#) presents the comparison between three different parameterizations for height from two different gap models and the forestry yield tables. SIBBORK uses the yield table parameterization, which involves piece-wise functions for all but one species.

Species	Height (m)	Biovolume (above-ground) (m <sup>3</sup> /tree)	Biomass (above- & below-ground) (t/tree)	Foliage Biomass (t/tree)	Forestry yield table applicability
<i>Abies sibirica</i>	-0.0049dbh <sup>3</sup> +0.9546dbh+1.37 (R <sup>2</sup> = 0.9993)	0.0001 dbh <sup>2.5371</sup> (R <sup>2</sup> = 0.9993)	0.00002dbh <sup>3</sup> -0.0003dbh <sup>2</sup> +0.0039dbh (R <sup>2</sup> = 0.9975)	for dbh < 33cm: 0.015 dbh <sup>2.1934</sup> for dbh > 33cm: 53.975log(dbh) - 156.59 (R <sup>2</sup> = 0.9993)	south & middle taiga
<i>Larix sibirica</i>	-0.0152dbh <sup>3</sup> +1.3806dbh+1.37 for dbh > 36cm: 6.0278log(dbh)+9.6025 (R <sup>2</sup> = 0.9675)	for dbh < 20cm: 0.0004 dbh <sup>2.3061</sup> for dbh > 20cm: 0.0013dbh <sup>2</sup> -0.0074dbh (R <sup>2</sup> = 0.9996)	0.0002 dbh <sup>2.5568</sup> (R <sup>2</sup> = 0.9999)	for dbh < 34cm: 0.0218 dbh <sup>2.0014</sup> for dbh > 34cm: 69.793log(dbh) - 220.71 (R <sup>2</sup> = 0.9789)	south & middle taiga
<i>Betula pendula</i> <i>Betula platyphylla</i> <i>Betula pubescens</i>	for dbh < 26.5cm: 1.0389dbh+1.37 for dbh > 26.5cm: 1.3444log(dbh)+24.501 (R <sup>2</sup> = 0.8455)	for dbh < 26.5cm: 0.0002 dbh <sup>2.5213</sup> (R <sup>2</sup> = 0.9997)	0.0002 dbh <sup>2.3793</sup> (R <sup>2</sup> = 0.9998)	for dbh < 22.4cm: 0.0492 dbh <sup>1.5835</sup> for dbh > 22.4cm: 6.5771log(dbh) - 13.672 (R <sup>2</sup> = 0.9387)	south & middle taiga
<i>Picea obovata</i>	0.0401dbh <sup>2</sup> -0.0516dbh+1.37 for dbh > 25cm: 21.928log(dbh) - 45.405 (R <sup>2</sup> = 0.974)	for dbh < 25cm: 0.00006 dbh <sup>2.8291</sup> (R <sup>2</sup> = 0.9973)	0.00006 dbh <sup>2.6887</sup> (R <sup>2</sup> = 0.9992)	for dbh < 27.3cm: 0.0497 dbh <sup>1.844</sup> for dbh > 27.3cm: 13.789log(dbh) - 23.48 (R <sup>2</sup> = 0.8652)	south & middle taiga
<i>Pinus sibirica</i>	for dbh < 38.5cm: -0.0073dbh <sup>2</sup> +0.913dbh+1.37 for dbh > 38.5cm: 0.3544log(dbh)-8.4582 (R <sup>2</sup> = 0.9731)	for dbh < 43cm: 0.0001 dbh <sup>2.514</sup> (R <sup>2</sup> = 0.9986)	0.00008 dbh <sup>2.5587</sup> for dbh > 43cm: 2.8067log(dbh)-9.4117 (R <sup>2</sup> = 0.9995)	for dbh < 33.6cm: 0.0075dbh <sup>2</sup> +0.2328dbh-0.2592 for dbh > 33.6cm: 19.537log(dbh) - 52.641 (R <sup>2</sup> = 0.9976)	Central Siberian Plateau
<i>Pinus sylvestris</i>	for dbh < 32cm: -0.0105dbh <sup>3</sup> +1.1644dbh+1.37 for dbh > 32cm: 12.739log(dbh) - 16.297 (R <sup>2</sup> = 0.9863)	for dbh < 40: 0.0003 dbh <sup>2.4137</sup> (R <sup>2</sup> = 0.9994)	0.0001 dbh <sup>2.3922</sup> (R <sup>2</sup> = 0.9993)	for dbh < 40cm: 0.0298 dbh <sup>1.7463</sup> for dbh > 40cm: 15.907log(dbh) - 39.909 (R <sup>2</sup> = 0.897)	Central & East Siberia
<i>Populus suaveolens</i> <i>Populus tremula</i>	for dbh < 34cm: 0.0013dbh <sup>2</sup> +0.736dbh+1.37 for dbh > 34cm: 13.358log(dbh)-19.19 (R <sup>2</sup> = 0.9272)	for dbh < 34cm: 0.0001 dbh <sup>2.5877</sup> (R <sup>2</sup> = 0.9989)	0.0001 dbh <sup>2.4599</sup> (R <sup>2</sup> = 0.9992)	for dbh < 28.3cm: 0.0281 dbh <sup>1.6509</sup> for dbh > 28.3cm: 7.6636log(dbh)-18.632 (R <sup>2</sup> = 0.9937)	south & middle taiga, Central & East Siberia

Fig. 2.23: Species-specific allometric equations derived from regional forestry yield tables.

Height equation used in FAREAST:

$$H = 1.3 + \left( \frac{H_{max}}{100} - 1.3 \right) \times \left( 1 - e^{\frac{-S \times DBH}{H_{max} - 1.3}} \right) \quad (2.9)$$

where  $H_{max}$  is the estimated maximum height a tree of a given species can achieve, and  $S$  is the slope of the H-DBH relationship for young saplings.

Height equation used in ZELIG:

$$H = \frac{237 + \frac{2 \times (H_{max} - 137)}{D_{max}} \times DBH - \frac{H_{max} - 137}{D_{max}}}{100} \quad (2.10)$$

where  $H_{max}$  and  $D_{max}$  are the estimated maximum height and diameter at breast height a tree of a given species can achieve. These maximum height and diameter values are difficult to estimate, and vary based on site conditions.

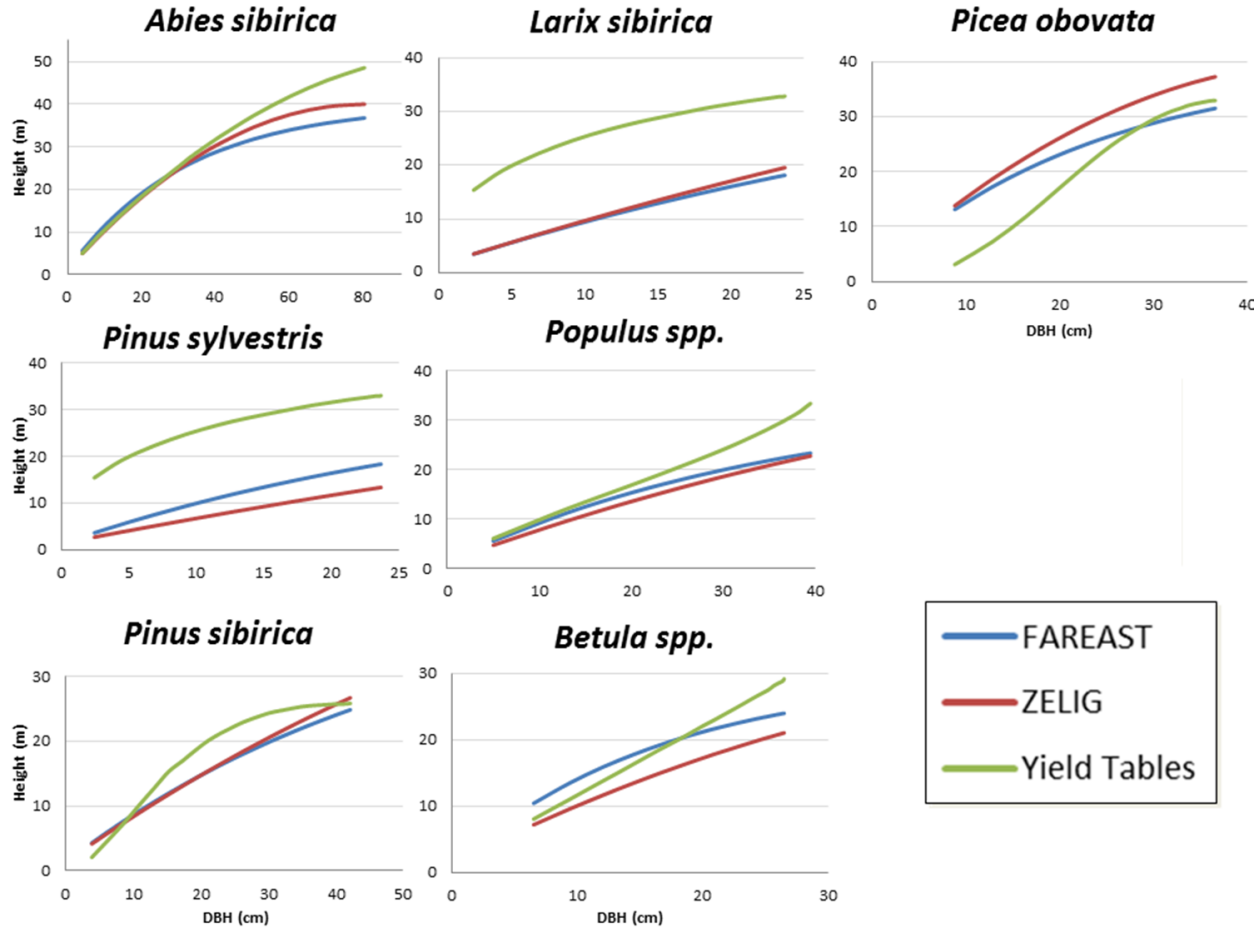


**Fig. 2.24:** Comparison of height parameterizations across models. SIBBORK is parameterized from forestry yield tables (green line).

### 2.3.2 Biovolume

Biovolume is a typical forestry survey parameter and represents predominantly the volume of the tree stem. SIBBORK computes biovolume in  $m^3/tree$  via a species-specific function of DBH derived from the average DBH, stem density, and average stand biovolume variables presented in the forestry yield tables (*Shvidenko et al.*, 2006). Species-specific equations for computing the biovolume of individual trees are presented in Figure 2.23. These equations represent lines of best fit for the stand biovolume ( $m^3/ha$ ) divided by stem density ( $stems/ha$ ) and the average DBH ( $cm$ ). Biovolume is not typically computed by gap models, however, as this is the parameter estimated in field surveys, including it in the model facilitates comparison along an additional variable. Furthermore, average DBH, stem density ( $stems/ha$ ), and biovolume ( $m^3/ha$ ) are reported within the same forestry yield table for each species, allowing for the direct derivation of an allometric relationship for biovolume as a function of DBH. This is in contrast to the allometric relationship between biomass ( $t/ha$ ) and average stand DBH, which is divided between forestry yield tables and tables of biological productivity, which were manually joined along the age variable (Figure 2.25).

### 2.3.3 Biomass

Biomass measurements are destructive and labor intensive. For this reason, biomass is not typically measured in field surveys, but is instead calculated from field-estimated stem biovolume using wood density. Focus on the tree stem can significantly underestimate the amount of total above- and below-ground biomass associated with each tree, since more than 30% of the biomass may be in the tree crown (*Monserud and Tchebakova*, 1996; *Shvidenko et al.*, 2006), and more than 25% of the biomass may be in the root system (*Schepaschenko et al.*, 1998; *Shvidenko et al.*, 2006). Nonetheless, the common approach is to estimate the tree stem volume and convert it to biomass by multiplying it by the wood density. The wood density can either be assumed the same for all trees (*Krankina et al.*, 1996; *Yan and Shugart*, 2005), or species- and region-specific values may be used to convert biovolume to biomass. There is a lot of variability in species-specific wood density values reported in the literature (*Monserud and Tchebakova*, 1996; *Schepaschenko et al.*, 1998; *Kajimoto et al.*, 1999; *Miao and Li*, 2007; *Falster et al.*, 2015), and the values used for the composition of the yield tables are not specified.

For SIBBORK, species-specific relationships were derived for above-ground biomass as a function of DBH based on the data presented in what were perceived to be overlapping forestry yield tables and tables of biological productivity for a given species and region. Since SIBBORK is an individual-based model, the relationship needs to represent the biomass per tree as a function of DBH. This was achieved by dividing the average stand biomass ( $tons/ha$ ) by stem density ( $stems/ha$ ), and fitting an equation to the relationship between this biomass and average stand DBH ( $cm$ ). This was accomplished using the stem density and DBH values provided in the yield table that corresponds to the same

## **Yield table of fully-stocked (normal) pine stands**

## 1.1. Ход роста полных (нормальных) сосновых древостояев

Age, year	Возраст, лет		Средняя высота, м	Средний диаметр, см	Число деревьев	Сумма площадей сечения, м <sup>2</sup> · га <sup>-1</sup>	Запас, м <sup>3</sup> · га <sup>-1</sup>	Изменение запаса, м <sup>3</sup> · га <sup>-1</sup> · год <sup>-1</sup>		Общая продуктивность, м <sup>3</sup> · га <sup>-1</sup>	Прирост по общей продуктивности, м <sup>3</sup> · га <sup>-1</sup> · год <sup>-1</sup>		Отпад, м <sup>3</sup> · га <sup>-1</sup> · год <sup>-1</sup>	
	Average Height, m	Average Diametr, cm						текущее	среднее		текущий	средний		
								Net Growth, м <sup>3</sup> · ha <sup>-1</sup> · year <sup>-1</sup>	Total volume, м <sup>3</sup> · ha <sup>-1</sup>	Gross Growth, м <sup>3</sup> · ha <sup>-1</sup> · year <sup>-1</sup>		Mortality, м <sup>3</sup> · ha <sup>-1</sup> · year <sup>-1</sup>		
								current	average		current	average		
	<b>lv бонитет</b>													
10	5.5	5.1	8277	17.0	57	9.95	5.65	61	11.22	6.15	1.27			
20	11.6	10.9	3263	30.4	178	13.51	8.89	205	16.80	10.27	3.29			
30	16.9	16.5	1863	39.7	316	13.74	10.53	386	18.80	12.85	5.06			
40	21.6	21.7	1245	46.2	448	12.46	11.19	574	18.70	14.36	6.24			
50	25.4	26.6	911	50.5	563	10.64	11.27	756	17.47	15.12	6.83			
60	28.6	31.0	709	53.4	660	8.77	11.00	922	15.71	15.37	6.95			
70	31.2	35.0	576	55.4	739	7.05	10.56	1070	13.77	15.28	6.72			

## Table of dynamics of biological productivity of fully-stocked pine stands

## **1.1. Динамика биологической продуктивности полных сосновых насаждений**

**Fig. 2.25:** The upper table contains the variables of average DBH, stem density, and stand biovolume. This facilitates the derivation of an allometric relationship for computing biovolume for each tree. The lower table contains information regarding biomass of different tree parts and total above-ground, as well as above- and below-ground biomass stand estimates. The common features between the two tables are the titles, which refer to the same species and ecotone, as well as the site index and the stand age.

species and ecotone as the biological productivity table. Foliage biomass, as well as the total above- and below-ground biomass, are similarly computed as a function of DBH. Figure 2.26 shows how the contribution of foliage and roots to the total above- and below-ground (AGBG) tree biomass changes over the course of a tree's lifetime.

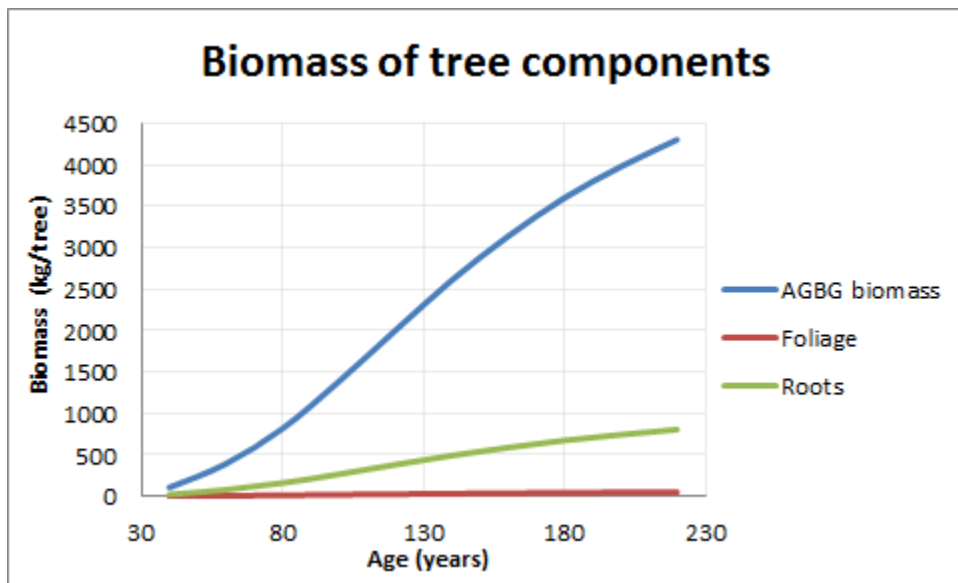


**Fig. 2.26:** Using Siberian larch as an example, the contribution of different tree components to total above- and below-ground tree biomass is shown for different stages in the tree's lifetime. Data obtained from Shvidenko *et al.* (2006).

This process to determining biomass allometry is very error-prone and depends on the yield tables and tables of biological productivity describing the same stands. Although species-specific equations for above-ground, as well as above- and below-ground biomass are included in SIBBORK, the verification and validation of these parameters is problematic, as few studies report above- and below-biomass estimates and the derivation of accurate biomass allometry may not even be feasible using the available forestry tables.

### 2.3.4 Foliage Biomass

Foliage biomass comprises 1-30% of total tree biomass (*Monserud and Tchekakova, 1996; Shvidenko et al., 2006*). According to the table of biological productivity, foliar biomass contributes more to the total biomass in the dark conifers fir, spruce, and Siberian cedar (8-13%). The denser canopy facilitates more light extinction, and this is why these species are collectively referred to as “dark” conifers. In contrast, light conifers - larch and pine - have lighter-colored, less dense canopies, which comprise up to 4 and 6% of total tree biomass, respectively. A larger proportion of young tree biomass is comprised of foliage. As the tree matures, foliage may constitute as little as 1% of total biomass.

Similar to tree biomass, foliage biomass is computed as a function of DBH based on the overlap of forestry yield tables and tables of biological productivity. This calculation is prone to the same errors as the above-ground biomass described in the previous section.

### 2.3.5 Leaf Area

Canopy leaf area estimates are of interest due to the control that the leaf area exerts on an array of physiological processes, from photosynthesis and respiration (*Asner et al.*, 2003) to water interception and sunlight availability (*Breda*, 2003), and ultimately the biological productivity. Numerous approaches to computing leaf area can be found in the literature, accompanied by several definitions of what should be considered leaf area (*Scurlock et al.*, 2001). For broadleaf trees, this is fairly simple - the leaf area can represent the area of one side of a leaf or two sides of a leaf. This is referred to as single-sided (projected) or double-sided (total) leaf area. Conifer needles can have cylindrical or triangular prism shapes, of which the latter has three sides. Leaf area can therefore be defined as one-sided (projected), two-sided, or three-sided (total). An additional definition for conifer needle leaf area estimates was suggested by Chen and Black (1992): “half the total intercepting area”, also known as hemisurface area (*Gower et al.*, 1999). In stand descriptions, often the leaf area index is used instead, which represents the leaf area per ground area. Much of the literature on leaf area (LA) and leaf area index (LAI) does not specify which definition was used to estimate the leaf area, which makes model parameterization and comparison of model output to published field-based estimates difficult. Furthermore, LA and LAI are site-specific, and are affected by soil nutrition and nitrogen content, soil moisture, and other environmental conditions (*Gower et al.*, 1999). This complicates the derivation of an allometric relationship between DBH and LA that could be applied to a multi-century simulation - a time frame over which environmental conditions could change significantly, especially when climate change is considered.

Leaf area is computed in SIBBORK in order to estimate the light environment throughout and below the canopy, however, no physiological process in the model depends on the leaf area. The computed leaf area is allocated evenly along the crown length of the tree (height - crown base) (*Urban*, 1990), and the horizontal extent of each tree’s canopy within each 1m vertical step is assumed to be homogeneously distributed across the plot area (*Shugart et al.*, 1988).

The original ZELIG model was created for mixed broadleaf temperate forests, and computed leaf area ( $m^2$ ) as a function of DBH ( $cm$ ) using the same equation form and coefficients for all species:

$$LA = 0.160694 \times DBH^{2.129} \quad (2.11)$$

A later version of ZELIG (v2.3) computed leaf area as a function of tree diameter and sapwood cross-sectional area at breast height:

$$LA = \pi \times \frac{DBH^2}{2} - \pi \times \left( \frac{DBH}{2} - r_{sapwood} \right) \times \left( Ratio_{\frac{sapwood}{leafarea}} \right) \quad (2.12)$$

where DBH is in *cm*,  $r_{sapwood}$  corresponds to the portion of the tree radius at breast height that represents the sapwood (*cm*), and the  $Ratio_{\frac{sapwood}{leafarea}}$  is the species-specific ratio of the sapwood area in the tree stem to the leaf area of the foliage. However, there is a significant difference in the vascular morphology of broadleaf and coniferous trees, and field-based estimates of conducting sapwood area are difficult (Vertessy *et al.*, 1995). In some broadleaf trees, the allometric relationship is observed between the few outer annual rings and leaf area, whereas in other broadleaf trees and in conifers the relationship is observed between the leaf area and the entire cross-sectional area of the sapwood (Albrektsen *et al.*, 1984; Breda, 2003). Even within plant functional types, there is significant variability in LA-sapwood area allometry (Waring *et al.*, 1982, Breda, 2003). Calculation of leaf area based on equation (2.12) may thus be appropriate for some tree species in the boreal forest, but not for others.

The FAREAST leaf area calculation is based on the Shinozaki pipe model (Shinozaki *et al.*, 1964) and uses the following equation:

$$LA = D_L \times (DBH \times \frac{H - CrownBase}{H - 1.3})^2 \quad (2.13)$$

where  $D_L$  is the ratio of the leaf area to the squared diameter at the base of the canopy crown - a ratio that is the same for all species in FAREAST. Height ( $H$ ) and the distance from the ground to the first branch ( $CrownBase$ ) are both in meters. Although the FAREAST model has been validated for China and Russia based on the ability to reproduce species composition and above-ground biomass, specifically the LA and the LAI calculations have never been validated (*Shugart, personal communication*). Both parameters are used to compute the light environment in the model, however, since FAREAST is a Monte Carlo simulation of independent plots, the light environment is only computed from directly overhead. Due to the differences between the Monte Carlo simulation and the spatially-explicit SIBBORK model, a LA or LAI parameterization that works well in FAREAST may not be appropriate for SIBBORK, where direct and diffuse light is computed along multiple light ray traces.

A method presented in Breda (2003) computes leaf area as a function of foliage biomass:

$$LA = B_f \times SLA \quad (2.14)$$

species	SLA ( $m^2/kg$ )	Reference
<i>Abies sibirica</i>	11.6	<i>Yan et al.</i> , 2010; <i>Wang et al.</i> , 2011
<i>Larix sibirica</i>	22.9	<i>Eguchi et al.</i> , 2004
<i>Betula pendula</i>	19.9	<i>Niinemets et al.</i> , 2002; <i>Repola et al.</i> , 2007
<i>Picea obovata</i>	12.9	<i>Tjoelker et al.</i> , 1998; <i>Hoffman and Usoltsev</i> , 2002
<i>Pinus sibirica</i>	15.2	<i>Tjoelker et al.</i> , 1998; <i>Hoffman and Usoltsev</i> , 2002; <i>Lindroth et al.</i> , 2008
<i>Pinus sylvestris</i>	13.4	<i>Tjoelker et al.</i> , 1998; <i>Hoffman and Usoltsev</i> , 2002; <i>Lindroth et al.</i> , 2008
<i>Populus tremula</i>	15.9	<i>Hoffman and Usoltsev</i> , 2002; <i>Breda</i> , 2003

**Fig. 2.27:** Specific leaf area (SLA) for boreal species obtained from the literature.

where  $B_f$  is the foliage biomass in kg, and SLA represents specific leaf area values for each species in  $m^2/kg$ . Published SLA values for boreal tree species are shown in Figure 2.27.

Specific leaf area generally represents the area-to-weight ratio of leaves or needles, but definitions for SLA diverge in the literature (Gower *et al.*, 1999). Broadleaf trees (birch, aspen) generally have higher SLA values than conifers, and larch exhibits the highest SLA of boreal conifers (Kloppel *et al.*, 1998). SLA varies widely between stands and seasons (Araki, 1972), depends on soil nitrogen and ambient  $CO_2$  concentrations (Curtis *et al.*, 2000), as well as soil moisture and leaf age (Landsberg and Gower, 1997; Ermolova and Utkin, 1998). Specific leaf area can vary significantly even within the crown of a single tree, with sun leaves thicker and heavier per unit area than the shade leaves (Araki, 1972; Ermolova and Utkin, 1998; Asner *et al.*, 2003).

However, this approach is attractive, since SLA values for different boreal species can be found in the literature, and the forestry tables of biological productivity specify a foliage biomass estimate for monospecies same-age cohorts (Figure 2.25). The latter creates a potential for deriving an allometric relationship between DBH and foliar biomass, provided the cross-correlation between forestry yield tables and tables of biological productivity is correct. However, it is important to keep in mind that SLA values are species- and site-specific, and can vary widely even within the crown of an individual tree. The SLA values in Figure 2.27 may not be fitting for some simulated sites, and downscaling the allometry from the stand-based tables of biological productivity to the individual trees in the simulation may not be appropriate.

In the simulation, LAI normalizes the sum of leaf areas of all trees on a plot by the area of the plot ( $100 m^2$ ). This is the parameter used in the exponent of the Beer-Lambert Law (equation (2.1)) for calculation of extinction of solar radiation as it travels through the forest canopy. Numerous approaches for LAI estimates exist in the literature, and some depend on the divergent definitions and measurement methodologies for LA and SLA (Barclay, 1998; Scurlock *et al.*, 2001; Asner *et al.*, 2003). LAI depends on time of year, canopy closure, stem density, stand age, and other structural parameters, such as the leaf/needle angle and the degree of damage experienced by a crown from disturbances such as fire or defoliators (Chen and Black, 1992; Chen, 1996; Scurlock *et al.*, 2001). Typical LAI indices for forests range 3-19, with highest LAI values reported for boreal coniferous forests, and values less than 6 in broadleaf and mixed

stands (*DeAngelis et al.*, 1981; *Schulze*, 1982; *Chen*, 1996; *Asner et al.*, 2003). LAI values in the teens reported for boreal and mixed forests may be a result of measurement methodologies or adjustments between definitions (*Barclay*, 1998). According to one of the definitions, LAI relates the one-sided leaf area to the ground area below the canopy, i.e. the shade cast by the canopy of a tree when the sun is directly overhead (*Barclay*, 1998). *Asner et al.* (2003) conducted a global survey of LAIs reported for different biomes, and estimated that the average LAI for boreal deciduous and evergreen forests are 2.6 and 2.7, respectively, although this analysis under-represents Russian forests and accounts for only one site in southeastern Siberia. Large scale average LAI values of less than 3.5 appear to characterize the middle and northern taiga ecotones, while LAI of 3.5-4.5 is estimated for the southern taiga region from a remote sensing and modeling-based product (*Asner et al.*, 2003). Furthermore, LAI values reported in the literature often represent area averages ( $ha^{-1}$ ) and do not represent the variability in LAI across the terrain or at point locations. A gap model, however, computes LAI for much smaller areas, and greater variability in LAI is expected on a plot by plot basis. The divergence in LAI values reported for boreal forests complicates the validation of the LAI calculations in the model, however, all SIBBORK-simulated LAI values fall within the broad range of LAIs reported in the literature for boreal species.

The SLA parameterization from equation (2.14) was adapted in SIBBORK. Model testing revealed that this approach may overestimate total leaf area and the leaf area index, with mature conifer forests exhibiting LAIs in the teens and even the lower 20s. Although the lower side of this range may agree with some of the values reported in the literature (*Chen et al.*, 2002; *DeRose et al.*, 2010) with adjustment factors for conifer needles and clumping of 1.5-2 (*Barclay*, 1998; *Scurlock et al.*, 2001), the LAI values at the higher end of this range are rarely found in the literature, but have indeed been measured in some forests (*DeAngelis et al.*, 1981). Moreover, the simulated stand structure and composition, both of which depend on the light environment computed using LAI, have been verified and validated for southern, middle and northern taiga locations on flat terrain, as well as in complex terrain at the southern extent of the boreal forest.

To determine the most appropriate leaf area parameterization for the boreal ecosystem, each of these four approaches should be used to compute LA and LAI for a stand under the historical climate conditions, and model output compared to published values of LAI for different monospecies stands. It will also be important to assess that the structure and composition of the stands are appropriately simulated with each of the four parameterizations. However, this involves scripting four different versions of the model, and conducting verification and validation testing with each version. This falls outside of the scope of this dissertation project, however, highlights an area for further refinement of the SIBBORK model. At this point, the framework of SIBBORK has been designed to allow for species-specific equations for the LA calculation, so that the most appropriate approach can be selected and employed for each species in the simulation.

A simpler, short-term solution to LAI overestimation could be a quality control check implemented to correct any plot-wide LAI of greater than a certain maximum threshold to a reasonable value in the lower teens. This approach has not been implemented, because within the simulated 3-D light environment, there is not much difference in the amount of light available in the lower portions of the canopy with an LAI of 15 or 22. Most of the light below a canopy with LAI of 15 is extinguished, which prevents shade-intolerant saplings from establishing in the subcanopy of dense coniferous trees, preserving realism in the simulation.

## 2.4 Environmental Effects on Vegetation Processes

Vegetation processes of sapling establishment, growth, and mortality are affected by environmental forcings. In ZELIG (*Urban*, 1990; *Urban et al.*, 1993; *Weishampel et al.*, 1996), the growth response of trees to the environmental factors of light availability, soil moisture, ambient temperature, expressed as growing degree days, and soil fertility, expressed as maximum biomass per plot, were parameterized as in Figure 2.28.

In SIBBORK, the environmental factors of growing degree days, soil moisture, soil fertility, permafrost, ground-level available light, as well as available light throughout and below the canopy are generated for the simulation area based on climatological record (*NCDC*, 2005a, 2005b) and lapse rates from DEM, hydrologic modeling based on DEM, soil datasets (*Stolbovoi and McCallum*, 2002; *Stolbovoi and Savin*, 2002), permafrost datasets (*Brown et al.*, 2002), and the Area Solar Radiation calculator based on DEM (*Fu and Rich*, 2002), respectively. The degree to which each species is affected by the presence or limited quantity of each factor is based on species-specific tolerances, which were obtained from the literature (*Shugart et al.*, 1992a; *Yan and Shugart*, 2005; *Larocque et al.*, 2016).

### 2.4.1 Available Light Factor

Available light is arguably the most important environmental constraint on vegetation growth and establishment (*Purves et al.*, 2008; *Purves and Pacala*, 2008), especially in environments with harsh and complex light regimes, such as the high-latitude boreal forests. In the absence of shade, trees are able to achieve optimal growth, provided other environmental factors are not limiting. In the shade, the growth rate diminishes until a species-specific compensation point is reached. At the compensation point, the energy gained from photosynthesis equals the energy expended on metabolism and respiration. Foliage and branches that are shaded to the point of acting as a drain on the plant's overall carbon budget are self-pruned. For example, shade-intolerant species may prune branches and foliage that receive less than 9% of above-canopy light, whereas shade tolerant species may be able to maintain foliage down to 5% of above-canopy light (Figure 2.28a).

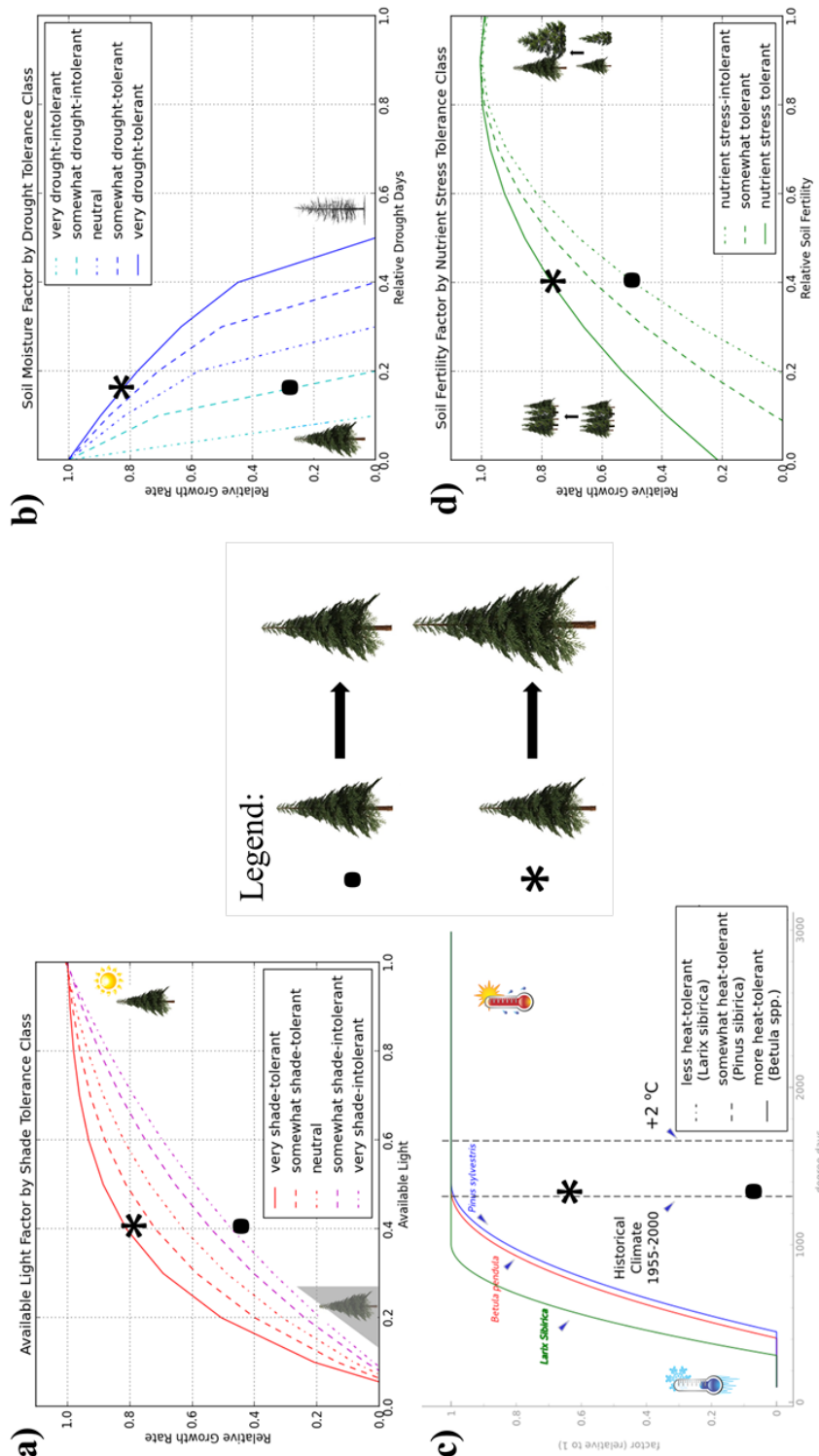


**Fig. 2.28:** Each simulated tree interacts with the surrounding environment based on species-specific tolerances to resource limitations. Growth responses are shown for (a) 5 shade tolerance classes to light limitations, (b) 5 drought tolerance classes to soil moisture limitations, (c) species-specific heat tolerance, reformulated from Pastor and Post (1986) based on Bugmann and Solomon (2000) and Bugmann (2001), and (d) 3 nutrient deficiency tolerance classes to nitrogen limitations. The \* in each case denotes the more tolerant species.

Tolerance class	$C_1$	$C_2$	$C_3$
1 (very shade tolerant)	1.01	4.62	0.05
2	1.04	3.44	0.06
3	1.11	2.52	0.07
4	1.24	1.78	0.08
5 (very shade intolerant)	1.49	1.23	0.09

**Fig. 2.29:** The shade tolerance class coefficients and compensation points were retained from ZELIG (Urban, 1990).

Following the approaches in other gap models (ZELIG, FAREAST), a shade tolerance class 1 (shade-tolerant) through 5 (shade-intolerant) is assigned to each species in the simulation based on literature descriptions (*Shugart et al.*, 1992a; *Smith and Hinckley*, 1995; *Yan and Shugart*, 2005; *Shuman*, 2010). The compensation point is computed based on equation:

$$ALF = C_1 \times (1 - e^{-C_2 \times (AL_h - C_3)}) \quad (2.15)$$

where  $ALF$  is the Available Light Factor with a value of 0 to 1, while  $C_1$ ,  $C_2$  and  $C_3$  are coefficients specific to the shade tolerance class. Specifically,  $C_2$  reflects the degree to which growth is affected by a decreasing amount of light, and  $C_3$  represents the compensation point for the specific shade tolerance class (Figure 2.29).  $AL_h$  is computed using Beer-Lambert Law (equation (2.1)) and LAI, and represents the fraction of above-canopy light available at each 1-meter vertical step through the canopy.

## 2.4.2 Growing Degree Days Factor

The growing degree days factor ( $GDDF$ ) is used to determine whether plant growth is limited by inadequate warmth over the course of the growing season. As in ZELIG, this function is initially generated as a parabola based on the maximum and minimum growing degrees that confound the species range (*Botkin et al.*, 1972a) via:

$$GDDF = \frac{4 \times (TY - min) \times (max - TY)}{(max - TY)^2} \quad (2.16)$$

where  $GDDF$  is the degree days factor with a value of 0 to 1,  $TY$  is the current year's growing degrees ( $GDD_5$ ) in the simulation, and  $min$  and  $max$  correspond to the maximum tolerated and minimum required growing degrees for the species. Generally, the maximum corresponds somewhat to the southern boundary of the geographical range the species inhabits. The left half of the parabola limits tree growth whenever not enough growing degrees are accumulated during the growing season. It is important to note that no growth occurs at the  $GDD_5$  minimum for a species, and very few representatives of the species may be found for several kilometers equatorward (or downslope) of this  $GDD_5$  isoline in pockets of favorable microclimates. If all other environmental factors are not limiting, some trees of the

species of interest may be found in locations experiencing annual  $GDD_5$  sums of  $100^{\circ}\text{C}$  or more above the  $GDD_5$  minimum for the species. The right half of the parabola in SIBBORK has been modified to a non-linear function and extended at the non-limiting value (1.0), based on evidence that plant growth is not limited by heat alone, when enough soil moisture is available (*Bugmann and Solomon*, 2000). The effects of GDDF on tree growth are shown in Figure 2.28c.

### 2.4.3 Soil Moisture Factor

Each species in the simulation is assigned to one of five drought tolerance classes (1 = very drought-intolerant, 5 = very drought-tolerant). Even the most drought-tolerant species require plant available water during at least 50% of the growing season (Figure 2.28b). The fraction of dry days during the growing season is compared to species-specific thresholds via the following equation:

$$SMF = \sqrt{\frac{(Tol/10 - DRT)}{(Tol/10)}} \quad (2.17)$$

where  $SMF$  is the Soil Moisture Factor with a value of 0 to 1,  $Tol$  refers to the species-specific drought-tolerance class (1 to 5), and  $DRT$  represents the minimum of  $\frac{Tol}{10}$  and the fraction of the growing season with no plant available water (soil moisture below wilting point).

### 2.4.4 Soil Fertility Factor

Although arboreal tree species inhabit regions with very slow decomposition rates and low soil nitrogen, even within these harsh conditions boreal species require different levels of soil nutrition for optimal growth. In SIBBORK, species are assigned to one of three nutrient stress tolerance classes (1 = very intolerant, 3 = very tolerant to poor soils). Just like the other environmental factors, the soil fertility factor ( $SFF$ ) ranges from 0 to 1 (Figure 2.28d). The species-specific  $SFF$  is computed based on relative soil fertility (equation (2.19)) and the amount of biovolume that potentially could be accumulated on a plot during each simulation year based on limitations of the other environmental factors:

$$SFF = C_1 \times N + C_2 \times N \times sf + C_3 \times N \times sf^2 \quad (2.18)$$

where  $C_1$ ,  $C_2$ , and  $C_3$  are regression constants (Figure 2.30) based on the species-specific tolerance to nutrient stress,  $N$  is the assigned nutrient stress tolerance class (1 to 3), and  $sf$  is the normalized soil fertility based on the soil fertility value specified for this region in the simulation and the amount of biovolume that could be accrued on the plot this

Tolerance class	$C_1$	$C_2$	$C_3$
1 (very intolerant)	-0.6274	3.6	-1.994
2	-0.2352	2.77	-1.55
3 (very tolerant)	0.2133	1.789	-1.014

**Fig. 2.30:** The regression coefficients for the different tolerance classes to poor soil nutrition were retained from ZELIG (Urban, 1990).

Growth on permafrost / permafrost presence	Present	Absent
Cannot grow on permafrost	0	1
Can grow on permafrost	1	1

**Fig. 2.31:** Boolean limitation of tree establishment and growth on permafrost based on species-specific tolerances to this environmental parameter.

year:

$$fertility_{relative} = \frac{SoilFertility}{BiovolumeIncrement_{optimal}} \quad (2.19)$$

In ZELIG, the optimal biomass increment is computed based on the optimal diameter increment and represents non-limiting conditions. In SIBBORK, the maximum possible biovolume increment is computed based on the limitations on growth exerted by the *ALGF* and *GDDF*. In this manner, the actual growth that could be attained is downscaled, rather than the optimal growth:

$$fertility_{relative} = \frac{SoilFertility}{BiovolumeIncrement_{MaximumPossible}} \quad (2.20)$$

## 2.4.5 Permafrost Factor

The permafrost parameterization is greatly simplified in SIBBORK. The permafrost presence (1) or absence (0) is specified for each plot, similar to elevation or soil fertility. Each species in the simulation is assigned to one of two groups based on whether it is capable of growing on permafrost (1) or not (0), and the permafrost factor is computed based on the site and species specifications (Figure 2.31). Of the 7 species in the simulation, Siberian larch (*Larix sibirica*), Siberian pine (*Pinus sibirica*) and spruce (*Picea obovata*) are able to grow on permafrost (Shugart *et al.*, 1992a; Tchebakova *et al.*, 2009a). As much as 80% of Siberia is underlain by permafrost - a factor that significantly affects species composition in those areas (Kotlyakov and Khromova, 2002; Tchebakova *et al.*, 2009a). The presence of permafrost for a region of interest can be obtained from the National Snow and Ice Data Center (<http://nsidc.org/data/gdd600.html>; Kotlyakov and Khromova, 2002). Alternatively, similar to the site index, the presence or absence of permafrost can be specified by the user for each plot.

The parameterization of permafrost can be expanded to include interaction with soil moisture and soil fertility, following the approaches in Bonan (1988).

## 2.4.6 Overall Growth Factor

The overall growth factor used to scale down annual tree ring growth is computed using all five environmental factors. The *Leibig's Law of the Minimum* is applied to below-ground effects (soil fertility, soil moisture, permafrost), to avoid unrealistically small annual growth. Regardless of whether soil moisture or soil fertility conditions are limiting, if a species is not able to grow on permafrost and the presence of permafrost has been specified for the plot, that species will not be able to establish on that plot. A multiplicative effect is assumed to occur from the limitations of the above-ground environmental factors (available light, growing degrees) and the minimum of the below-ground factors.

$$\text{GrowthFactor} = \text{ALGF} \times \text{GDDF} \times \min(\text{SMF}, \text{SFF}, \text{Permafrost}) \quad (2.21)$$

Using solely the environmental conditions as the limiting factor on species establishment and growth, SIBBORK simulates appropriate species composition for forests in northern, middle, and southern taiga, and even at the southernmost boreal forest boundary in the complex terrain of Altay-Sayan mountains, without an explicit specification of species ranges in the driver.

*The model source code is available at <http://www.github.com/sibbork/SIBBORK>*

---

## CHAPTER

## EIGHT

---

## REFERENCES

- Acevedo, M. F., Urban, D. L. and H. H. Shugart (1996). Models of forest dynamics based on roles of tree species. *Ecological Modelling*, 87, 267-284.
- Acevedo, M. F. (2013). *Simulation of Ecological and Environmental Models*. CRC Press, Taylor & Francis Group, New York.
- Ajtay, G. L., Ketner, P., & Duvigneaud, P. (1979). Terrestrial primary production and phytomass. *The Global Carbon Cycle*, 13, 129-182.
- Aksenen, D., Dobrynin, D., Dubinin, M., Egorov, A., Isaev, A., Karpachevskiy, M., Laestadius, L., Potapov, P., Purekhovskiy, A., Turubanpva, S., and Yaroshenko, A. (2002). *Atlas of Russia's intact forest landscapes*. Russian NGOs Forest Club, Moscow, Russia. Available at <http://www.forest.ru/eng/publications/intact/> [accessed 4 February 2015]
- Albrektson, A. (1984). Sapwood basal area and needle mass of Scots pine (*Pinus sylvestris* L.) trees in central Sweden. *Forestry*, 57 (1), 35-43.
- Alexeyev, V.A. (1998). Forest health status in Russia. In: *Proceedings of the International Symposium of the USDA Forest Service*. General technical report PSW-GTR-166, USDA Forest Service, Pacific Southwest Research Station, Berkeley, CA, USA, 267-270.
- Allen, C. D., Macalady, A. K., Chenchouni, H., Bachelet, D., McDowell, N., Vennetier, M., et al. (2010). A global overview of drought and heat-induced tree mortality reveals emerging climate change risks for forests. *Forest Ecology and Management*, 259 (4), 660-684.
- Allison, S. D., & Treseder, K. K. (2008). Warming and drying suppress microbial activity and carbon cycling in boreal forest soils. *Global Change Biology*, 14 (12), 2898-2909.
- Anderegg, W. R. L., Kane, J. M., and L. D. L. Anderegg (2012). Consequences of widespread tree mortality triggered by drought and temperature stress. *Nature Climate Change*, DOI: 10.1038/nclimate1635.
- Angelstam, P. (1992). Conservation of communities-the importance of edges, surroundings and landscape mosaic structure. In: *Ecological principles of nature conservation*. Springer US. p 9-70.
- Anonymous (1990). *Forest Fund of the USSR*. State Committee for Forestry, Moscow, Russia 1-2. (in Russian)
- Antonio, N., Tome, M., Tome, J., Soares, P., & Fontes, L. (2007). Effect of tree, stand, and site variables on the allometry of Eucalyptus globulus tree biomass. *Canadian Journal of Forest Research*, 37 (5), 895-906.
- Anuchin, N.P. (1986). *Forest Encyclopedia*, Vol II. Soviet Encyclopedia, Moscow, USSR. p455-457. (in Russian)
- Araki,M. (1972). The Studies on the Specific Leaf Area of Forest Trees (II). *Japanese Forestry Society*, 54 (6), 184-191.

- Arctic Atlas.* (1985). USSR Academy of Sciences, Leningrad. (In Russian)
- Ashcroft, M. B., Chisholm, L. A., & French, K. O. (2009). Climate change at the landscape scale: predicting fine-grained spatial heterogeneity in warming and potential refugia for vegetation. *Global Change Biology*, 15 (3), 656-667.
- Ashton, M. S., Tyrrell, M. L., Spalding, D., & Gentry, B. (Eds.). (2012). *Managing forest carbon in a changing climate*. Springer Science & Business Media.
- Asner, G. P., Scurlock, J. M., & A Hicke, J. (2003). Global synthesis of leaf area index observations: implications for ecological and remote sensing studies. *Global Ecology and Biogeography*, 12 (3), 191-205.
- Atlas of USSR.* (1983). USSR Academy of Sciences, Leningrad. (In Russian)
- Atkin, O.K. et al. (2007). Respiration as a percentage of daily photosynthesis in whole plants is homeostatic at moderate, but not high, growth temperatures. *New Phytologist*, 174, 367-380.
- Babushkina, E. A., Knorre, A. A., Vaganov, E. A., & Bryukhanova, M. V. (2010). Transformation of climatic response in radial increment of trees depending on topoeological conditions of their occurrence. *Geography and Natural Resources*, 32 (1), 80-86. (in Russian)
- Baldocchi, D., Kelliher, F. M., Black, T. A., & Jarvis, P. (2000). Climate and vegetation controls on boreal zone energy exchange. *Global Change Biology*, 6 (S1), 69-83.
- Balzter, H., Gerard, F. F., George, C. T., Rowland, C. S., Jupp, T. E., McCallum, I., ... & Schmullius, C. (2005). Impact of the Arctic Oscillation pattern on interannual forest fire variability in Central Siberia. *Geophysical Research Letters*, 32 (14), .
- Barber, V. A., Juday, G. P. and B. P. Finney (2000). Reduced growth of Alaskan white spruce in the twentieth century from temperature-induced drought stress. *Nature*, 405, 668-672.
- Barchenkov, A. P. (2010). Changes in morphology of regenerating organs of Siberian larch along the River Yenisei. *Conifers of the Boreal Zone*, 27 (1-2), 36-42. (in Russian)
- Barclay, H. J. (1998). Conversion of total leaf area to projected leaf area in lodgepole pine and Douglas-fir. *Tree Physiology*, 18 (3), 185-193.
- Barlage, M., Zeng, X., Wei, H., & Mitchell, K. E. (2005). A global  $0.05^{\circ}$  maximum albedo dataset of snow-covered land based on MODIS observations. *Geophysical Research Letters*, 32 (17).
- Bartalev, S. (2010). Hybrid Biomass and Land Cover Map for Central Siberia.
- Bartalev, S. A., V. A. Egorov, D. V. Ershov, A. S. Isaev, E. A. Loupian, D. E. Plotnikov, and I. A. Uvarov. 2011. The Vegetation Mapping over Russia Using MODIS Spectroradiometer Satellite Data. *Contemporary Earth Remote Sensing From Space*, 8, 285-302. (in Russian)
- Basilevich, V.I. (1986). Biological productivity of soil vegetation formations in the USSR. *Izvestia Akademii nauk SSSR - Geography*, 2, 49-66.
- Bauweraerts, I., Ameye, M., Werten, T. M., McGuire, M. A., Teskey, R. O., & Steppe, K. (2014). Water availability is the decisive factor for the growth of two tree species in the occurrence of consecutive heat waves. *Agricultural and Forest Meteorology*, 189, 19-29.
- Beaudoin, A., Le Toan, T., Goze, S., Nezry, E., Lopes, A., Mougin, E., ... & Shin, R. T. (1994). Retrieval of forest biomass from SAR data. *International Journal of Remote Sensing*, 15 (14), 2777-2796.
- Bentz, B. J., Regniere, J., Fettig, C. J., Hansen, E. M., Hayes, J. L., Hicke, J. A., ... & Seybold, S. J. (2010). Climate change and bark beetles of the western United States and Canada: direct and indirect effects. *BioScience*, 60 (8), 602-613.
- Betts, A. K., & Ball, J. H. (1997). Albedo over the boreal forest. *Journal of Geophysical Research*, 103, 28-901.
- Betts, R. A. (2000). Offset of the potential carbon sink from the boreal forestation by decreases in surface albedo. *Nature*, 408, 187-190.

- Bhatti, J. S., Van Kooten, G. C., Apps, M. J., Laird, L. D., Campbell, I. D., Campbell, C., ... & Banfield, E. (2003). Carbon balance and climate change in boreal forests. In: *Towards Sustainable Management of the Boreal Forest*, p799-855. National Research Council Research Press, Ottawa. ON.
- Blunden, J., Arndt, D. S., Achberger, C., Ackerman, S. A., Albalil, A., Alexander, P., et al. (2013). State of the Climate in 2012. *Bulletin of the American Meteorological Society*, 94 (8), S1-S238.
- Boisier, J. P., de Noblet-Ducoudre, N., & Ciais, P. (2013). Inferring past land use-induced changes in surface albedo from satellite observations: a useful tool to evaluate model simulations. *Biogeosciences*, 10 (3), 1501-1516.
- Bolin, B. (1986). How much  $CO_2$  will remain in the atmosphere. In: B. Bolin, B.R. Doos, J. Jager, and R.A. Warrick (editors), *The Greenhouse Effect, Climate Change, and Ecosystems*. John Wiley, Chichester. p93-155.
- Bonan, G. (1988). Dissertation: Environmental Processes and Vegetation Patterns in Boreal Forests. University of Virginia, Charlottesville, Va.
- Bonan, G. B. (1988). A simulation model of environmental processes and vegetation patterns in boreal forests: test case Fairbanks, Alaska. Working Paper WP-88-63. International Institute for Applied Systems Analysis, Laxenburg, Austria. 63 pp.
- Bonan, G. B. and H. H. Shugart (1989) Environmental Factors and Ecological Processes in Boreal Forests. *Annual Review of Ecology and Systematics*, 20, 1-28.
- Bonan, G. B., Shugart, H. H. and D. L. Urban. (1990). The sensitivity of some high latitude boreal forests to climatic parameters. *Climatic Change*, 16, 9-31.
- Bonan, G. B., Pollard, D. and S. L. Thompson. (1992). Effects of boreal forest vegetation on global climate. *Nature*, 359, 716-718.
- Bonan, G. B., Chapin III, F. S., & Thompson, S. L. (1995). Boreal forest and tundra ecosystems as components of the climate system. *Climatic Change*, 29 (2), 145-167.
- Bonan, G.B. (2008) Forests and climate change: Forcings, feedbacks, and the climate benefits of forests. *Science*, 320, 1444-1449.
- Bond-Lamberty, B., Fisk, J. P., Holm, J. A., Bailey, V., Bohrer, G., & Gough, C. M. (2015). Moderate forest disturbance as a stringent test for gap and big-leaf models. *Biogeosciences*, 12 (2), 513-526.
- Botkin, D. B., Janak, J. F. and J. R. Wallis. (1972a). Rationale, limitations, and assumptions of a Northeastern forest growth simulator. *IBM Journal of Research and Development*, 16, 101-116.
- Botkin, D. B., Janak, J. F. and J. R. Wallis. (1972b). Some ecological consequences of a computer model of forest growth. *Journal of Ecology*, 60, 849-872.
- Botkin, D. B. (1993). *Forest Dynamics: An ecological model*. Oxford University Press, Oxford, UK.
- Bradshaw, F. J. (1992). Quantifying edge effect and patch size for multiple-use silviculture - a discussion paper. *Forest Ecology and Management*, 48 (3), 249-264.
- Bragg, D. C. (2001). Potential relative increment (PRI): a new method to empirically derive optimal tree diameter growth. *Ecological Modelling*, 137 (1), 77-92.
- Bragg, D. C. (2003). Optimal diameter growth equations for major tree species of the Midsouth. *Southern Journal of Applied Forestry*, 27 (1), 5-10.
- Brazhnik, K., and H.H. Shugart (2015). SIBBORK: New Spatially-Explicit Gap Model for Boreal Forest in 3-Dimensional Terrain. *Ecological Modelling*, in review.
- Breda, N.J. (2003). Ground-based measurements of leaf area index: a review of methods, instruments and current controversies. *Journal of Experimental Botany*, 54 (392), 2403-2417.
- Briffa, K. R., Schweingruber, F. H., Jones, P. D., Osborn, T. J., Shiyatov, S. G., & Vaganov, E. A. (1998). Reduced sensitivity of recent tree-growth to temperature at high northern latitudes. *Nature*, 391 (6668), 678-682.

- Broadbent, E. N., Asner, G. P., Keller, M., Knapp, D. E., Oliveira, P. J., & Silva, J. N. (2008). Forest fragmentation and edge effects from deforestation and selective logging in the Brazilian Amazon. *Biological Conservation*, 141 (7), 1745-1757.
- Brooks, J. R., Flanagan, L. B., Buchmann, N., & Ehleringer, J. R. (1997a). Carbon isotope composition of boreal plants: functional grouping of life forms. *Oecologia*, 110 (3), 301-311.
- Brooks, J. R., Flanagan, L. B., Varney, G. T., & Ehleringer, J. R. (1997b). Vertical gradients in photosynthetic gas exchange characteristics and refixation of respired  $CO_2$  within boreal forest canopies. *Tree Physiology*, 17 (1), 1-12.
- Brown, J., Ferrians Jr, O. J., Heginbottom, J. A., & Melnikov, E. S. (2002). Circum-Arctic Map of Permafrost and Ground-Ice Conditions, version 2. National Snow and Ice Data Center, Boulder.
- Bryson, R.A., Baerreis, D.A., and W.M. Wendland. (1970). The character of late-glacial and post-glacial climate changes. In: Dort, W., and J.K. Jones (eds.), Pleistocene and Recent Environments of the Central Great Plains. University Press of Kansas, Lawrence. pp.53-74.
- Buchman, R. G., Pederson, S. P. and N. R. Walters (1983) A tree survival model with application to species of the Great Lakes region. *Canadian Journal of Forest Research*, 13, 601-608.
- Buermann, W., Parida, B., Jung, M., MacDonald, G. M., Tucker, C. J., & Reichstein, M. (2014). Recent shift in Eurasian boreal forest greening response may be associated with warmer and drier summers. *Geophysical Research Letters*, 41 (6), 1995-2002.
- Bugmann, H., Fischlin, A., & Kienast, F. (1996). Model convergence and state variable update in forest gap models. *Ecological Modelling*, 89 (1), 197-208.
- Bugmann, H. K. and A. M. Solomon (2000). Explaining Forest Composition and Biomass across Multiple Biogeographical Regions. *Ecological Applications*, 10 (1), 95-114.
- Bugmann, H. K. (2001). A review of forest gap models. *Climatic Change*, 51, 259-305.
- Bulygina, O., Korshunova, N. N., Razuvayev, V. N., & Groisman, P. Y. (2014, December). Climate Extreme Events over Northern Eurasia in Changing Climate. In: AGU Fall Meeting Abstracts (Vol. 1, p. 0453).
- Bunn, A. G., Goetz, S. J., Kimball, J. S., & Zhang, K. (2007). Northern High-Latitude Ecosystems Respond to Climate Change. *EOS Transactions*, 88, 333-335.
- Burton, P. J., Kneeshaw, D. D., & Coates, K. D. (1999). Managing forest harvesting to maintain old growth in boreal and sub-boreal forests. *The Forestry Chronicle*, 75 (4), 623-631.
- Burton, P. J., Messier, C., and Smith, D. W., eds. *Towards Sustainable Management of the Boreal Forest*. Ottawa, ON, CAN: NRC Research Press, 2003.
- Buryak, L. V., Kalenskaya, O. P., Tolmachev, A. V., & Yankovskii, R. V. (2009). Forest fires and their after-effects in the Sushensky Bor National Park. *Lesnoe Khozyaistvo*, 3, 37-39.
- Buryak, L. V., Sukhinin, A. I., Kalenskaya, O. P., & Ponomarev, E. I. (2011). Effects of fires in ribbon-like pine forests of southern Siberia. *Contemporary Problems of Ecology*, 4 (3), 248-253.
- Busing, R. T. and A. M. Solomon (2004) A comparison of forest survey data with forest dynamics simulators FORCLIM and ZELIG along climatic gradients in the Pacific Northwest. U. S. Geological Survey Scientific Investigations Report 2004-5087.
- Busing, R. T. and D. Mailly (2004) Advances in spatial, individual-based modeling of forest dynamics. *Journal of Vegetation Science*, 15, 831-842.
- Cale, W. G., O'Neill, R. V., & Shugart, H. H. (1983). Development and application of desirable ecological models. *Ecological Modelling*, 18 (3), 171-186.
- Campbell, G. S. (1977). *An Introduction to Environmental Biophysics*. Springer-Verlag, New York, NY.
- Campbell, G. S. and J. M. Norman (1998). *An Introduction to Environmental Biophysics*. Springer Science & Business Media, LLC, New York, New York.

- Chapin III, F. S., Callaghan, T. V., Bergeron, Y., Fukuda, M., Johnstone, J. F., Juday, G., & Zimov, S. A. (2004). Global change and the boreal forest: thresholds, shifting states or gradual change? *AMBIO: A Journal of the Human Environment*, 33 (6), 361-365.
- Chapin, F. S. III, Oswood, M. W., Van Cleve, K., Viereck, L. A., and D. L. Verbyla. (2006a). Alaska's Changing Boreal Forest. Oxford University Press, Oxford, UK.
- Chapin III, F. S., Viereck, L. A., Adams, P., Van Cleve, K., Fastie, C. L., Ott, R. A., ... & Johnstone, J. F. (2006b). Successional processes in the Alaskan boreal forest. In: *Alaska's changing boreal forest*. Oxford University Press, Oxford, p100-120.
- Chen, J.M., & Black, T.A. (1992). Defining leaf area index for non-flat leaves. *Plant, Cell & Environment*, 15 (4), 421-429.
- Chen, J., Franklin, J. F., & Spies, T. A. (1992). Vegetation responses to edge environments in old-growth Douglas-fir forests. *Ecological Applications*, 2 (4), 387-396.
- Chen, J. M. (1996). Optically-based methods for measuring seasonal variation of leaf area index in boreal conifer stands. *Agricultural and Forest Meteorology*, 80 (2), 135-163.
- Chen, J. M., Rich, P. M., Gower, S. T., Norman, J. M., & Plummer, S. (1997). Leaf area index of boreal forests: theory, techniques, and measurements. *Journal of Geophysical Research: Atmospheres (1984-2012)*, 102 (D24), 29429-29443.
- Chen, J. M., Pavlic, G., Brown, L., Cihlar, J., Leblanc, S. G., White, H. P., Hall, R. J., Peddle, D. R., King, D. J., Trofymow, J. A., Swift, E., Van der Sanden, J. & Pellikka, P. K. E. (2002). Derivation and validation of Canada-wide coarse-resolution leaf area index maps using high-resolution satellite imagery and ground measurements. *Remote Sensing of Environment*, 80 (1), 165-184.
- Chen, X., Vierling, L., Deering, D., & Conley, A. (2005). Monitoring boreal forest leaf area index across a Siberian burn chronosequence: a MODIS validation study. *International Journal of Remote Sensing*, 26 (24), 5433-5451.
- Chlachula, J., & Sukhova, M. G. (2011). Regional manifestations of present climate change in the Altai, Siberia. International Proceedings of Chemical, Biological and Environmental Engineering. Environmental Engineering and Applications, Edited by Li Xuan, 17, 134-139.
- Chytry, M., Danihelka, J., Kubesova, S., Lustyk, P., Ermakov, N., Hajek, M., ... & Pisut, I. (2008). Diversity of forest vegetation across a strong gradient of climatic continentality: Western Sayan Mountains, southern Siberia. *Plant Ecology*, 196 (1), 61-83.
- Clark, W. C., Jones, D. D., & Holling, C. S. (1979). Lessons for ecological policy design: a case study of ecosystem management. *Ecological Modelling*, 7 (1), 1-53.
- Clark, J. S. (1998). Why trees migrate so fast: confronting theory with dispersal biology and the paleorecord. *The American Naturalist*, 152 (2), 204-224.
- Cochrane, M. A., Alencar, A., Schulze, M. D., Souza, C. M., Nepstad, D. C., Lefebvre, P., & Davidson, E. A. (1999). Positive feedbacks in the fire dynamic of closed canopy tropical forests. *Science*, 284 (5421), 1832-1835.
- Coffin, D. P., & Urban, D. L. (1993). Implications of natural history traits to system-level dynamics: comparisons of a grassland and a forest. *Ecological Modelling*, 67 (2), 147-178.
- Collinge, S. K. (1996). Ecological consequences of habitat fragmentation: implications for landscape architecture and planning. *Landscape and Urban Planning*, 36 (1), 59-77.
- Conard, S. G., Sukhinin, A. I., Stocks, B. J., Cahoon, D. R., Davidenko, E. P. and G. A. Ivanova (2002) Determining effects of area burned and fire severity on carbon cycling and emissions in Siberia. *Climatic Change*, 55, 197-211.
- Conard, S. G., Sukhinin, A. I., Ivanova, G. A., Hao, W. M., & McRae, D. J. (2004). Modeling and monitoring effects of area burned and fire severity on carbon cycling, emissions, and forest health and sustainability in Central Siberia: February 2004 Progress Report, 36 p.

- Cox, P. M., Betts, R. A., Jones, C. D., Spall, S. A., & Totterdell, I. J. (2000). Acceleration of global warming due to carbon-cycle feedbacks in a coupled climate model. *Nature*, 408 (6809), 184-187.
- Crawford, R. M. M., Jeffree, C. E., & Rees, W. G. (2003). Paludification and forest retreat in northern oceanic environments. *Annals of Botany*, 91 (2), 213-226.
- Cuevas-Gonzales, M. A. R. Í. A., Gerard, F., Balzter, H., & Riano, D. (2009). Analysing forest recovery after wildfire disturbance in boreal Siberia using remotely sensed vegetation indices. *Global Change Biology*, 15 (3), 561-577.
- Curtis, P. S., Vogel, C. S., Wang, X., Pregitzer, K. S., Zak, D. R., Lussenhop, J., Kubiske, M., & Teeri, J. A. (2000). Gas exchange, leaf nitrogen, and growth efficiency of *Populus tremuloides* in a  $CO_2$ -enriched atmosphere. *Ecological Applications*, 10 (1), 3-17.
- Cvetkov, P.A. (2002) Determination of fire danger in Siberian forests. *Lesnoe Khozaistvo*, 5, 43-45. (in Russian)
- Dale, V. H., Joyce, L. A., McNulty, S., Neilson, R. P., Ayres, M. P., Flannigan, M. D., ... & Michael Wotton, B. (2001). Climate change and forest disturbances: climate change can affect forests by altering the frequency, intensity, duration, and timing of fire, drought, introduced species, insect and pathogen outbreaks, hurricanes, windstorms, ice storms, or landslides. *BioScience*, 51 (9), 723-734.
- de Groot, W. J., Cantin, A. S., Flannigan, M. D., Soja, A. J., Gowman, L. M., & Newbery, A. (2013). A comparison of Canadian and Russian boreal forest fire regimes. *Forest Ecology and Management*, 294, 23-34.
- Denman, K.L. et al. (2007). In: *Climate Change 2007: The Physical Science Basis. Contribution of Working Group I to the Fourth Assessment Report of the Intergovernmental Panel on Climate Change*, S. Solomon et al., Eds. (Cambridge Univ. Press, Cambridge, 2007) pp. 499-587.
- Devi, N., Hagedorn, F., Moiseev, P., Bugmann, H., Shiyatov, S., Mazepa, V., & Rigling, A. (2008). Expanding forests and changing growth forms of Siberian larch at the Polar Urals treeline during the 20th century. *Global Change Biology*, 14 (7), 1581-1591.
- Deyeva N. M. (1985). Biomass amount in forest communities of the northern-western part of Plateau Putorana, *Botanicheskii Zhurnal* (Russian Botanical Journal), 70 (1), 54-58. (in Russian)
- Deyeva N. M. (1987). Vegetative mass structure in forest phytocoenoses of the northern-western part of Plateau Putorana, *Botanicheskii Zhurnal* (Russian Botanical Journal), 72 (4), 505-511. (in Russian)
- Dirnbock, T., Dullinger, S., & Grabherr, G. (2003). A regional impact assessment of climate and land-use change on alpine vegetation. *Journal of Biogeography*, 30 (3), 401-417.
- Dislich, C. and A. Huth (2012). Modelling the impact of shallow landslides on forest structure in tropical montane forests. *Ecological Modelling*, 239, 40-53, DOI: 10.1016/j.ecolmodel.2012.04.016
- Dore, S., Kolb, T. E., Montes-Helu, M., Sullivan, B. W., Winslow, W. D., Hart, S. C., ... & Hungate, B. A. (2008). Long-term impact of a stand-replacing fire on ecosystem  $CO_2$  exchange of a Ponderosa pine forest. *Global Change Biology*, 14 (8), 1801-1820.
- Dulamsuren, C., Hauck, M., & Mühlenberg, M. (2005a) Vegetation at the taiga forest-steppe borderline in the western Khentey Mountains, northern Mongolia. In: *Annales Botanici Fennici* (pp. 411-426). Finnish Zoological and Botanical Publishing Board.
- Dulamsuren, C., Hauck, M., & Mühlenberg, M. (2005b) Ground vegetation in the Mongolian taiga forest-steppe ecotone does not offer evidence for the human origin of grasslands. *Applied Vegetation Science*, 8 (2), 149-154.
- Dulamsuren, C., Hauck, M., Bader, M., Osokhjargal, D., Oyungerel, S., Nyambayar, S., ... & Leuschner, C. (2009). Water relations and photosynthetic performance in *Larix sibirica* growing in the forest-steppe ecotone of northern Mongolia. *Tree Physiology*, 29 (1), 99-110.
- Dulamsuren, C., Hauck, M., Leuschner, H. H., & Leuschner, C. (2011). Climate response of tree-ring width in *Larix sibirica* growing in the drought-stressed forest-steppe ecotone of northern Mongolia. *Annals of Forest Science*, 68 (2), 275-282.

- Dymond, C. C., Neilson, E. T., Stinson, G., Porter, K., MacLean, D. A., Gray, D. R., ... & Kurz, W. A. (2010). Future spruce budworm outbreak may create a carbon source in eastern Canadian forests. *Ecosystems*, 13 (6), 917-931.
- Easterling, D. R., Horton, B., Jones, P. D., Peterson, T. C., Karl, T. R., Parker, D. E. et al (1997). Maximum and minimum temperature trends for the globe. *Science*, 277, 364-367.
- Eguchi, N., Fukatsu, E., Funada, R., Tobita, H., Kitao, M., Maruyama, Y., & Koike, T. (2004). Changes in morphology, anatomy, and photosynthetic capacity of needles of Japanese larch (*Larix kaempferi*) seedlings grown in high  $CO_2$  concentrations. *Photosynthetica*, 42 (2), 173-178.
- Emanuel, W. R., Shugart, H. H. and M. P. Stevenson (1985). Climate change and the broad scale distribution of terrestrial ecosystem complexes. *Climatic Change*, 7, 29-43.
- Englhart, S., Keuck, V., & Siegert, F. (2011). Aboveground biomass retrieval in tropical forests - The potential of combined X-and L-band SAR data use. *Remote Sensing of Environment*, 115 (5), 1260-1271.
- Erler, A. E. T., Shuman, J. K., Soukhavolosky, V., Kovalev, A., Stevens, T. and H. H. Shugart (2008). Modeling and assessing insect disturbance on boreal forests in the Krasnoyarsk region of Russia by employing the FAREAST gap model and local forest inventory and disturbance data. Poster at the American Geophysical Union conference, San Francisco, CA, USA.
- Ermolova, L. S., & Utkin, A. I. (1998). Specific leaf area of dominant forest-forming species of Russia. *Russian Journal of Ecology*, 29 (3), 152-156.
- Ershov, D.V. and Isaev, A.S., eds. (2006). GIS database of Siberian Silkworm forest damages in Usolsky forest enterprise of the Krasnoyarsk region. Russian Academy of Science Center for Forest Ecology and Productivity Forest Ecosystems Monitoring Laboratory, Moscow, Russia.
- Esper, J., & Schweingruber, F. H. (2004). Large-scale treeline changes recorded in Siberia. *Geophysical Research Letters*, 31 (6). DOI: 10.1029/2003GL019178
- ESRI 2012 ESRI ArcGIS version 10.1 [computer program] ESRI, Redlands, CA, USA .
- Falster, D. S., Duursma, R. A., Ishihara, M. I., Barneche, D. R., FitzJohn, R. G., Varhammar, A., ... & McCulloh, K. (2015). BAAD: a Biomass And Allometry Database for woody plants. *Ecological Archives* E096-128.
- Ferreira, L. V., & Laurance, W. F. (1997). Effects of forest fragmentation on mortality and damage of selected trees in central Amazonia. *Conservation Biology*, 797-801.
- Fisher, J. B., Whittaker, R. J., & Malhi, Y. (2011). ET come home: potential evapotranspiration in geographical ecology. *Global Ecology and Biogeography*, 20 (1), 1-18.
- Folland, C. K. and T. R. Karl. (2001) Observed climate variability and change. In: *Climate change 2001: the scientific basis. Contribution of WORKING Group 1 to the third IPCC scientific assessment*. Edited by Houghton, J. T., Ding, Y., Griggs, D. J., Noguer, M., Van der Linden, P. J., Xiaosu, D., Maskell, K., and C. A. Johnson. Cambridge University Press, Cambridge, UK. pp. 99-182.
- Fransson, J. E. S. (1999). Estimation of stem volume in boreal forests using ERS-1 C-and JERS-1 L-band SAR data. *International Journal of Remote Sensing*, 20 (1), 123-137.
- Fu, P., & Rich, P. M. (2002). A geometric solar radiation model with applications in agriculture and forestry. *Computers and electronics in agriculture*, 37 (1), 25-35.
- Furyaev, V.V., Pleshnikov, F.I., Zlobina, L.P. and E.A. Furyaev. (2004). Transformation of structure and ecological function of forests under the influence of fire in central Siberia. *Lesovedenie*, 6, 50-57.
- Gerard, F., Plummer, S., Wadsworth, R., Sanfeliu, A. F., Iliffe, L., Balzter, H., & Wyatt, B. (2003). Forest fire scar detection in the boreal forest with multitemporal SPOT-VEGETATION data. *IEEE Transactions on Geoscience and Remote Sensing*, 41 (11), 2575-2585.
- Germania, I.G. (2003) Global and regional problems of forest fires. (in Russian)

- Germino, M. J., Smith, W. K., & Resor, A. C. (2002). Conifer seedling distribution and survival in an alpine-treeline ecotone. *Plant Ecology*, 162 (2), 157-168.
- Goetz, S. J., Mack, M. C., Gurney, K. R., Randerson, J. T., & Houghton, R. A. (2007). Ecosystem responses to recent climate change and fire disturbance at northern high latitudes: observations and model results contrasting northern Eurasia and North America. *Environmental Research Letters*, 2 (4), 045031.
- Goodale, G. L., Apps, M. J., Birdsey, R. A., Field, C. B., Heath, L. S., Houghton, R. A., Jenkins, J. C., Kohlmaier, G. H., Kurz, W., Liu, S., Nabuurs, G. H., Nilsson, S. and A. Z. Shvidenko (2002) Forest carbon sinks in the Northern Hemisphere. *Ecological Applications*, 12, 891-899.
- Gorchakovskiy, P. L., & Shiyatov, S. G. (1978). The upper forest limit in the mountains of the boreal zone of the USSR. *Arctic and Alpine Research*, 10 (2), 349-363.
- Goulden, M. L., Munger, J. W., Fan, S. M., Daube, B. C., & Wofsy, S. C. (1996). Exchange of carbon dioxide by a deciduous forest: response to interannual climate variability. *Science*, 271 (5255), 1576-1578.
- Gower, S. T., & Richards, J. H. (1990). Larches: deciduous conifers in an evergreen world. *BioScience*, 40 (11), 818-826.
- Gower, S. T., Kucharik, C. J., & Norman, J. M. (1999). Direct and indirect estimation of leaf area index, f APAR, and net primary production of terrestrial ecosystems. *Remote Sensing of Environment*, 70 (1), 29-51.
- Gower, S. T., Krankina, O., Olson, R. J., Apps, M., Linder, S., & Wang, C. (2001). Net primary production and carbon allocation patterns of boreal forest ecosystems. *Ecological Applications*, 11 (5), 1395-1411.
- Grace, J., Lloyd, J., McIntyre, J., Miranda, A. C., Meir, P., Miranda, H. S., ... & Gash, J. (1995). Carbon dioxide uptake by an undisturbed tropical rain forest in southwest Amazonia, 1992 to 1993. SCIENCE-NEW YORK THEN WASHINGTON-, 778-778.
- Grace, J., Berninger, F., & Nagy, L. (2002). Impacts of climate change on the tree line. *Annals of Botany*, 90 (4), 537-544.
- Grimm, V., & Railsback, S. F. (2005). *Individual-based modeling and ecology*. Princeton University Press, Princeton, New Jersey, USA.
- Grimm, V., Revilla, E., Berger, U., Jeltsch, F., Mooij, W. M., Railsback, S. F., et al. (2005). Pattern-oriented modeling of agent-based complex systems: lessons from ecology. *Science*, 310 (5750), 987-991.
- Groisman, P. Y., Sherstyukov, B. G., Razuvayev, V. N., Knight, R. W., Enloe, J. G., Stroumentova, N. S., ... & Karl, T. R. (2007). Potential forest fire danger over Northern Eurasia: changes during the 20th century. *Global and Planetary Change*, 56 (3), 371-386.
- Groisman, P., & Soja, A. J. (2009). Ongoing climatic change in Northern Eurasia: justification for expedient research. *Environmental Research Letters*, 4 (4), 045002.
- Groisman, P. Y., Blyakharchuk, T. A., Chernokulsky, A. V., Arzhanov, M. M., Marchesini, L. B., Bogdanova, E. G., et al. (2013). Climate changes in Siberia. In *Regional Environmental Changes in Siberia and Their Global Consequences*. Springer Netherlands. p. 57-109.
- Groisman, P. Y., & Gutman, G. (2013). *Environmental Changes in Siberia: Regional Changes and their Global Consequences*. Springer, Dordrecht. 357p.
- Gruza, G. V., Ran'kova, E. Y., Razuvayev, V. N., and O. N. Bulygina. (1999). Indicators of climate change in the Russian Federation. In Weather and climate extremes. Edited by Karl, T., R., Nicholls, N., and A. Ghazi. Kluwer Academic Publishers, Dordrecht, Netherlands. p. 219-242.
- Gruza, G.V., Bardin, M.Yu, Rankova, E.Ya., Rocheva, E.V, Platova, T.V, et al. (2015) A Report on Climate Features on the Territory of the Russian Federation in 2014. Obtained from <http://www.meteorf.ru> (in Russian)
- Gustafson, E. J., Shvidenko, A. Z., Sturtevant, B. R., & Scheller, R. M. (2010). Predicting global change effects on forest biomass and composition in south-central Siberia. *Ecological Applications*, 20 (3), 700-715.

- Hamilton, R. A. Woodland Owner Notes: Forest Soils and Site Index. North Carolina Cooperative Extension Service, USDA.
- Hansen, J., Ruedy, R., Glascoe, J. and M. Sato. (1999). GISS analysis of surface temperature change. *Journal of Geophysical Research*, 104, 30997-31022.
- Hansen, M. C., Potapov, P. V., Moore, R., Hancher, M., Turubanova, S. A., Tyukavina, A., ... & Townshend, J. R. G. (2013). High-resolution global maps of 21st-century forest cover change. *Science*, 342 (6160), 850-853.
- Hayden, B. P. (1998). Ecosystem feedbacks on climate at the landscape scale. *Philosophical Transactions of the Royal Society of London B: Biological Sciences*, 353 (1365), 5-18.
- Hely, C., Flannigan, M., Bergeron, Y., & McRae, D. (2001). Role of vegetation and weather on fire behavior in the Canadian mixedwood boreal forest using two fire behavior prediction systems. *Canadian Journal of Forest Research*, 31 (3), 430-441.
- Hoffmann, C. W., & Usoltsev, V. A. (2002). Tree-crown biomass estimation in forest species of the Ural and of Kazakhstan. *Forest Ecology and Management*, 158 (1), 59-69.
- Hogg, E. H., Brandt, J. P., & Michaelian, M. (2008). Impacts of a regional drought on the productivity, dieback, and biomass of western Canadian aspen forests. *Canadian Journal of Forest Research*, 38 (6), 1373-1384.
- Hogg, E. H., & Hurdle, P. A. (1995). The aspen parkland in western Canada: a dry-climate analogue for the future boreal forest? Springer Netherlands. pp. 391-400.
- Holcomb, S. S. (2001). An examination of the riparian bottomland forest in North Central Texas through ecology, history, field study, and computer simulation (Doctoral dissertation, University of North Texas).
- Hollinger, D. Y., Ollinger, S. V., Richardson, A. D., Meyers, T. P., Dail, D. B., Martin, M. E., Scott, N. A., Arkebauer, T. J., Baldocchi, D. D., and K. L. Clark. (2010). Albedo estimates for land surface models and support for a new paradigm based on foliage nitrogen concentrations. *Global Change Biology*, 16, 696-710.
- Holm, J. A., Shugart, H. H., Van Bloem, S. J. and G. Larocque. (2012) Gap model validation in a subtropical dry forest and predicting poor transition of abandoned fields into secondary forests in Puerto Rico. *Ecological Modelling*, 233, 70-82.
- Holm, J. A., Chambers, J. Q., Collins, W. D., & Higuchi, N. (2014). Forest response to increased disturbance in the central Amazon and comparison to western Amazonian forests. *Biogeosciences*, 11 (20), 5773-5794.
- Holtmeier, F. K., & Broll, G. (2005). Sensitivity and response of northern hemisphere altitudinal and polar treelines to environmental change at landscape and local scales. *Global Ecology and Biogeography*, 14 (5), 395-410.
- Houghton, R. A., Butman, D., Bunn, A. G., Krainka, O. N., Schlesinger, P., and T. A. Stone. (2007). Mapping Russian forest biomass with data from satellites and forest inventories. *Environmental Research Letters*, 2, 045032, doi:10.1088/1748-9326/2/4/045032
- Huth, A., Ditzer, T., & Bossel, H. (1998). *The rain forest growth model FORMIX3: model description and analysis of forest growth and logging scenarios for the Deramakot Forest Reserve (Malaysia)*.
- Hüttich, C., Korets, M., Bartalev, S., Zharko, V., Schepaschenko, D., Shvidenko, A., and Schmullius, C. (2014): Exploiting Growing Stock Volume Maps for Large Scale Forest Resource Assessment: Cross-Comparisons of ASAR- and PALSAR-Based GSV Estimates with Forest Inventory in Central Siberia. *Forests*, 5 (8), 1753-1776.
- Hytteborn, H., Maslov, A.A., Nazimova, D.I. and L.P. Rysin (2005). Boreal Forests of Eurasia. In: F Andersson (editor) *Ecosystems of the World, 6: Coniferous Forests*. Elsevier B V, Amsterdam, Netherlands. p23-99.
- IPCC, 2007: Climate Change 2007: The Physical Science Basis. Contribution of Working Group I to the Fourth Assessment Report of the Intergovernmental Panel on Climate Change [Solomon, S., D. Qin, M. Manning, Z. Chen, M. Marquis, K.B. Averyt, M.Tignor and H.L. Miller (eds.)]. Cambridge University Press, Cambridge, United Kingdom and New York, NY, USA.
- IPCC, 2013: Climate Change 2013: The Physical Science Basis. Contribution of Working Group I to the Fifth Assessment Report of the Intergovernmental Panel on Climate Change [Stocker, T.G., Qin, D., Plattner, G.-K., Tignor,

M., Allen, S.K., Boschung, J., Nauels, A., Xia, Y., Bex, V. and P.M. Midgley (eds.)]. Cambridge University Press, Cambridge, UK and New York, NY, 1535 pp.

Isachenko, A. G. (1985). *Landscape of the USSR* (map atlas). Leningrad University Press, USSR, 320pp.

Isaev A.S., Ovchinnikova T.M., Pal'nikova E.N., Sukhovolski V.G. and O. V. Tarasova (2000) The influence of insects on boreal ecosystems under global climate change. - In: *Disturbance of Boreal Forest Ecosystem: Human Impacts and Natural Processes* (International Boreal Forest Research Association 1997 Annual Meeting Proceedings). US Department of Agriculture Forest Service. North Central Research Station General Technical Report NC-209, pp.115-123.

Isaev, A. S., Khlebopros, R. G., Nedorezov, L. V., Kondakov, Yu. P., Kiselev, V. V., and V. G. Sukhovol'sky. (2001). *Population dynamic of forest insects*. Nauka (Science), Moscow, Russia. (In Russian)

Isachenko, A.G., Shlyapnikov, A.A., Robozertseva, O.D., and A. Z. Filipetskaya (1988) The landscape map of the USSR. General Ministry of Geodesy and Cartography of the USSR, Moscow, USSR. (in Russian).

Istomov, S. V. (2005). The current dynamics of the upper treeline in West Sayan mountains, actual questions of research and protection of the plant world. Transactions of the Reserve - Tigiretsky, 211-214.

Ivanova, G. A., Ivanov, V. A., Kukavskaya, E. A., & Soja, A. J. (2010). The frequency of forest fires in Scots pine stands of Tuva, Russia. *Environmental Research Letters*, 5 (1), 015002.

Jackson, R. B., Randerson, J. T., Canadell, J. G., Anderson, R. G., Avissar, R., Baldocchi, D. D., ... & Pataki, D. E. (2008). Protecting climate with forests. *Environmental Research Letters*, 3 (4), 044006.

Jiang, H., Peng, C., Apps, M. J., Zhang, Y., Woodard, P. M. and Z. Wang (1999) Modelling the next primary productivity of temperate forest ecosystems in China with a GAP model. *Ecological Modelling*, 122, 225-238.

Johnstone, J. F., Chapin III, F. S., Foote, J., Kemmett, S., Price, K., & Viereck, L. (2004). Decadal observations of tree regeneration following fire in boreal forests. *Canadian Journal of Forest Research*, 34 (2), 267-273.

Jupp, T. E., Taylor, C. M., Balzter, H., & George, C. T. (2006). A statistical model linking Siberian forest fire scars with early summer rainfall anomalies. *Geophysical Research Letters*, 33 (14).

Kajimoto, T., Matsuura, Y., Sofronov, M. A., Volokitina, A. V., Mori, S., Osawa, A., & Abaimov, A. P. (1999). Above- and belowground biomass and net primary productivity of a *Larix gmelinii* stand near Tura, central Siberia. *Tree Physiology*, 19 (12), 815-822.

Kammer, P. M., Schöb, C., & Choler, P. (2007). Increasing species richness on mountain summits: Upward migration due to anthropogenic climate change or re-colonisation? *Journal of Vegetation Science*, 18 (2), 301-306.

Kashian, D. M., Romme, W. H., Tinker, D. B., Turner, M. G., & Ryan, M. G. (2006). Carbon storage on landscapes with stand-replacing fires. *BioScience*, 56 (7), 598-606.

Kasischke, E. S., Christensen, N. L., Jr. and Stocks, B. J. (1994). Fire, global warming and the mass carbon balance in boreal forests. *Ecological Applications*, 5, 437-451.

Kasischke, E. S. and N. H. F. French (1995) Locating and estimating the areal extent of wildfires in Alaskan boreal forests using multiple-season AVHRR NDVI composite data. *Remote Sensing of Environment*, 51, 263-275.

Kasischke E.S., Hyer E.J., French N.H.F., Suchinin A.I., Hewson J.H., Stocks B.J. (2004). Carbon emissions from boreal forest fires: 1996 to 2002. *Global Biogeochemical Cycles*, 19:GB1012, doi:10.1029/2004, GB002300

Keane, R. E., Austin, M., Field, C., Huth, A., Lexer, M. J., Peters, D., ... & Wyckoff, P. (2001). Tree mortality in gap models: application to climate change. *Climatic Change*, 51 (3-4), 509-540.

Kharuk, V. I., & Fedotova, E. V. (2003). Forest-tundra ecotone dynamics. Arctic environment variability in the context of global change, 281-299.

Kharuk, V. I., Ranson, K. J., Kuz'michev, V. V., & Im, S. T. (2003). Landsat-based analysis of insect outbreaks in southern Siberia. *Canadian Journal of Remote Sensing*, 29 (2), 286-297.

- Kharuk, V. I., Dvinskaya, M. L., & Ranson, K. J. (2005). The spatiotemporal pattern of fires in northern Taiga larch forests of central Siberia. *Russian Journal of Ecology*, 36 (5), 302-311.
- Kharuk, V. I., Ranson, K. J., Im, S. T., & Naurzbaev, M. M. (2006). Forest-tundra larch forests and climatic trends. *Russian Journal of Ecology*, 37 (5), 291-298.
- Kharuk, V. I., Ranson, K. and M. Dvinskaya. (2007). Evidence of evergreen conifer invasion into Larch dominated forests during recent decades in central Siberia. *Eurasian Journal of Forest Research*, 10, 163-171.
- Kharuk, V. I., Ranson, K. J., Sergey, T. I. and M. L. Dvinskaya. (2009). Response of *Pinus sibirica* and *Larix sibirica* to climate change in southern Siberian alpine forest-tundra ecotone. *Scandinavian Journal of Forest Research*, 24, 130-139.
- Kharuk, V. I., Im, S. T., & Dvinskaya, M. L. (2010a). Forest-tundra ecotone response to climate change in the Western Sayan Mountains, Siberia. *Scandinavian Journal of Forest Research*, 25 (3), 224-233.
- Kharuk, V. I., Ranson, K. J., Im, S. T., & Vdovin, A. S. (2010b). Spatial distribution and temporal dynamics of high-elevation forest stands in southern Siberia. *Global Ecology and Biogeography*, 19 (6), 822-830.
- Kharuk, V. I., Im, S. T., Dvinskaya, M. L., & Ranson, K. J. (2010c). Climate-induced mountain tree-line evolution in southern Siberia. *Scandinavian Journal of Forest Research*, 25 (5), 446-454.
- Kharuk V.I., Ranson K.J., and Dvinskaya M.L. (2010d) Wildfire dynamics in Mid-Siberian larch dominated forests. In: Balzter H (ed) *Environmental Change in Siberia*. Springer, London, pp 83-100.
- Kharuk, V. I., Ranson, K. J., Dvinskaya, M. L., & Im, S. T. (2011). Wildfires in northern Siberian larch dominated communities. *Environmental Research Letters*, 6 (4), 045208.
- Kharuk, V. I., Ranson, K. J., Oskorbin, P. A., Im, S. T., & Dvinskaya, M. L. (2013a). Climate induced birch mortality in Trans-Baikal lake region, Siberia. *Forest Ecology and Management*, 289, 385-392.
- Kharuk, V. I., Im, S. T., Oskorbin, P. A., Petrov, I. A., & Ranson, K. J. (2013b). Siberian pine decline and mortality in southern siberian mountains. *Forest Ecology and Management*, 310, 312-320.
- King, G. A., & Neilson, R. P. (1992). The transient response of vegetation to climate change: a potential source of CO<sub>2</sub> to the atmosphere. *Water, Air, and Soil Pollution*, 64 (1-2), 365-383.
- Kloepfel, B. D., Gower, S. T., Treichel, I. W., & Kharuk, S. (1998). Foliar carbon isotope discrimination in *Larix* species and sympatric evergreen conifers: a global comparison. *Oecologia*, 114 (2), 153-159.
- Knorre, A. A., Kirdyanov, A. V., & Vaganov, E. A. (2006). Climatically induced interannual variability in aboveground production in forest-tundra and northern taiga of central Siberia. *Oecologia*, 147 (1), 86-95.
- Kobak, K. I. (1988). Budyko, M. I. (ed). *Biotical compounds of carbon cycle*. Gidrometeoizdat, Leningrad, USSR.
- Kobayashi, H., Delbart, N., Suzuki, R., & Kushida, K. (2010). A satellite-based method for monitoring seasonality in the overstory leaf area index of Siberian larch forest. *Journal of Geophysical Research: Biogeosciences* (2005-2012), 115 (G1).
- Kohler, P., Chave, J., Riera, B., Huth, A. (2003). Simulating long-term response of tropical wet forests to fragmentation. *Ecosystems*, 6 (2), 0114-0128.
- Köhler, P., & Huth, A. (2007). Impacts of recruitment limitation and canopy disturbance on tropical tree species richness. *Ecological Modelling*, 203 (3), 511-517.
- Kohyama, T. (2005). Scaling up from shifting-gap mosaic to geographic distribution in the modeling of forest dynamics. *Ecological Research*, 20, 305-312.
- Kolchugina, T. P., & Vinson, T. S. (1995). Role of Russian forests in the global carbon balance. *Ambio*, 258-264.
- Kolosova, L.N., ed. (1982). Geographic Atlas for school teachers, 4th ed. General Ministry of Geodesy and Cartography of the USSR, Moscow, USSR. (in Russian)

- Kondakov, Y. (1974). Regularities of the Siberian moth outbreaks. Ecology of forest animal populations. Nauka, Novosibirsk, Russia. pp.206-265. (in Russian)
- Kondakov, Y.L. (2002). Massive outbreaks of Siberian silkworm in forests of Krasnoyarsky Krai. *Entomological Investigations in Siberia*, 2, 25-74. (in Russian)
- Körner, C. (1998). A re-assessment of high elevation treeline positions and their explanation. *Oecologia*, 115 (4), 445-459.
- Korovin, G. N. (1996). Analysis of the distribution of forest fires in Russia. In: *Fire in ecosystems of boreal Eurasia*. Springer Netherlands. pp. 112-128.
- Kotlyakov, V. and T. Khromova. (2002). Maps of permafrost and ground ice. In Stolbovoi V. and I. McCallum, eds. Land Resources of Russia. Laxenburg, Austria: International Institute for Applied Systems Analysis and the Russian Academy of Science. CD-ROM. Distributed by the National Snow and Ice Data Center, Boulder.
- Krankina, O. N., & Dixon, R. K. (1992). Forest management in Russia: challenges and opportunities in the era of perestroika. *Journal of Forestry (USA)*.
- Krankina, O. N., & Dixon, R. K. (1994). Forest management options to conserve and sequester terrestrial carbon in the Russian Federation. *World Resources Review*, 6 (1), 88-101.
- Krankina, O. N., Harmon, M. E., & Winjum, J. K. (1996). Carbon storage and sequestration in the Russian forest sector. *AMBIO*, 25, 284-288.
- Krankina, O. N., Houghton, R. A., Harmon, M. E., Hogg, E. H., Butman, D., Yatskov, M., Huso, M., Treyfeld, R. F., Razuvayev, V. N., and G. Spycher. (2005) Effects of climate, disturbance, and species on forest biomass across Russia. *Canadian Journal of Forest Research*, 35, 2281-2293.
- Kryuchkov, V.V. (1973). The effect of permafrost on the northern tree line. In Permafrost: Proceedings of the Second International Conference (USSR Contribution), pp.136-138. Washington, D.C.: National Academy of Science.
- Kukavskaya, E. A., Buryak, L. V., Ivanova, G. A., Conard, S. G., Kalenskaya, O. P., Zhila, S. V., & McRae, D. J. (2013). Influence of logging on the effects of wildfire in Siberia. *Environmental Research Letters*, 8 (4), 045034.
- Kukavskaya, E., Buryak, L. V., Conard, S. G., Petkov, A., Barrett, K., Kalenskaya, O. P., & Ivanova, G. (2014). Effects of Repeated Fires in the Forest Ecosystems of the Zabaikalye Region, Southern Siberia. In: AGU Fall Meeting Abstracts (Vol. 1, p. 0456).
- Kulagin, A. Y., Davydych, A. N., & Zaitsev, G. A. (2006). Specific features of the growth of Siberian spruce (*Picea obovata* Ledeb.) at early stages of ontogeny in broadleaf-conifer forests of the Ufa plateau. *Russian Journal of Ecology*, 37 (1), 66-69.
- Kull, O., & Tulva, I. (2000). Modelling canopy growth and steady-state leaf area index in an aspen stand. *Annals of forest science*, 57(5), 611-621.
- Kullman, L. (2000). Tree-limit rise and recent warming: a geoecological case study from the Swedish Scandes. *Norsk Geografisk Tidsskrift*, 54 (2), 49-59.
- Kullman, L. (2001). 20th century climate warming and tree-limit rise in the southern Scandes of Sweden. *Ambio: A journal of the Human Environment*, 30 (2), 72-80.
- Kullman, L. (2004). A face of global warming - "ice birches" and a changing alpine plant cover. *Geoöko*, 25, 181-202.
- Kullman, L., & Kjällgren, L. (2006). Holocene pine tree-line evolution in the Swedish Scandes: Recent tree-line rise and climate change in a long-term perspective. *Boreas*, 35 (1), 159-168.
- Kulmala, M., Suni, T., Lehtinen, K. E. J., Maso, M. D., Boy, M., Reissell, A., ... & Hari, P. (2004). A new feedback mechanism linking forests, aerosols, and climate. *Atmospheric Chemistry and Physics*, 4 (2), 557-562.
- Kurz, W. A., Apps, M. J., Stocks, B. J., & Volney, W. J. A. (1995a). *Global climate change: disturbance regimes and biospheric feedbacks of temperate and boreal forests*. Oxford University Press, New York. p199-133.

- Kurz, W. A., Apps, M. J., Beukema, S. J., & Lekstrum, T. (1995b). 20th century carbon budget of Canadian forests. *Tellus B*, 47 (1-2), 170-177.
- Kurz, W. A. and M. J. Apps (1999) A 70-year retrospective analysis of carbon fluxes in the Canadian forest sector. *Ecological Applications*, 9, 526-547.
- Kurz, W. A., Dymond, C. C., Stinson, G., Rampley, G. J., Neilson, E. T., Carroll, A. L., ... & Safranyik, L. (2008). Mountain pine beetle and forest carbon feedback to climate change. *Nature*, 452 (7190), 987-990.
- Kuusinen, N., Tomppo, E., Shuai, Y., & Berninger, F. (2014). Effects of forest age on albedo in boreal forests estimated from MODIS and Landsat albedo retrievals. *Remote Sensing of Environment*, 145, 145-153.
- Landsberg, J. J., & Gower, S. T. (1997). *Applications of physiological ecology to forest management*. Academic Press.
- Larcher, W. (1995). *Plant physiological ecology*. Springer, Berlin, Germany.
- Larocque, G. R., Archambault, L. and C. Delisle. (2006) Modelling forest succession in two southeastern Canadian mixedwood ecosystem types using the ZELIG model. *Ecological Modelling*, 199, 350-362.
- Larocque, G. R., Archambault, L. and C. Delisle. (2011) Development of the gap model ZELIG-CFS to predict the dynamics of American mixed forest types with complex structures. *Ecological Modelling*, 222, 2570-2583.
- Larocque, G.R., H.H. Shugart, W. Xi and J.A. Holm. (2016). Forest succession models (in press). G.R. Larocque (ed.), *Ecological Forest Management Handbook*. CRC Press, Taylor and Francis Group, London.
- Lauenroth, W. K., Urban, D. L., Coffin, D. P., Parton, W. J., Shugart, H. H., Kirchner, T. B., and T. M. Smith (1993) Modeling vegetation structure - ecosystem process interactions across sites and ecosystems. *Ecological Modelling*, 67, 49-80.
- Laurance, W. F., Delamônica, P., Laurance, S. G., Vasconcelos, H. L., & Lovejoy, T. E. (2000). Conservation: rainforest fragmentation kills big trees. *Nature*, 404 (6780), 836-836.
- Laurance, W. F., Lovejoy, T. E., Vasconcelos, H. L., Bruna, E. M., Didham, R. K., Stouffer, P. C., ... & Sampaio, E. (2002). Ecosystem decay of Amazonian forest fragments: a 22-year investigation. *Conservation Biology*, 16 (3), 605-618.
- Laurance, W. F. (2008). Theory meets reality: how habitat fragmentation research has transcended island biogeographic theory. *Biological Conservation*, 141 (7), 1731-1744.
- Law, B. E. (2014). Regional analysis of drought and heat impacts on forests: current and future science directions. *Global Change Biology*, 20 (12), 3595-3599.
- Lawrence, P. J., Feddema, J. J., Bonan, G. B., Meehl, G. A., O'Neill, B. C., Oleson, K. W., ... & Thornton, P. E. (2012). Simulating the biogeochemical and biogeophysical impacts of transient land cover change and wood harvest in the Community Climate System Model (CCSM4) from 1850 to 2100. *Journal of Climate*, 25 (9), 3071-3095.
- Le Toan, T., Beaudoin, A., Riou, J., & Guyon, D. (1992). Relating forest biomass to SAR data. *Geoscience and Remote Sensing, IEEE Transactions on*, 30 (2), 403-411.
- Leemans, R. and Prentice, I. C. (1989) *FORSKA, a General Forest Succession Model*. Institute of Ecological Botany, Uppsala, pp. 70.
- Lenoir, J., Gégout, J. C., Marquet, P. A., De Ruffray, P., & Brisse, H. (2008). A significant upward shift in plant species optimum elevation during the 20th century. *Science*, 320 (5884), 1768-1771.
- Lindroth, A., Grelle, A., & Morén, A. S. (1998). Long-term measurements of boreal forest carbon balance reveal large temperature sensitivity. *Global Change Biology*, 4 (4), 443-450.
- Lindroth, A., Lagergren, F., Aurela, M., Bjarnadottir, B., Christensen, T., Dellwik, E., ... & Vesala, T. (2008). Leaf area index is the principal scaling parameter for both gross photosynthesis and ecosystem respiration of Northern deciduous and coniferous forests. *Tellus B*, 60 (2), 129-142.
- Liu, J., & Ashton, P. S. (1998). FORMOSAIC: an individual-based spatially explicit model for simulating forest dynamics in landscape mosaics. *Ecological Modelling*, 106 (2), 177-200.

- Liu, H., Randerson, J. T., Lindfors, J., & Chapin, F. S. (2005). Changes in the surface energy budget after fire in boreal ecosystems of interior Alaska: An annual perspective. *Journal of Geophysical Research: Atmospheres* (1984-2012), 110 (D13).
- Loboda, T. V., & Csiszar, I. A. (2007). Reconstruction of fire spread within wildland fire events in Northern Eurasia from the MODIS active fire product. *Global and Planetary Change*, 56 (3), 258-273.
- Logan, J. A., J. Régnière and J. A. Powell (2003) Assessing the impacts of global warming on forest pest dynamics. *Frontiers in Ecology and in the Environment*, 1, 130-137.
- Luyssaert, S., Schulze, E. D., Börner, A., Knöhl, A., Hessenmöller, D., Law, B. E., ... & Grace, J. (2008). Old-growth forests as global carbon sinks. *Nature*, 455 (7210), 213-215.
- Lyamzev, N. and A. Isaev (2002) in Stolbovoi and McCallum.
- Lydolph, P. E. (1977). *Climates of the Soviet Union. World Survey of Climatology*, vol. 7. Elsevier Scientific Publishing Company, New York.
- Ma, Z., Peng, C., Zhu, Q., Chen, H., Yu, G., Li, W., ... & Zhang, W. (2012). Regional drought-induced reduction in the biomass carbon sink of Canada's boreal forests. *Proceedings of the National Academy of Sciences*, 109 (7), 2423-2427.
- MacDonald, G. M., Velichko, A. A., Kremenetski, C. V., Borisova, O. K., Goleva, A. A., Andreev, A. A., Cwynar, L.C., Riding, R.T., Forman, S.L., Edwards, T.W.D., Aravena, R., Hammarlund, D., Szeicz, J.M., and Gattaulin, V. N. (2000). Holocene treeline history and climate change across northern Eurasia. *Quaternary Research*, 53 (3), 302-311.
- Malevsky-Malevich, S. P., Molkentin, E. K., Nadyozhina, E. D., & Shklyarevich, O. B. (2008). An assessment of potential change in wildfire activity in the Russian boreal forest zone induced by climate warming during the twenty-first century. *Climatic Change*, 86 (3-4), 463-474.
- Malysheva, N.V. (1993). Forest density map. In: *Ecological Atlas of Russia* (2002). Kiselyova, N.M., ed. "Karta" Publishing House, St. Petersburg, Russia.
- Manabe, S. and R. J. Stouffer (1980) Sensitivity of a global climate to an increase in  $CO_2$  concentration in the atmosphere. *Journal of Geophysical Research*, 85, 5529-5554.
- Mankin, J B, R V O'Neil, H H Shugart and B W Rust (1977). The importance of validation in ecosystem analysis. In: G. S. Innis (editor) *New Directions in the Analysis of Ecological Systems, Part I: Simulation Councils*, La Jolla, CA. p63-71.
- Matsumoto, K., Ohta, T., Nakai, T., Kuwada, T., Daikoku, K. I., Iida, S. I., ... & Hattori, S. (2008). Energy consumption and evapotranspiration at several boreal and temperate forests in the Far East. *Agricultural and Forest Meteorology*, 148 (12), 1978-1989.
- Maximov, T., Ohta, T., & Dolman, A. J. (2008). Water and energy exchange in East Siberian forest: A synthesis. *Agricultural and Forest Meteorology*, 148 (12), 2013-2018.
- McDowell, N. G., Beerling, D. J., Breshears, D. D., Fisher, R. A., Raffa, K. F., & Stitt, M. (2011). The interdependence of mechanisms underlying climate-driven vegetation mortality. *Trends in Ecology & Evolution*, 26 (10), 523-532.
- Meleshko, V. P., Kattsov, V. M., Govorkova, V. A., Sporyshev, P. V., Shkol'nik, I. M., & Shneerov, B. E. (2008). Climate of Russia in the 21st century. Part 3. Future climate changes calculated with an ensemble of coupled atmosphere-ocean general circulation CMIP3 models. *Russian Meteorology and Hydrology*, 33 (9), 541-552. (in Russian)
- Messier, C., Smith, D. W., & Adamowicz, W. L. (Eds.). (2003). *Towards sustainable management of the boreal forest*. Ottawa, Ont: NRC Research Press. pp. 1-40
- METI and NASA Release Version 2 ASTER Global DEM (2011). U.S. Geological Survey / NASA LP DAAC. Retrieved 13 November 2013.
- Miao, Z., & Li, C. (2007). *Biomass estimates for major boreal forest species in west-central Canada* (Vol. 2). Canadian Wood Fibre Centre.

- Mielke, D.L., Shugart, H.H., and D.C. West. (1978) Stand model for upland forests of Southern Arkansas (No. ORNL/TM-6225). Oak Ridge National Lab, Tennessee, USA.
- Milakovskiy, B., Frey, B., & James, T. (2012). Carbon dynamics in the boreal forest. In: *Managing Forest Carbon in a Changing Climate*. Springer Netherlands. p 109-135.
- Miller, C. and D. L. Urban (1999) A model of surface fire, climate and forest pattern in the Sierra Nevada, California. *Ecological Modelling*, 114, 113-135.
- Mitrofanov D. P. (1977) *Chemical composition of forest plants in Siberia*. Nauka, Novosibirsk, USSR. 120 pp. (in Russian)
- Mladenoff, D. J., & He, H. S. (1999). Design, behavior and application of LANDIS, an object-oriented model of forest landscape disturbance and succession. Spatial modeling of forest landscape change: approaches and applications. Cambridge University Press, Cambridge, UK, 125-162.
- Mladenoff, D. J. (2004). LANDIS and forest landscape models. *Ecological Modelling*, 180 (1), 7-19.
- Moiseev, P. A. (2002). Effect of climatic changes on radial increment and age structure formation in high-mountain larch forests of the Kuznetsk Ala Tau. *Russian Journal of Ecology*, 33 (1), 7-13.
- Mokhov, I. I., Chernokulsky, A. V., & Shkolnik, I. M. (2006, December). Regional model assessments of fire risks under global climate changes. In: *Doklady earth sciences* (Vol. 411, No. 2, pp. 1485-1488). MAIK Nauka/Interperiodica.
- Mokhov, I. I., & Chernokulsky, A. V. (2010). Regional model assessments of forest fire risks in the Asian part of Russia under climate change. *Geography and Natural Resources*, 31 (2), 165-169.
- Mollicone, D., Eva, H. D., & Achard, F. (2006). Ecology: human role in Russian wild fires. *Nature*, 440 (7083), 436-437.
- Monserud, R. A., Tchekabakova, N. M., & Leemans, R. (1993). Global vegetation change predicted by the modified Budyko model. *Climatic Change*, 25 (1), 59-83.
- Monserud, R. A., & Tchekabakova, N. M. (1996). A vegetation model for the Sayan Mountains, southern Siberia. *Canadian Journal of Forest Research*, 26 (6), 1055-1068.
- Monsi, M., Uchijima, Z., & Oikawa, T. (1973). Structure of foliage canopies and photosynthesis. *Annual Review of Ecology and Systematics*, 301-327.
- Morris, R. F. (1963). The dynamics of epidemic spruce budworm populations. *Memoirs of the Entomological Society of Canada*, 95 (31), 1-12.
- Nakai, Y., Matsuura, Y., Kajimoto, T., Abaimov, A. P., Yamamoto, S., & Zyryanova, O. A. (2008). Eddy covariance  $CO_2$  flux above a Gmelin larch forest on continuous permafrost in Central Siberia during a growing season. *Theoretical and Applied Climatology*, 93 (3-4), 133-147.
- National Climate Data Center (NCDC). (1998). Technical Report 98-03. Available from NOAA National Climatic Data Center, Asheville, NC, USA.
- National Climate Data Center (NCDC). (2005a). Global Synoptic Climatology Network C the former USSR Version 1.0. Available from NOAA National Climatic Data Center, Asheville, NC, USA.
- National Climate Data Center (NCDC). (2005b). Daily and sub-daily precipitation for the former USSR Version 1.0. Available from NOAA National Climatic Data Center, Asheville, NC, USA.
- Neigh, C. S., Nelson, R. F., Ranson, K. J., Margolis, H. A., Montesano, P. M., Sun, G., ... & Andersen, H. E. (2013). Taking stock of circumboreal forest carbon with ground measurements, airborne and spaceborne LiDAR. *Remote Sensing of Environment*, 137, 274-287.
- Ninemets, U., PORTSMUTH, A., & Truu, L. (2002). Leaf structural and photosynthetic characteristics, and biomass allocation to foliage in relation to foliar nitrogen content and tree size in three Betula species. *Annals of Botany*, 89 (2), 191-204.

- Nikolov N. and H. Helmisaari. (1992). Silvics of the circumpolar boreal forest tree species, pp 9-84. In: Shugart H. H., R. Leemans and G.B. Bonan (eds). *A systems analysis of the global boreal forest*. Cambridge University Press, Cambridge, UK.
- Noskova, N.E. and I.N. Tretyakova. (2006). The effects of stress on reproductive abilities of pine. *Conifers of the Boreal Zone*, 23 (3), 54-63.
- Noskova, N.E., Tretyakova, I.N., and E.N. Muratova. (2009) Microsporogenesis and pollen formation in Scotch pine (*Pinus sylvestris* L.) under modern climatic conditions of Siberia. *Biology Bulletin*, 36 (3), 317-322.
- Ogureeva, G.N. (1973). *Botanical geography of Altay*. Russian Academy of Sciences Press, Moscow, USSR. 188p.
- Ohta, T., Maximov, T. C., Dolman, A. J., Nakai, T., van der Molen, M. K., Kononov, A. V., ... & Yabuki, H. (2008). Interannual variation of water balance and summer evapotranspiration in an eastern Siberian larch forest over a 7-year period (1998-2006). *Agricultural and Forest Meteorology*, 148 (12), 1941-1953.
- Oker-Blom, P. (1986). Photosynthetic radiation regime and canopy structure in modeled forest stands. *Acta Forestalia Fennica*, 197, 1-44.
- Olchev, A., & Novenko, E. (2011). Estimation of potential and actual evapotranspiration of boreal forest ecosystems in the European part of Russia during the Holocene. *Environmental Research Letters*, 6 (4), 045213.
- Oleson KW, Lawrence DM, Bonan GB et al. (2013) Technical Description of Version 4.5 of the Community Land Model (CLM), pp. 308-310. National Center for Atmospheric Research, Boulder, CO.
- Ollinger, S. V., Richardson, A. D., Martin, M. E., Hollinger, D. Y., Frolking, S. E., Reich, P. B., ... & Schmid, H. P. (2008). Canopy nitrogen, carbon assimilation, and albedo in temperate and boreal forests: Functional relations and potential climate feedbacks. *Proceedings of the National Academy of Sciences*, 105 (49), 19336-19341.
- Onuchin, V.S. (1962). Several morphological features of Siberian larch in Tuva. In: *Larch: compilation*. Krasnoyarsk: STI, 29(1), 22-35. (in Russian)
- Onuchin A. A. (1986). Transformation of solid precipitation with forests of Khamar-Daban Mountains: Dissertation. Krasnoyarsk: V.N. Sukachev Forest Institute, 182 p. (in Russian).
- Osawa, A., Zyryanova, O. A., Matsuura, Y., Kajimoto, T., and R. W. Wein (2010). *Permafrost Ecosystems: Siberian Larch Forests, Ecological Studies*. Springer, New York, NY.
- Ovchinnikov, D.V. and E.A. Vaganov (1999). Dendrochronological characteristics of *Larix sibirica* L. at the upper treeline in Mountain Altai. *Nauka*, 6 (2), 145-152. (in Russian)
- Pabst, R. J., Goslin, M. N., Spies, T. A., and S. L. Garman. (2006). Use of the ZELIG forest simulation model in the coastal landscape analysis and modeling study (CLAMS). Presentation to Spanish forestry researchers (Sept 22, 2006), Corvallis, OR.
- Pabst, R. J., Goslin, M. N., Garman, S. L., & Spies, T. A. (2008). Calibrating and testing a gap model for simulating forest management in the Oregon Coast Range. *Forest Ecology and Management*, 256 (5), 958-972.
- Pacala, S. W., Canham, C. D., & Silander Jr, J. A. (1993). Forest models defined by field measurements: I. The design of a northeastern forest simulator. *Canadian Journal of Forest Research*, 23 (10), 1980-1988.
- Pastor, J. and W. M. Post. (1986). Influence of climate, soil moisture, and succession on forest carbon and nitrogen cycles. *Biogeochemistry*, 2, 3-27.
- Pastor, J. and W. M. Post. (1988). Response of northern forests to  $CO_2$ -induced climate change. *Letters to Nature*, 334, 55-58.
- Patenaude, G., Hill, R. A., Milne, R., Gaveau, D. L., Briggs, B. B. J., & Dawson, T. P. (2004). Quantifying forest above ground carbon content using LiDAR remote sensing. *Remote Sensing of Environment*, 93 (3), 368-380.
- Pautova V. N. (1976). Aboveground plant mass and transpiration of some communities in forest-tundra zone. *Transactions of Limnological Institute of SO AN USSR*, 22 (42), 92-128. (in Russian)

- Petrov, V. V., & N. B. Ponomareva (1977). Initial States of Secondary Successional Growth Post Fire in Coniferous Forest. *Vestnik Moskovskogo Universiteta: Biologiya*, Moscow State University Press, Moscow, USSR.
- Pielke, R. A., & Vidale, P. L. (1995). The boreal forest and the polar front. *Journal of Geophysical Research: Atmospheres* (1984-2012), 100 (D12), 25755-25758.
- Polikarpov, N. P., Chebakova, N. M., & Nazimova, D. I. (1986). *Klimat i gornye lesa Sibiri* (Climate and mountain forests of Siberia). Nauka Publishing House, Novosibirsk, USSR.
- Post, W. M. and J. Pastor (1996) Linkages - an individual-based forest ecosystem model. *Climatic Change*, 34, 253-261.
- Prentice, K. C. and I Y. Fung (1990). The sensitivity of terrestrial carbon storage to climate change. *Nature*, 346, 48-51.
- Prentice, I. C., Sykes, M. T., & Cramer, W. (1993). A simulation model for the transient effects of climate change on forest landscapes. *Ecological Modelling*, 65 (1), 51-70.
- Purves, D. and S. Pacala (2008). Predictive Models of Forest Dynamics Science, *Science*, 320 (5882) 1452-1453.
- Purves, D.W., Lichstein, J.W., Strigul, N, and S.W. Pacala. (2008). Predicting and understanding forest dynamics using a simple tractable model. *Proceedings of the National Academy of Sciences*, 105 (44), 17-18-17022.
- Radkevich, V. A. (1997) *Ecology textbook*. 3rd ed. Ministry of Higher Education. 159pp.
- Rakovskaya, E.M., and M.I. Davydova. (1990). *Physical Geography of USSR*, v2. "Akademiya" Publishing House, Moscow, USSR.
- Randerson, J. T., Liu, H., Flanner, M. G., Chambers, S. D., Jin, Y., Hess, P. G., ... & Zender, C. S. (2006). The impact of boreal forest fire on climate warming. *Science*, 314 (5802), 1130-1132.
- Reimers, N.F. (1990). *Nature utilization: dictionary-encyclopedia*. Thought Press, Moscow, USSR.
- Reiners, W. A., & Driese, K. L. (2004). *Transport processes in nature: propagation of ecological influences through environmental space* (Vol. 1). Cambridge University Press.
- Repola, J., Ojansuu, R., & Kukkola, M. (2007). Biomass functions for Scots pine, Norway spruce and birch in Finland. In: *Working Papers of the Finnish Forest Research Institute* 53. Finnish Forest Research Institute.
- Resler, L. M., Butler, D. R., & Malanson, G. P. (2005). Topographic shelter and conifer establishment and mortality in an alpine environment, Glacier National Park, Montana. *Physical Geography*, 26 (2), 112-125.
- Rogers, B. M., Soja, A. J., Goulden, M. L., & Randerson, J. T. (2015). Influence of tree species on continental differences in boreal fires and climate feedbacks. *Nature Geoscience*.
- Röser, C., Montagnani, L., Schulze, E. D., Mollicone, D., Kolle, O., Meroni, M., et al. (2002). Net  $CO_2$  exchange rates in three different successional stages of the Dark Taiga of central Siberia. *Tellus B*, 54 (5), 642-654.
- Running, S. W., Nemani, R. R. and R. D. Hungerford (1987) Extrapolation of synoptic meteorological data in mountainous terrain and its use for simulating forest evapotranspiration and photosynthesis. *Canadian Journal of Forest Research*, 17, 472-483.
- Samoilova, G. S. (1973). *Types of landscapes in mountains of Southern Siberia*. Neklyudova, M.P., ed. Moscow State University Press, Moscow, USSR. (in Russian)
- SAS v9.3 (2010) SAS Institute Inc., Cary, NC, USA.
- Savva, Y. V., Schweingruber, F. H., Vaganov, E. A., & Milyutin, L. I. (2003). Influence of climate changes on treering characteristics of Scots pine provenances in southern Siberia (forest-steppe). *IAWA Journal*, 24 (4), 371-383.
- Scheller, R.M., and J.B. Domingo. (2012) LANDIS-II Base Fire v3.0 Extension User Guide. University of Wisconsin, Madison, Wisconsin, USA. (<http://www.landis-ii.org/extensions/base-fire>)
- Scholze, M., Knorr, W., Arnell, N. W., & Prentice, I. C. (2006). A climate-change risk analysis for world ecosystems. *Proceedings of the National Academy of Sciences*, 103 (35), 13116-13120.

- Schepashenko, D., Shvidenko, A., & Nilsson, S. (1998). Phytomass (live biomass) and carbon of Siberian forests. *Biomass and Bioenergy*, 14 (1), 21-31.
- Schepaschenko D, McCallum I, Shvidenko A, Fritz S, Kraxner F, Obersteiner M (2010) A new hybrid land cover dataset for Russia: a methodology for integrating statistics, remote sensing and in-situ information. *J Land Use Sci*. doi: 10.1080/1747423X.2010.511681 (Published online 22 Dec 2010)
- Schulze, E. D. (1982). Plant life forms and their carbon, water and nutrient relations. In: *Physiological Plant Ecology* II. Springer Berlin Heidelberg. pp. 615-676.
- Schulze, E. D., Schulze, W., Koch, H., Arneth, A., Bauer, G., Kelliher, F. M., ... & Issajev, A. (1995). Aboveground biomass and nitrogen nutrition in a chronosequence of pristine Dahurian Larix stands in eastern Siberia. *Canadian Journal of Forest Research*, 25 (6), 943-960.
- Schulze, E. D., Vygodskaya, N. N., Tchekabakova, N. M., Czimczik, C. I., Kozlov, D. N., Lloyd, J., ... & Wirth, C. (2002). The Eurosiberian Transect: an introduction to the experimental region. *Tellus B*, 54 (5), 421-428.
- Schulze ED, Wirth C, Mollicone D, Ziegler W. (2005). Succession after stand replacing disturbances by fire, wind throw, and insects in the dark taiga of Central Siberia. *Oecologia*, 146 (1), 77-88.
- Schuur, E. A. G., McGuire, A. D., Schädel, C., Grosse, G., Harden, J. W., Hayes, D. J., ... & Vonk, J. E. (2015). Climate change and the permafrost carbon feedback. *Nature*, 520 (7546), 171-179.
- Scurlock, J. M. O., Asner, G. P., & Gower, S. T. (2001). Worldwide historical estimates of leaf area index, 1932-2000. ORNL Technical Memorandum ORNL/TM-2001/268. Oak Ridge National Laboratory, Oak Ridge, Tenn. <http://www.osti.gov/bridge>.
- Sedel'nikov, V.P. (1979) *Flora and vegetation of high-mountain areas in the Kusnetsk Altay*. Nauka, Novosibirsk, USSR. (in Russian)
- Seedre, M., Taylor, A. R., Chen, H. Y. H., and K. Jogiste. (2013). Deadwood density of five boreal tree species in relation to field-assignment decay class. *Forest Science*, 59 (3), 261-266.
- Serreze, M. C., Walsh, J. E., Chapin, F. S., III, Osterkamp, T., Dyurgerov, M., Romanovsky, V., Oechel, W. C., Morison, J., Zhang, T., and R. G. Barry (2000) Observational evidence of recent change in the Northern high-latitude environment. *Climatic Change*, 46, 159-207.
- Shibistova, O., Lloyd, J. O. N., Evgrafova, S., Savushkina, N., Zrazhevskaya, G., Arneth, A., ... & SCHULZE, E. D. (2002a). Seasonal and spatial variability in soil  $CO_2$  efflux rates for a central Siberian *Pinus sylvestris* forest. *Tellus B*, 54 (5), 552-567.
- Shibistova, O., Lloyd, J., Zrazhevskaya, G., Arneth, A., Kolle, O., Knohl, A., ... & Schmerler, J. (2002b). Annual ecosystem respiration budget for a *Pinus sylvestris* stand in central Siberia. *Tellus B*, 54 (5), 568-589.
- Shinozaki, K., Yoda, K., Hozumi, K., & Kira, T. (1964). A quantitative analysis of plant form-the pipe model theory: I. Basic analyses. *Japanese Journal of Ecology*, 14 (3), 97-105.
- Shugart, H. H. and D. C. West (1977) Development of an Appalachian deciduous forest succession model and its application to assessment of the impact of the chestnut blight. *Journal of Environmental Management*, 5, 161-179.
- Shugart, H. H. and D. C. West (1979) Size and pattern of simulated forest stands. *Forest Science*, 25, 120-122.
- Shugart, H.H. and D.C. West (1980). Forest Succession models. *Biosciences*, 30, 308-313.
- Shugart, H. H. (1984). *A theory of forest dynamics*. Springer-Verlag, New York.
- Shugart, H.H., Antonovsky, M.J., Jarvis P.G., and Sandford A.P. (1986).  $CO_2$ , climatic change and forest ecosystems: Assessing the response of global forests to the direct effects of increasing  $CO_2$  and climatic change pp. 475-521. In: *The Greenhouse Effect, Climatic Change and Ecosystems (SCOPE 29)* eds. Bolin, B., Döös, B.R., Jager J. and Warrick R.A. (eds). John Wiley & Sons, New York.
- Shugart, H. H. (1987). Dynamic Ecosystem Consequences of Tree Birth and Death Patterns. *Biosciences*, 37 (8), 596-601.

- Shugart, H.H., Bonan, G.B. & Rastetter, E.B. (1988a). Niche theory and community organization. *Canadian Journal of Botany*, 66, 2634-2639.
- Shugart, H.H., P.J. Michaels, T.M. Smith, D.A. Weinstein and E.B. Rastetter. (1988b). Simulation Models of Forest Succession. In: T. Rosswall, R.G. Woodmansee and P.G. Risser (eds.), *Scales and Global Changes: Spatial and Temporal Variability in Biospheric and Geospheric Processes*. John Wiley and Sons, Ltd., London. pp. 125-151.
- Shugart, H. H., Leemans, R. and G. B. Bonan, eds. (1992a). *A Systems Analysis of the Global Boreal Forest*. Cambridge University Press, Cambridge.
- Shugart, H. H., Smith, T. M. and W. M. Post. (1992b). The potential for application of individual-based simulation models for assessing the effects of global change. *Annual Reviews of Ecology and Systematics*, 23, 15-38.
- Shugart, H. H., Emanuel, W. R. and G. Shao. (1996). Models of forest structure for conditions of climatic change. *Commonwealth Forestry Review*, 75, 51-64.
- Shugart, H. H. (1998). *Terrestrial ecosystems in changing environments*. Cambridge University Press, Cambridge.
- Shugart, H. H. (2000). The importance of structure in the longer-term dynamics of ecosystems. *Journal of Geophysical Research - Atmospheres*, 105, 20065-20075.
- Shugart, H. H. (2003). *A theory of forest dynamics: The ecological implications of forest succession models*. Blackburn Press, Caldwell, NJ.
- Shugart, H. H., Shuman, J. K., Yan, X., and N. Zhang. (2006). Eurasian forest cover and climate feedbacks. *iLEAPS Newsletter*, 3, 20-21.
- Shugart, H. H. (2007). *How the earthquake bird got its name and other tales of an unbalanced nature*. Yale University Press, USA.
- Shugart, H. H. and F. I. Woodward. (2011). *Global Change and the Terrestrial Biosphere: Achievements and Challenges*. Wiley-Blackwell, Oxford, UK.
- Shkol'nik, I., V. Meleshko, S. Efimov, and E. Stafeeva, (2012). Changes in climate extremes on the territory of Siberia by the middle of the 21st century: An ensemble forecast based on the MGO regional climate model. *Russian Meteorology and Hydrology*, 37, 71-84.
- Shuman, J.K. and H. H. Shugart. (2009). Evaluating the sensitivity of Eurasian forest biomass to climate change using a dynamic vegetation model. *Environmental Research Letters*, 4, 045024.
- Shuman, J.K. (2010). Dissertation: Russian forest dynamics and response to changing climate: A simulation study. University of Virginia, Charlottesville, VA.
- Shuman, J. K., H. H. Shugart and T. L. O'Halloran. (2011). Sensitivity of Siberian larch forest to climate change. *Global Change Biology*, 17, 2370-2384.
- Shumilova, L. V. (1962). *Botanical geography of Siberia*. Tomsk State University, Tomsk, USSR. 440p.
- Shvidenko, A. Z., & Nilsson, S. (2000). Fire and the carbon budget of Russian forests. In: *Fire, climate change, and carbon cycling in the boreal forest*. Springer New York. pp. 289-311.
- Shvidenko, A., & Nilsson, S. (2002). Dynamics of Russian forests and the carbon budget in 1961-1998: An assessment based on long-term forest inventory data. *Climatic change*, 55 (1-2), 5-37.
- Shvidenko, A. and S. Nilsson. (2003). Dynamics of Russian forests and the carbon budget in 1961-1998: An assessment based on long-term forest inventory data. *Climatic change*, 55 (1-2), 5-37.
- Shvidenko, A. and S. Nilsson. (2003b). A synthesis of the impact of Russian forests on the global carbon budget for 1961-1998. *Tellus*, 55B, 391-415.
- Shvidenko, A. Z., Schepaschenko, D. G., Nilsson, C., and Yu. I. Buluy. (2006). *Tables and models of growth and productivity of forests of major forest forming species of northern Eurasia* (standard and reference materials). Ministry of Natural Resources of the Russian Federation, Moscow, Russia.

- Simard, M., Pinto, N., Fisher, J. B., & Baccini, A. (2011). Mapping forest canopy height globally with spaceborne lidar. *Journal of Geophysical Research: Biogeosciences* (2005-2012), 116 (G4).
- Sitch, S., Huntingford, C., Gedney, N., Levy, P. E., Lomas, M., Piao, S. L., ... & Woodward, F. I. (2008). Evaluation of the terrestrial carbon cycle, future plant geography and climate-carbon cycle feedbacks using five Dynamic Global Vegetation Models (DGVMs). *Global Change Biology*, 14 (9), 2015-2039.
- Smith, T. M. and D. L. Urban. (1988). Scale and the resolution of forest structural pattern. *Vegetatio*, 74, 143-150.
- Smith, T. M., Shugart, H. H., Bonan, G. B., and J. B. Smith. (1992). Modeling the potential response of vegetation to global climate change. *Advances in Ecological Research*, 22, 93-116.
- Smith, T. M. and H. H. Shugart. (1993). The transient response of terrestrial carbon storage to a perturbed climate. *Nature*, 361, 523-526.
- Smith, W. K., Hinckley, T. M., & Ewel, K. C. (1995). Ecophysiology of coniferous forests. *Trends in Ecology and Evolution*, 10 (8), 343.
- Sofronov, M.A., Sofronova, T.M., and A.V. Volokitina. (2004). Evaluation of fire danger based on weather conditions using meteorological forecasts. *Lesnoe Khozaistvo*, 6, 31-32. (in Russian)
- Soja, A. J., Cofer, W. R., Shugart, H. H., Sukhinin, A. I., Stackhouse, P. W., McRae, D. J., and S. G. Conard. (2004). Estimating fire emissions and disparities in boreal Siberia (1998-2002). *Journal of Geophysical Research*, 109 (D14S06) doi:10.1029/2004JD004570.
- Soja, A. J., Shugart, H. H., Sukhinin, A., Conard, S., & Stackhouse Jr, P. W. (2006). Satellite-derived mean fire return intervals as indicators of change in Siberia (1995-2002). *Mitigation and Adaptation Strategies for Global Change*, 11 (1), 75-96.
- Soja, A. J., Tchekakova, N. M., French, N. H., Flannigan, M. D., Shugart, H. H., Stocks, B. J., Sukhinin, A. I., Parfenova, E. I., and F. S. Chapin III. (2007). Climate-induced boreal forest change: Predictions versus current observations. *Global and Planetary Change*, 56, 274-296.
- Solomon, A. M. (1986). Transient Response of Forests to  $CO_2$  Induced Climate Change: Simulation Modeling Experiments in Eastern North America. *Oecologia*, 68, 567-579.
- Spracklen, D. V., Bonn, B., & Carslaw, K. S. (2008). Boreal forests, aerosols and the impacts on clouds and climate. *Philosophical Transactions of the Royal Society A: Mathematical, Physical and Engineering Sciences*, 366 (1885), 4613-4626.
- Stepanovskikh, A. S. (2003) *Applied Ecology: preservation of environment*. Unity-Dana Press, Moscow, Russia.
- Stevens, G. C., & Fox, J. F. (1991). The causes of treeline. *Annual Review of Ecology and Systematics*, 177-191.
- Stocks, B. J., Fosberg, M. A., Lynham, T. J., Mearns, L., Wotton, B. M., Yang, Q., ... & McKenney, D. W. (1998). Climate change and forest fire potential in Russian and Canadian boreal forests. *Climatic Change*, 38 (1), 1-13.
- Stolbovoi, V. and I. McCallum, eds. (2002). CD-ROM Land Resources of Russia. International Institute for Applied Systems Analysis and the Russian Academy of Science, Laxenburg, Austria.
- Stolbovoi, V. and I. Savin. (2002). Maps of soil characteristics. In Stolbovoi, V. and I. McCallum, eds (2002) CD-ROM Land Resources of Russia. International Institute for Applied Systems Analysis and the Russian Academy of Science, Laxenburg, Austria.
- Strauss, J., Schirrmeyer, L., Grosse, G., Wetterich, S., Ulrich, M., Herzschuh, U., and H.-W. Hubberten. (2013). The deep permafrost carbon pool of the yedoma region in Siberia and Alaska. *Geophys Research Letters*, 40, 6165-6170.
- Sturtevant, B.R., Miranda, B.R., Scheller, R.M., and D. Shinneman. (2008). LANDIS-II dynamic fire system extension. Verion 1. User guide. Univeristy of Wisconsin, Madison, Wisconsin, USA.
- Sturtevant, B.R., R.M. Scheller, B.R. Miranda, D. Shinneman, A.D. Syphard. (2009). Simulating dynamic and mixed-severity fire regimes: A process-based fire extension for LANDIS-II. *Ecological Modelling*, 220, 3380-3393.

- Sullivan, A. D., & Clutter, J. L. (1972). A simultaneous growth and yield model for loblolly pine. *Forest Science*, 18 (1), 76-86.
- Sun, G., Ranson, K. J., Kharuk, V. I., Im, S. T., & Naurzbaev, M. M. (2011). Characterization and monitoring of tundra-taiga transition zone with multi-sensor satellite data. In: *Eurasian Arctic Land Cover and Land Use in a Changing Climate*, pp. 53-77. Springer Netherlands.
- Suzuki, K. and T. Ohta. (2003). Effect of larch forest density on snow surface energy balance. *Journal of Hydrometeorology*, 4, 1181-1193.
- Sykes, M. T., & Prentice, I. C. (1995). Boreal forest futures: modelling the controls on tree species range limits and transient responses to climate change. In: *Boreal Forests and Global Change*, pp. 415-428. Springer Netherlands.
- Tarnocai, C., Canadell, J. G., Schuur, E. A. G., Kuhry, P., Mazhitova, G., & Zimov, S. (2009). Soil organic carbon pools in the northern circumpolar permafrost region. *Global Biogeochemical Cycles*, 23 (2).
- Tchebakova, N. M., Monserud, R. A., & Parfenova, E. I. (2001). *Phytomass change in the mountain forests of southern Siberia under climate warming*. US Department of Energy National Energy Technology Laboratory.
- Tchebakova, N.M. (2006). Dissertation (doctorate): Possible transformation of vegetation cover in Siberia for different climate change scenarios. Krasnoyarsk, Russia. 60pp. (in Russian)
- Tchebakova, N. M., & Parfenova, E. I. (2006). Prediction of forest shifts under climate change at the end of the 20th century in Central Siberia. *Computer Technology*, 11 (part 3), 77-86.
- Tchebakova, N. M., Parfenova, E., & Soja, A. J. (2009a). The effects of climate, permafrost and fire on vegetation change in Siberia in a changing climate. *Environmental Research Letters*, 4 (4), 045013.
- Tchebakova, N. M., Rehfeldt, G. E. and E. I. Parfenova. (2009b). From vegetation zones to climatypes: Effect of climate warming on Siberian exosystems, pp. 427-447. In: Osawa, A., Zyranova, O. A., Matsurura, Y., Kajimoto, T. and R. W. Wein (eds). *Permafrost Ecosystems of Siberian Larch Forests*. Springer-Verlag, New York.
- Tchebakova, N. M., Parfenova, E. I., & Soja, A. J. (2011). Climate change and climate-induced hot spots in forest shifts in central Siberia from observed data. *Regional Environmental Change*, 11 (4), 817-827.
- Thornthwaite, C. W. and J. R. Mather. (1957). Instructions and tables for computing potential evapotranspiration and the water balance. *Publications in Climatology*, 10, 183-311.
- Tietjen, B., & Huth, A. (2006). Modelling dynamics of managed tropical rainforests - aggregated approach. *Ecological Modelling*, 199 (4), 421-432.
- Timoshok, E. E., Narozhnyi, Y. K., Dirks, M. N., & Berezov, A. A. (2003). Experience in combined glaciological and botanical studies on the primary plant successions on young moraines in the Central Altai. *Russian Journal of Ecology*, 34 (2), 91-97.
- Timoshok, E. E., Timoshok, E. N., & Skorokhodov, S. N. (2014). Ecology of Siberian stone pine (*Pinus sibirica* Du Tour) and Siberian larch (*Larix sibirica* Ledeb.) in the Altai mountain glacial basins. *Russian Journal of Ecology*, 45 (3), 194-200.
- Tinner, W., & Kaltenrieder, P. (2005). Rapid responses of high-mountain vegetation to early Holocene environmental changes in the Swiss Alps. *Journal of Ecology*, 93 (5), 936-947.
- Tjoelker, M. G., Oleksyn, J., & Reich, P. B. (1998). Seedlings of five boreal tree species differ in acclimation of net photosynthesis to elevated  $CO_2$  and temperature. *Tree Physiology*, 18 (11), 715-726.
- Tretyakova, I.N. and N.E. Noskova. (2004). Scotch pine pollen under conditions of environmental stress. *Russian Journal of Ecology*, 35 (1), 20-26.
- Tretyakova, I. N. (2006). Characteristics of organ formation and their morphogenetic potential in Siberian larch. *Achievements of Modern Biology*, 126 (5), 472-480. (in Russian)
- Urban, D.L. (1990). A versatile model to simulate forest pattern: A user's guide to ZELIG version 1.0. Department of Environmental Sciences, University of Virginia, Charlottesville, VA, 108 pp.

- Urban, D.L., G.B. Bonan, T.M. Smith, and H.H. Shugart. (1991). Spatial applications of gap models. *Forest Ecology and Management*, 42, 95-110.
- Urban, D. L., & Shugart, H. H. (1992). Individual-based models of forest succession. In: *Plant succession: theory and prediction*. Chapman and Hall, London. pp. 249-292.
- Urban, D. L. Harmon, M. E. and C. B. Halpern. (1993). Potential response of Pacific Northwest forests to climatic change, effects of stand age and initial composition. *Climatic Change*, 23, 247-266.
- Urban, D. L. (2000). Using model analysis to design monitoring programs for landscape management and impact assessment. *Ecological Applications*, 10, 1820-1832.
- Valendik, E. N. (1996). Temporal and spatial distribution of forest fires in Siberia. In: *Fire in Ecosystems of Boreal Eurasia*. Springer Netherlands. pp. 129-138.
- Valendik, E.N., Verkhovec, S.V., Kisilyakhov, E.K. and A.Yu. Lantukh. (2004a). The role of the silkworm in the fire potential of forests of the Lower Angara river basin. *Lesnoe Khozaistvo*, 6, 27-29. (In Russian)
- Valendik, E.N., Verkhovec, S.V., Kisilyakhov, E.K., Kosov, I.V. and N.A. Tyul'panov. (2004b). Preparation of silkworm-infested forest for regeneration through fire. *Lesnoe Khozaistvo*, 3, 41-42. (In Russian)
- Vaschuk, L. N. and A. Z. Shvidenko. (2006). *Dynamics of Forests of Irkutsk Region*. Irkutsk printing house N1, Irkutsk, Russia.
- Vertessy, R. A., Benyon, R. G., O'sullivan, S. K., & Gribben, P. R. (1995). Relationships between stem diameter, sapwood area, leaf area and transpiration in a young mountain ash forest. *Tree Physiology*, 15 (9), 559-567.
- Viereck, L. A., Van Cleve, K., & Dyrness, C. T. (1986). Forest ecosystem distribution in the taiga environment. In: *Forest ecosystems in the Alaskan taiga*. Springer New York. pp. 22-43.
- Volney, W. J. A. and R. A. Fleming. (2000). Climate Change and impacts of boreal forest insects. *Agriculture, Ecosystems and Environment*, 82, 283-294.
- Vygodskaya, N. N., Groisman, P. Ya., Tchebakova, N. M., Kurbatova, J. A., Panfyorov, O., Parfenova, E. I., and A. F. Sogachev. (2007). Ecosystems and climate interactions in the boreal zone of northern Eurasia. *Environmental Research Letters*, 2, 045033.
- Wang, J., Zhang, C., Xia, F., Zhao, X., Wu, L., & Gadow, K. V. (2011). Biomass structure and allometry of *Abies nephrolepis* (Maxim) in Northeast China. *Silva Fennica*, 45 (2), 211-226.
- Waring, R. H., Schroeder, P. E., & Oren, R. (1982). Application of the pipe model theory to predict canopy leaf area. *Canadian Journal of Forest Research*, 12 (3), 556-560.
- Waring, R. H., & Schlesinger, W. H. (1985). *Forest ecosystems: concepts and management*. Academic Press, Inc. Harcourt Brace Jovanovich, Publishers.
- Watt, A. S. (1947). Pattern and process in the plant community. *The Journal of Ecology*, 35, 1-22.
- Wegge, P., Rølstad, J., & Gjerde, I. (1992). Effects of boreal forest fragmentation on capercaillie grouse: empirical evidence and management implications. In: *Wildlife 2001: populations*. Springer Netherlands. pp. 738-749.
- Weishampel, J.F., D.L. Urban, H.H. Shugart, and J.B. Smith. (1992). A comparison of semivariograms from a forest transect gap model and remotely sensed data. *Journal of Vegetation Science*, 3, 521-526.
- Weishampel, J.F. (1994). Dissertation: Spatial dynamics of primary forest succession: Modeling the Glacier Bay 'chronosequence'. University of Virginia, Charlottesville, VA.
- Weishampel, J. F., & Urban, D. L. (1996). Coupling a spatially-explicit forest gap model with a 3-D solar routine to simulate latitudinal effects. *Ecological Modelling*, 86 (1), 101-111.
- Welp, L. R., Randerson, J. T., & Liu, H. P. (2007). The sensitivity of carbon fluxes to spring warming and summer drought depends on plant functional type in boreal forest ecosystems. *Agricultural and Forest Meteorology*, 147 (3), 172-185.

- Wertin, T. M., McGuire, M. A., & Teskey, R. O. (2012). Effects of predicted future and current atmospheric temperature and  $[CO_2]$  and high and low soil moisture on gas exchange and growth of *Pinus taeda* seedlings at cool and warm sites in the species range. *Tree Physiology*, 32 (7), 847-858.
- Westerling, A. L., Hidalgo, H. G., Cayan, D. R., and T. W. Swetnam. (2006). Warming and earlier spring increase western US forest wildfire activity. *Science*, 313, 940-943.
- Wilkinson, M., Juday, G. P., Barber, V. A., & Zald, H. S. (2004). Recent climate warming forces contrasting growth responses of white spruce at treeline in Alaska through temperature thresholds. *Global Change Biology*, 10 (10), 1724-1736.
- Winjum, J. K., Dixon, R. K., & Schroeder, P. E. (1992). Estimating the global potential of forest and agroforest management practices to sequester carbon. In: *Natural Sinks of :math:'CO\_2'*. Springer Netherlands. pp. 213-227.
- Wirth, C., Schulze, E. D., Lüthker, B., Grigoriev, S., Siry, M., Hardes, G., ... & Vygodskaya, N. N. (2002). Fire and site type effects on the long-term carbon and nitrogen balance in pristine Siberian Scots pine forests. *Plant and Soil*, 242 (1), 41-63.
- Wirth, C. (2005). Fire regime and tree diversity in boreal forests: implications for the carbon cycle. In: *Forest Diversity and Function*. Springer Berlin Heidelberg. pp. 309-344.
- Woodward, F. I. (1987). *Climate and Plant Distribution*. Cambridge University Press, Cambridge.
- Yamazaki, T., Yabuki, H., Ishii, Y., Ohta, T., & Ohata, T. (2004). Water and energy exchanges at forests and a grassland in eastern Siberia evaluated using a one-dimensional land surface model. *Journal of Hydrometeorology*, 5 (3), 504-515.
- Yan X. and H. H. Shugart. (2005). A forest gap model to simulate dynamics and patterns of eastern Eurasian forests. *Journal of Biogeography*, 32, 1641-1658.
- Yan, M. J., Yamanaka, N., Yamamoto, F., & Du, S. (2010). Responses of leaf gas exchange, water relations, and water consumption in seedlings of four semiarid tree species to soil drying. *Acta Physiologiae Plantarum*, 32 (1), 183-189.
- Yang, J., He, H. S., & Gustafson, E. J. (2004). A hierarchical fire frequency model to simulate temporal patterns of fire regimes in LANDIS. *Ecological Modelling*, 180 (1), 119-133.
- Yatskov, M., Harmon, M. E., & Kruckina, O. N. (2003). A chronosequence of wood decomposition in the boreal forests of Russia. *Canadian Journal of Forest Research*, 33 (7), 1211-1226.
- Zhang, N., Shugart, H. H. and X. Yan. (2009). Simulating the effects of climate changes on eastern Eurasian forests. *Climatic Change*, 95, 341-361.
- Zhang, K., Kimball, J. S., Nemani, R. R., & Running, S. W. (2010). A continuous satellite-derived global record of land surface evapotranspiration from 1983 to 2006. *Water Resources Research*, 46 (9).
- Zhang, N., Yasunari, T., & Ohta, T. (2011). Dynamics of the larch taiga-permafrost coupled system in Siberia under climate change. *Environmental Research Letters*, 6 (2), 024003.